ISSN-print: 2073-0764

ISSN-online: 2959-4340

TuJNaS

Thamar University Journal of Natural & Applied Sciences

A peer-reviewed Open-Access Journal

Volume 10

Issue (2)

December 2025

Thamar University Publications

Thamar University Journal of
Natural and Applied Sciences (*TUJNAS*)

Thamar University Journal of Natural & Applied Sciences (TUJNAS) is a peer-reviewed journal. It is an open-access journal published by Thamar University, Dhamar, Yemen twice a year. The aim of the journal is to publish original and review articles in the fields of science, agriculture, engineering, medicine, environment, and computer science. The journal is published in English only.

The journal has the following international standard codes:

ISSN-print: 2073-0764

ISSN-online: 2959-4340

For more information on editorial policy, manuscript submission, ethics, etc., please visit the TUJNAS Journal website:

https://www.tu.edu.ye/journals/index.php/TUJNAS

Vision, Mission, and Aims

Vision

Through several procedures, TUJNAS aspires to be a leading regional and international natural and applied sciences journal. TUJNAS strives for inclusion in major indexing services such as Scopus and Web of Science to boost scholarly visibility and citation impact. It publishes open-access research aligned with the UN SDGs. The journal continuously refines its editorial policies, ethical guidelines, and production workflows in line with COPE and ICMJE recommendations to ensure the timely, transparent, and reliable publication of high-quality scientific content.

Mission

TUJNAS exists to publish rigorous, high-impact research in natural and applied sciences. It upholds academic integrity through a strict double-masked peer review process, safeguarding quality and originality. The journal fosters interdisciplinary collaboration to bridge theoretical science with practical applications, driving innovative solutions to global and local challenges. Committed to open science, it provides free, immediate access to research, enhancing engagement among researchers, practitioners, and policymakers. The journal aims to address pressing societal and scientific issues worldwide by prioritizing actionable insights.

Aims

1. Broad disciplinary coverage: by publishing contributions in:

- Pure Sciences: Biology, Chemistry, Physics, Mathematics, Earth and Environmental Sciences.
- Applied Sciences & Engineering: Civil, Mechanical, Electrical, Chemical, Environmental, Mechatronics, and Renewable Energy Engineering.
- Life and Health Sciences: Agriculture, Veterinary Medicine, Pharmacology, Biotechnology, Clinical Medicine, Public Health, Biomedical Engineering, and Health Informatics.
- Computer & Information Technology: Data Science, Artificial Intelligence, Software Engineering, Network Systems, Cybersecurity, and Health Informatics.

2. Diverse article types: by encouraging submission of:

- Original Research Articles presenting novel empirical or theoretical insights.
- Review Articles synthesizing and critically evaluating current knowledge.
- Case Studies highlighting unique applications or phenomena in real-world contexts.
- Editorials offering expert perspectives on emerging trends or policy issues.
- Short communications deliver concise, timely findings of high relevance.

3. Regional engagement and global outreach:

- Support Early-Career Researchers by offering clear author guidelines, mentorship through the review process, and rapid turnarounds.
- Highlight Local Contexts to address Yemen-specific environmental, agricultural, and health challenges while drawing lessons of broader relevance.
- Promote international collaboration by soliciting contributions from global experts and forming editorial alliances with related journals and societies.

4. Ethics and Transparency:

- Enforce strict adherence to authorship criteria, conflict-of-interest declarations, and research ethics (including human/animal welfare and data integrity).
- Embrace transparent archival of data and methods to enable reproducibility and long-term accessibility.

Editorial Team

General Supervisor

Prof. Dr. Mohammed Mohammed Al-Haifi

Position: Rector of the University, Thamar University, Dhamar, Yemen.

Address: University Presidency, Thamar University, P O Box 87246 Dhamar, Yemen.

E-Mail: dralhaifi@tu.edu.ye

Editor-in-chief

Prof. Dr. Adulkarem Esmail Zabiba

Position: Vice-Rector of Postgraduate and Scientific Research, Thamar University, Dhamar, Yemen.

Address: Vice Presidency of the University for Postgraduate Studies and Scientific Research, Thamar University, P O Box 87246 Dhamar, Yemen.

E-Mail: karimzabiba@tu.edu.ye

Editorial Director

Prof. Dr. Abdullah Ahmed Ali Ahmed

Position: Professor of Nanoscience, Physics Department, Faculty of Applied Sciences, Thamar University, Dhamar, Yemen.

Address: Faculty of Applied Sciences, Thamar University, P O Box 87246 Dhamar, Yemen.

E-Mail: abdullah2803@tu.edu.ye

Editorial Director Assistant

Assoc. Prof. Annas Saeed Ahmad Al-Sharabi

Position: Associate Prof. of Superconductor, Physics Department, Faculty of Applied Sciences, Thamar University, Dhamar, Yemen.

Address: Faculty of Applied Sciences, Thamar University, P O Box 87246 Dhamar, Yemen.

E-Mail: annas.AlSharabi@tu.edu.ye

✉ All correspondence should be sent to: ✉

Editorial Director,

Thamar University Journal of

Natural and Applied Sciences (TUJNAS)

Thamar University, P O Box: 87246 Dhamar, Republic of Yemen
E-Mail: tujnas@tu.edu.ye

Advisory Board

Assoc. Prof. Abdul Ghani Ali Mohammed

Position: Dean of Faculty of Agriculture & Veterinary Medicine, Thamar University, Dhamar, Yemen.

Address: Faculty of Agriculture & Veterinary Medicine, Thamar University, Dhamar, Yemen.

E-Mail: abdulghani.ali@tu.edu.ye

Assist. Prof. Fouad Mohammed Y. Al-Jarmouzi

Position: Dean of Faculty of Engineering, Thamar University, Dhamar, Yemen.

Address: Faculty of Engineering, Thamar University, Dhamar, Yemen.

E-Mail: aljarmouzi@tu.edu.ye

Assist. Prof. Nashwan Hamid Saleh Al-Tairi

Position: Dean of Faculty of Dentistry, Thamar University, Dhamar, Yemen.

Address: Faculty of Dentistry, Thamar University, Dhamar, Yemen.

E-Mail: nashwanh9@tu.edu.ye

Assoc. Prof. Adel Ali Ahmed Amran

Position: Dean of Faculty of Medical Science, Thamar University, Dhamar, Yemen.

Address: Faculty of Medical Science, Thamar University, Dhamar, Yemen.

E-Mail: adelamran@tu.edu.ye

Assist. Dr. Abdullah Al-Murtadha

Position: Dean of Faculty of Medicine, Thamar University, Dhamar, Yemen.

Address: Faculty of Medicine, Thamar University, Dhamar, Yemen.

E-Mail: abdullah.almurtadha@tu.edu.ye

Editorial Board

Prof. Dr. Levan Chkhartishvili (Georgia)

Research field: Semiconducting and Powder Composite Materials.

Position: Professor at the Department of Engineering Physics, Faculty of Informatics and Control Systems, Georgian Technical University, and researcher at F. Tavadze Metallurgy and Materials Science Institute, Semiconducting and Powder Composite Materials Laboratory.

Affiliation: Department of Engineering Physics, Faculty of Informatics and Control Systems, Georgian Technical University, 77 M. Kostava Ave., GTU Campus 4, Room 307, Tbilisi, 0160, Georgia.

E-Mail: levanchkhartishvili@gtu.ge , chkharti2003@yahoo.com

Prof. Dr. Saeed M. Al-Ghalibi (Yemen)

Research field: Bacteriology, Fungi, Medical microbiology, and Food Microbiology.

Position: Deputy Dean of Faculty of Science for Academic Affairs and Graduate Studies, Faculty of Science, Sana'a University, Sana'a, Yemen

Affiliation: Department of Biology, Faculty of Science, Sana'a University, Sana'a, Yemen.

E-Mail: s.alghalabi@su.edu.ye , Alghalibi@gmail.com

Prof. Dr. Abdulkarim A. Amad (Yemen)

Research field: Animal nutrition and production feed and feeding.

Affiliation: Faculty of Agriculture, Thamar University, Dhamar, Yemen and Institute of Animal Nutrition, Department of Veterinary Medicine, Frei Universität Berlin, Berlin, Germany.

E-Mail: abdulkarim.Amad@tu.edu.ye , abeerobeid@yahoo.com

Prof. Dr. Nabil M. Al-Areeq (Yemen)

Research field: Petroleum Geology, Hydrology, Sedimentology, Integrated Water Resources Management, Data analysis and Resolving of Water Related Conflicts.

Position: Centre Director of Water Resources and Environment, Thamar University, Dhamar, Yemen.

Affiliation: Department of Geology and Environment, Faculty of Applied Science, Thamar University, Dhamar, Yemen.

E-Mail: alareeqnabil@tu.edu.ye , nabilalareeq@yahoo.com

Prof. Dr. Ibrahim Radman Al Shaibani (Yemen)

Research field: Veterinary Parasitology.

Position: Vice Dean for students' affair, Faculty of Veterinary Medicine, Thamar University, Dhamar, Yemen.

Affiliation: Faculty of Veterinary Medicine, Thamar University, Dhamar, Yemen.

E-Mail: ibrahim.alshaibani@tu.edu.ye , dr_ibra67@yahoo.com

Prof. Dr. Salah Mahdi Saleem Al-Bader (Iraq)

Research field: Fungal taxonomy, Fungal ecology, and Natural products as antifungal agents.

Affiliation: Department of Medical Laboratory Sciences, College of Science, Knowledge University, Erbil, Iraq.

E-Mail: salah.mahdi@knu.edu.iq

Prof. Dr. Abeer Omer A. Obeid (Yemen)

Research field: Organic chemistry, Polymers, Liquid Crystals, and synthesis of heterocyclic compounds, as well as Anti-cancer and Antibacterial applications.

Affiliation: Department of Chemistry, Faculty of Science, Sana'a University, Sana'a, Yemen.

E-Mail: ab.obaid@su.edu.ye , abeerobeid@yahoo.com

Prof. Dr. Abduh M. Abdulwahab (Yemen)

Research field: Single Crystal, Crystal Structure, Physical Characterization of Solid-State Materials and Solid-State Physics.

Affiliation: Department of Physics, Faculty of Applied Sciences, Thamar University, Dhamar, Yemen.

E-Mail: abduh.abdulwahab@tu.edu.ye , abduhabdulwahab@yahoo.com

Prof. Dr. Omar M. A. Al Shuja'a (Yemen)

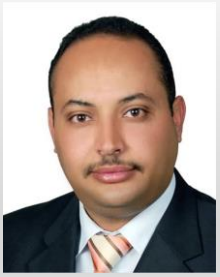

Research field: Materials Chemistry, Polymer Chemistry, and Physical Chemistry.

Position: Dean of the Center for Development and Quality Assurance, Al-Nasser University, Sana'a, Yemen.

Affiliation: Department of Chemistry, Faculty of Applied Sciences, Thamar University, Dhamar, Yemen.

E-Mail: omrshugaa@tu.edu.ye , abduhabdulwahab@yahoo.com

Assoc. Prof. AbdulSalam M. Al-Makdad (Yemen)

Research field: Diagnosis, management, and care of acute and chronic liver disease and GI diseases. Diagnostic and interventional GI endoscopy.

Position: President of the internal medicine department in AL-Wahda Teaching Hospital Maabar, Maabar City, Dhamar, Yemen.

Affiliation: Department of Internal Medicine, Faculty of Medicine, Thamar University, Dhamar, Yemen.

E-Mail: aalmakdad@tu.edu.ye

Assoc. Prof. Shaimaa A. A. Momen (Egypt)

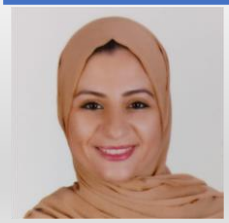

Research field: Entomology.

Affiliation: Department of Entomology, Faculty of Science, Ain Shams University, Khalifa El-Maamon Street, 11566, Cairo, Egypt.

E-Mail: Shaimaa_momen@sci.asu.edu.eg , Shaimaa_momen@hotmail.com

Assoc. Prof. Essam A. Al-Moraissi (Yemen)

Research field: Oral and maxillofacial surgery, craniomaxillofacial trauma, temporomandibular joint disorders, orthognathic surgery, surgical pathology, cleft lip and palate, implant dentistry, lower third molar surgery, regenerative medicine, and adult mesenchymal stem cells.

Affiliation: Department of Oral and Maxillofacial Surgery, Faculty of Dentistry, Thamar University, Dhamar, Yemen.

E-Mail: dressamalmoraissi@tu.edu.ye

Assoc. Prof. Salah Abdul-Jabbar Jassim (Iraq)

Research field: Thin Films, Semiconductor Devices, and Solid-State Physics.

Affiliation: Department of Dentistry, AL Kunooze University College, Basrah, Iraq.

E-Mail: salah.abdul.jabbar@kunoozu.edu.iq , salahjassim200@yahoo.com , salah.jassim@alayen.edu.iq

Assoc. Prof. Amin Saif Ahmed (Yemen)

Research field: Energy and control systems engineering.

Affiliation: Department Mechatronics, Al-Saeed College of Engineering and Information Technology, Taiz University, Taiz, Yemen.

E-Mail: sameeralromima@yahoo.com , sameeralromima@gmail.com

Assoc. Prof. Dina Salah Eldin M. Abdelrhman (Egypt)

Research field: Gold Nanoparticles, Photochemistry, Nanotechnology, and Nanomedicine.

Affiliation: Biophysics, Physics Department, Faculty of Science, Ain Shams University, Khalifa El-Maamon Street, 11566, Cairo, Egypt.

E-Mail: dinasalah@sci.asu.edu.eg , dandy741@hotmail.com , dandy741@gmail.com

Assoc. Prof. Fawaz M. A. Al-Badaii (Yemen)

Research field: Microbiology, Antimicrobial resistance, Environmental Science, Heavy metals, and Adsorption Water quality.

Affiliation: Department of Biology, Faculty of Applied Sciences, Thamar University, Dhamar, Yemen.

E-Mail: fawaz.AlBadai@tu.edu.ye , abdualwhab1974@gmail.com

Assoc. Prof. Abdulwahab B. Alwany (Yemen)

Research field: Solid State Physics, Thein Films, Materials Science, and Nanoscience.

Affiliation: Department of Physics, Faculty of Science, Ibb University, Ibb, Yemen.

E-Mail: abdualwhab@yahoo.com , abdualwhab1974@gmail.com

Assoc. Prof. Ali Abdullah A. Al-Mehdar (Yemen)

Research field: Pharmacology & Therapeutics.

Affiliation: Department of Pharmacology and Toxicology, Faculty of Faculty of Medicine, Thamar University, Dhamar, Yemen.

E-Mail: ali.almehdar@tu.edu.ye , alialmehdar2006@yahoo.com

Assoc. Prof. Sameer A. M. Abdulrahman (Yemen)

Research field: Pharmaceutical Analytical Chemistry and Water Treatment.

Affiliation: Department of Chemistry, Faculty of Education and Sciences-Rada'a, Albaydha University, Albaydha 14517, Yemen.

E-Mail: sameeralromima@yahoo.com , sameeralromima@gmail.com

Assoc. Prof. Nada M. Al-Hamdani (Yemen)

Research field: Histology, and Physiology, specializing in Endocrinology.

Affiliation: Department of Biology, Faculty of Science, Sana'a University, Sana'a, Yemen.

E-Mail: n.alhamdni@su.edu.ye , hamdaninadam@gmail.com

Assoc. Prof. Abdulbari A. A. Saeed (UK)

Research field: Preparation and characterization of mesoporous from solid waste as catalysis for water purification, Separation technology using an adsorption process, Water and wastewater treatment, and Biofuel production from organic solid waste.

Affiliation: School of Engineering, Institute for Infrastructure and Environment (IIE), University of Edinburgh, Edinburgh EH9 3JL, UK.

E-Mail: alborani_75@yahoo.co.uk , Abdulbari.Saeed@ed.ac.uk

Assoc. Prof. Yahya Qaid Hasan Ali (Yemen)

Research field: Differential Equations, Numerical Analysis, and Adomian Decomposition Method.

Affiliation: Department of Mathematics, Faculty of Applied Sciences, Thamar University, Dhamar, Yemen.

E-Mail: qaid.Yahya@tu.edu.ye , yahya217@yahoo.com

Assoc. Prof. Abdullah Alwarafi (Yemen)

Research field: Social Pharmacy.

Position: Vice Dean for Student Affairs, Faculty of Dentistry, Ibb University, Ibb, Yemen

Affiliation: Pharmacy Department, Faculty of Dentistry, Ibb University, Ibb, Yemen.

E-Mail: abdullahalwarafi@gmail.com , dentistry@ibbuniv.edu.ye

Prof. Dr. Ahmed A. M. Alakwa (Yemen)

Research field: Agricultural Economics.

Position: Head of Scientific Research, Vice Presidency of the University for Postgraduate Studies and Scientific Research, Thamar University, P O Box 87246 Dhamar, Yemen

Affiliation: Faculty of Agriculture, Thamar University, Dhamar, Yemen.

E-Mail: Hawali.ahmed@tu.edu.ye , alakwaahmed55@gmail.com

Prof. Dr. Ahmed Ali Saleh Obayeha (Yemen)

Research field: Orthodontics, Pediatric Dentistry, and Preventive Medicine.

Position: Dean of the Faculty of Dentistry, Al-Razi University, Sana'a, Yemen

Affiliation: Faculty of Dentistry Sana'a University, Sana'a, Yemen.

E-Mail: a.Obaya@su.edu.ye , Ahmedobeyah@yahoo.com

Assoc. Prof. Fathi Ahmed ELShawish (Yemen)

Research field: Identification and characterization of genetic sources of indigenous and introduced fruits, propagation and breeding of fruit crops, and design and layout of gardens.

Position: Deputy Dean for Postgraduate Studies and Scientific Research, Faculty of Agriculture, Thamar University, Dhamar, Yemen

Affiliation: Faculty of Agriculture, Thamar University, Dhamar, Yemen.

E-Mail: Fathi.ELShawish@tu.edu.ye ,

Assoc. Prof. Khalid Al-Hussaini (Yemen)

Research field: Information & Communication Technology (ICT), Computer Communications (Networks), Communication Engineering, and Computer Engineering.

Position: University Rector's Advisor for Academic Development & Automation and Vice Dean for Student Affairs, Faculty of Computer Science & Information Systems, Thamar University, Dhamar, Yemen.

Affiliation: Department of Information Technology, Faculty of Computer Science & Information System, Thamar University, Dhamar, Yemen.

E-Mail: khalid.alhussaini@tu.edu.ye

Assoc. Prof. Rasheed M. Alsanafi (Yemen)

Research field: Surveying & Urban Engineering and Planning, Civil Engineering.

Position: Postgraduate Studies and Scientific Research, Faculty of Engineering, Thamar University, Dhamar, Yemen.

Affiliation: Department of Civil Engineering Faculty of Engineering, Thamar University, Dhamar, Yemen.

E-Mail: alsanafy@tu.edu.ye , alsanafy@hotmail.com

Assoc. Prof. Kamal O. I. Ba'hakem (Yemen)

Research field: Surgical Gastroenterology, Upper & Lower GIT Endoscopy (diagnostic and therapeutic), Bleeding emergency GIT, Major conventional GIT surgery including biliary tree reconstructions, ERCP specialist, and General Surgeon.

Position: Vice director of AL-Wahda Teaching Hospital Maabar, Thamar University, Yemen.

Affiliation: Department of Surgery, Faculty of Medicine, Thamar University, Dhamar, Yemen.

E-Mail: mkamel1970@yahoo.com , khemo1970@gmail.com

Prof. Dr. Mohammad Ghaffar Faraj (Iraq)

Research field: Polymer Solar Cells and Solar Energy.

Affiliation: Department of Physics, Faculty of Science and Health, Koya University, Koya, Kurdistan Region, Iraq.

E-Mail: mohammad.ghaffar@koyauniversity.org

Prof. Dr. Saad S. AL-Tobaili (Yemen)

Research field: Graph Theory and Mathematical Modeling relationships.

Affiliation: Department of Mathematics, Faculty of Science, Hadhramout University, Mukalla, Hadhramout, Yemen.

E-Mail: saadaltabili1@yahoo.com

Prof. Dr. Majid Raissan Al Bahrani (Iraq)

Research field: Nano-Energy Materials & Devices, Solid-State Physics, Graphene, Carbon Nanotube, and Organic Photovoltaics.

Affiliation: Physics Department, College of Sciences, University of Thi-Qar, Nasiriyah, Iraq.

E-Mail: majidphy2016@utq.edu.iq or m20111973@yahoo.com

Assoc. Prof. Hassan A. M. Al-Khawlani (Yemen)

Research field: Horticulture and Biotechnology.

Affiliation: Agriculture research & extension authority (AREA), Dhamar, Yemen.

E-Mail: alkholanihassaan@gmail.com

Assoc. Prof. Mohammed Jassim Mohammed Ali (Iraq)

Research field: Integrated Optics & Photonic Devices, Optical Sensors & Biosensors, Solid-State Physics & Materials Characterization, Nanotechnology, Atomic & Molecular Spectroscopy, Computational Physics and Simulation.

Affiliation: Physics Department, College of Sciences, Mustansiriyah University, Baghdad, Iraq.

E-Mail: mohammedjassim@uomustansiriyah.edu.iq or mohammedjassim78@gmail.com

Assoc. Prof. Amin M. A. AlWaseai (Yemen)

Research field: Biotechnology and Food Technology.

Position: Head of Biotechnology & Food Technology Department, Faculty of Agriculture, Thamar University, Dhamar, Yemen.

Affiliation: Department of Biotechnology & Food Technology, Faculty of Agriculture, Thamar University, Dhamar, Yemen.

E-Mail: amin.alwaseai@tu.edu.ye , amin_alwaseai2000@yahoo.com

Prof. Dr. Adil N. Ayyash (Iraq)

Research field: Theoretical Physics, Molecular Physics and Spectroscopy, Spectral Analysis of Materials, and Computational Physics.

Affiliation: Department of Physics, College of Science, University of Anbar, Anbar, Iraq.

E-Mail: sc.adil_nameh78@uoanbar.edu.iq

Assoc. Prof. Rana Ismael Khaleel (Iraq)

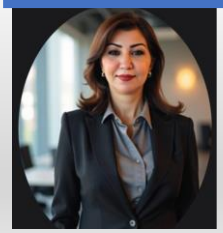

Research field: Medical Physics.

Affiliation: Physics Department, College of Sciences, Mustansiriyah University, Baghdad, Iraq.

E-Mail: khleelrana79@uomustansiriyah.edu.iq

Technical Team

Technical Editing by:

Mr. Mohammed Subaie

Volume 10, Issue 2, December 2025

Articles

TUJNAS

Original Article

Thamar University Journal of Natural & Applied Sciences 10(2) (2025) 1– 8

DOI: https://doi.org/10.59167/tujnas.v10i2.3011

Some Coefficient Estimates for Subclass of Starlike Functions Associated with the Sine Function Defined by Subordination

Safa'a Hamood Mohammed Al-Saqqaf

Department of Mathematics, College of Education - Saber, University of Lahej, Yemen.

Email: safaalsaqqaf1@gmail.com

Received: 3 July 2025. Received (in revised form): 22 September 2025. Accepted: 6 October 2025. Published: 28 December 2025.

Abstract:

In this article, we investigate the logarithmic coefficients for a subclass of starlike functions with respect to symmetric conjugate points associated with the sine function. Although this class has been previously studied in the context of coefficient bounds and geometric properties, the logarithmic coefficients, especially higher-order ones, have not been extensively addressed in the literature. We derive explicit formulas for the first six logarithmic coefficients γ_1 through γ_6 for functions in this class. We establish precise bounds for the Hankel coefficients, Hankel determinants $H_{2,1}(f)$, $H_{2,2}(f)$, $H_{3,1}(f)$ and $H_{4,1}(f)$ associated with the class $\mathcal{S}^*_{SC}(\sin z)$. In addition, we derive sharp estimates for the Hankel determinant for the Logarithmic coefficients $H_{2,1}(F_f/2)$ and $H_{2,2}(F_f/2)$ within the same class.

Keywords: Analytic functions; Starlike functions; Coefficient estimates; Logarithmic coefficients; Subordination; Hankel determinant

1. Introduction and preliminaries

This article lies within the framework of geometric function theory, with a particular focus on the study of starlike functions- an important class of univalent analytic functions defined in the open unit disk.

The study of logarithmic coefficients, especially those of higher order, plays a vital role in understanding the growth, distortion, and geometric behavior of analytic functions.

In this work, we consider a subclass of starlike functions with respect to symmetric conjugate points associated with the sine function. The sine function, being a classical transcendental function, possesses rich analytic and geometric properties that motivate the present investigation.

Let $\mathcal{A}$ denote the class of functions f that are analytic in the unit disk

$D = \{z: z \in \mathbb{C}\ and\ |z| < 1\}$, and that has a Maclaurin series expansion of the form

$$f(z) = z + \sum_{m=2}^{\infty} a_m z^m \quad , \quad (z \in D). \tag{1.1}$$

A subclass of $\mathcal{A}$, denoted by $\mathcal{S}$, consists of functions that are univalent and normalized such that $f(0) = 0, f'(0) = 1$. Let $\mathcal{S}^*$denote the subclass of $\mathcal{S}$ consisting of starlike functions, i.e., $f \in \mathcal{S}^*$ if and only if:

$$\mathcal{R}e\ \frac{zf'(z)}{f(z)} > 0 \ , z \in D. \tag{1.2}$$

Let $\mathcal{B}$ denote the family of Schwarz functions $w(z)$, that are analytic in D given by

$$w(z) = \sum_{n=1}^{\infty} b_n z^n \quad , \quad (z \in D),$$

and satisfying $w(0) = 0$ and $|w(z)| < 1$ for all $z \in D$. Given analytic functions f and g in D, we say that f is subordinated to g, written $f \prec g$, if there exists a Schwarz function $w(z)$ such that $f(z) = g\big(w(z)\big), z \in D$.

When g is univalent and $f(0) = g(0)$, then $f(D) \subset g(D)$.

For fixed constants A and B satisfying $-1 \le B < A \le 1$, denoted by $P[A, B]$, the family of functions

$$p(z) = 1 + \sum_{n=1}^{\infty} c_n z^n .$$

A function $p(z)$, analytic in the unit disk D, belongs to the Janowski class $P[A, B]$ if and only if

$$p(z) = \frac{1 + Aw(z)}{1 + Bw(z)}, \quad (z \in D),$$

where $w(z)$ is the Schwarz function. This class $P[A, B]$ is known as the Janowski class and was introduced by Janowski [7].

Class $P[A, B] \subset P[1, -1] = P$, then it reduces to the class P, the well-known class of functions with positive real part consists of functions p that satisfy $\mathcal{R}e\ p(z) > 0$ and $p(0) = 1$.

We now introduce a subclass of starlike functions with respect to symmetric conjugate points connected to the sine function as follows:

Definition 1.1.

Let $\mathcal{S}^*_{SC}(\sin z)$ denote the class of analytic functions f satisfying the subordination condition:

$$\frac{zf'(z)}{h(z)} \prec \varphi(z), z \in D, \tag{1.3}$$

where $h(z)=\frac{f(z)-\overline{f(-\bar{z})}}{2}$ and $\varphi(z)=1+\sin z$.

It is worth noting that several studies, including those by El-Ashwah and Thomas [6] and Ping and Janteng [18] have investigated subclasses of starlike functions with respect to symmetric conjugate points, particularly using classical subordination conditions such as $\frac{1+z}{1-z}$ or Janowski-type functions, i.e.,

$$\mathcal{S}^*_{SC}=\left\{f\in\mathcal{A}:\mathcal{R}e\left(\frac{zf'(z)}{h(z)}\right)>0\,,z\in D\right\},$$

and

$$\mathcal{S}^*_{SC}[A,B]=\left\{f\in\mathcal{A}:\mathcal{R}e\left(\frac{zf'(z)}{h(z)}\right)\prec\frac{1+Az}{1+Bz}\,,-1\le B<A\le 1\,,z\in D\right\}.$$

However, most of these works have focused on coefficient estimates, geometric properties, or second Hankel determinants. In contrast, this work introduces a distinct subclass $\mathcal{S}^*_{SC}(\sin z)$, defined by subordination associated with the sine function $\varphi(z)=1+\sin z$, and presents a comprehensive study of the logarithmic coefficients γ_1 to γ_6 as well as higher-order Hankel determinants $H_{2,1}(F_f/2)$, $H_{2,2}(F_f/2)$, $H_{2,1}(f), H_{2,2}(f), H_{3,1}(f)$ and $H_{4,1}(f)$ while the general framework aligns with prior literature in geometric function theory, this article distinguishes itself by providing new sharp bounds for both Taylor coefficients up to and logarithmic coefficients, which have received limited attention in previous research. This extension bridges a gap in the literature and contributes to a deeper understanding of analytic behavior in sine-associated subclasses $\mathcal{S}^*_{SC}$ and $\mathcal{S}^*_{SC}[A,B]$.

In 2023, Mohamad et al. [15] introduced the subclass of star-like functions with respect to symmetric conjugate points associated with the sine function. Some coefficient functionals for this class are considered. Bounds of Taylor coefficients, logarithmic coefficients, and the Hankel and Toeplitz determinants whose entries are logarithmic coefficients are provided. Comparison with Mohamad et al. (2023):

1- Main Similarity:

Both articles study a subclass of starlike analytic functions with respect to symmetric conjugate points associated with the sine function. They use a similar subordination condition of the form: $\frac{zf'(z)}{h(z)}\prec\varphi(z), z\in D$.

2- Key Differences: It can be tabulated in the following table (Table 1).

Table 1: Key differences of comparison with Mohamad et al. (2023).

Aspect	Current work	Mohamad *et al.* (2023) [15]
Order of coefficients	Computes Taylor coefficient up to a_7, logarithmic coefficients up to γ_6, and Hankel determinants up to the fourth order for Taylor and second logarithmic coefficients	Mainly deals with lower order, typically up to a_5, logarithmic coefficients up to γ_4, and Hankel determinants up to the second logarithmic coefficients.
Depth of Analysis	Offers a more comprehensive and detailed investigation of higher-order coefficients, including Hankel determinants.	Focuses on a specific class with limited analysis of the coefficient order.
Scientific Contribution	Presents new and original results that extend beyond previous works by including higher-order terms and advanced determinant Analysis	Provides a complementary study within a narrower, symmetry-based framework.

The Fekete-Szegö inequality is a well-known result concerning the coefficients of univalent analytic functions, initially formulated by Fekete and Szegö in 1933 in connection with the Bieberbach conjecture. A related and important problem in the theory of univalent functions is the study of Hankel determinants, which have proven helpful in the investigation of singularities and power series with integral coefficients.

For the functions $f\in\mathcal{A}$ of the form (1.1), in 1976, Noonan and Thomas [16] stated the ℓ^{th} Hankel determinant as

$$H_{\ell,n}(f)=\begin{vmatrix} a_n & a_{n+1} & \cdots & a_{n+\ell-1}\\ a_{n+1} & a_{n+2} & \cdots & a_{n+\ell-2}\\ \vdots & \vdots & \cdots & \vdots\\ a_{n+\ell-1} & a_{n+\ell} & \cdots & a_{n+2(\ell-1)}\end{vmatrix}, \tag{1.4}$$

$(a_1=1\,\ell, n\in N=\{1,2,\cdots.\})$.

In particular, we have

$$H_{2,1}(f)=\begin{vmatrix} a_1 & a_2\\ a_2 & a_3\end{vmatrix}=a_3-{a_2}^2\ (a_1=1, n=1, \ell=2)\,, \tag{1.5}$$

$$H_{2,2}(f)=\begin{vmatrix} a_2 & a_3\\ a_3 & a_4\end{vmatrix}=a_2a_4-{a_3}^2\ (n=2,\ell=2), \tag{1.6}$$

$$H_{3,1}(f)=\begin{vmatrix} a_1 & a_2 & a_3\\ a_2 & a_3 & a_4\\ a_3 & a_4 & a_5\end{vmatrix}=a_3a_5-a_3^3-a_4^2-a_2^2a_5+2a_2a_3a_4$$
$$=a_3H_{2,2}(f)+a_4I+a_5H_{2,1}(f), \tag{1.7}$$

where $I=a_2a_3-a_4$, and

$$H_{4,1}(f)=\begin{vmatrix} a_1 & a_2 & a_3 & a_4\\ a_2 & a_3 & a_4 & a_5\\ a_3 & a_4 & a_5 & a_6\\ a_4 & a_5 & a_6 & a_7\end{vmatrix}$$
$$=-a_4\begin{vmatrix} a_2 & a_3 & a_4\\ a_3 & a_4 & a_5\\ a_4 & a_5 & a_6\end{vmatrix}+a_5\begin{vmatrix} a_1 & a_3 & a_4\\ a_2 & a_4 & a_5\\ a_3 & a_5 & a_6\end{vmatrix}$$
$$-a_6\begin{vmatrix} a_1 & a_2 & a_4\\ a_2 & a_3 & a_5\\ a_3 & a_4 & a_6\end{vmatrix}+a_7\begin{vmatrix} a_1 & a_2 & a_3\\ a_2 & a_3 & a_4\\ a_3 & a_4 & a_5\end{vmatrix}$$
$$=-a_4[a_4(a_3a_5-a_4^2)-a_5(a_2a_5-a_3a_4)+a_6(a_2a_4-{a_3}^2)]$$
$$+a_5[a_3(a_3a_5-a_4^2)-a_5(a_5-a_2a_4)+a_6(a_4-a_2a_3)]$$
$$-a_6[a_3(a_2a_5-a_3a_4)-a_4(a_5-a_2a_4)+a_6(a_3-{a_2}^2)]+a_7H_{3,1}(f)$$
$$=a_7H_{3,1}(f)-a_6\rho_1+a_5\rho_2-a_4\rho_3, \tag{1.8}$$

where $\rho_1=a_3(a_2a_5-a_3a_4)-a_4(a_5-a_2a_4)+a_6(a_3-{a_2}^2)$,

$$\rho_2=a_3(a_3a_5-a_4^2)-a_5(a_5-a_2a_4)+a_6(a_4-a_2a_3),$$

$$\rho_3=a_4(a_3a_5-a_4^2)-a_5(a_2a_5-a_3a_4)+a_6(a_2a_4-{a_3}^2).$$

We note that $H_{2,1}(f)$ is the well-known Fekete-Szegö functional [10], which is generalized as

$$\nabla(\mu,f)=|a_3-\mu{a_2}^2|, \tag{1.9}$$

for $\mu\in\mathbb{C}$.

Recently, the Hankel determinants of a function $f\in\mathcal{A}$ whose elements are logarithmic coefficients of $f\in\mathcal{A}$ have been introduced by Kowalczyk and Lecko [10, 11]

$$H_{\ell,n}(F_f/2)=\begin{vmatrix} \gamma_n & \gamma_{n+1} & \cdots & \gamma_{n+\ell-1}\\ \gamma_{n+1} & \gamma_{n+2} & \cdots & \gamma_{n+\ell-2}\\ \vdots & \vdots & \cdots & \vdots\\ \gamma_{n+\ell-1} & \gamma_{n+\ell} & \cdots & \gamma_{n+2(\ell-1)}\end{vmatrix}.$$

The logarithmic coefficients are defined in the series form

$$\log\frac{f(z)}{z}=2\sum_{n=1}^{\infty}\gamma_nz^n\,. \tag{1.10}$$

Taking both sides and using (1.1) or differentiating (1.10) and using (1.1), we get

$$\gamma_1=\frac{1}{2}a_2\ , \tag{1.11}$$

$$\gamma_2=\frac{1}{2}\left(a_3-\frac{1}{2}a_2^2\right), \tag{1.12}$$

$$\gamma_3=\frac{1}{2}\left(a_4-a_2a_3+\frac{1}{3}a_2^3\right), \tag{1.13}$$

$$\gamma_4=\frac{1}{2}\left(a_5-a_2a_4+a_2^2a_3-\frac{1}{2}a_3^2-\frac{1}{4}a_2^4\right), \tag{1.14}$$

$$\gamma_5=\frac{1}{2}\left(a_6-a_2a_5-a_3a_4+a_2^2a_4+a_2a_3^2-a_3a_2^3+\frac{1}{5}a_2^5\right), \tag{1.15}$$

$$\gamma_6=\frac{1}{2}\left(a_7-a_2a_6-a_3a_5+a_2^2a_5-\frac{3}{2}a_2^2a_3^2-a_4a_2^3-\frac{1}{2}a_4^2+2a_2a_3a_4+\frac{1}{3}a_3^3+a_3a_2^4-\frac{1}{6}a_2^6\right). \tag{1.16}$$

The logarithmic coefficients have great importance; for instance, these coefficients helped Kayumov [8] to solve Brennan's conjecture for conformal mapping, and the estimation of the logarithmic coefficients can be transferred to the Taylor coefficients of univalent functions via the Lebedev–Milin inequalities [4] (for details).

Some recent works on this problem that relate to the theory of univalent functions have been studied in [1, 14, 18], but only a few articles have been published for the class of starlike functions with respect to other points. Motivated by these works, in this article, we obtain the upper bounds of the Taylor coefficients $|a_n|, n=2,3,4,5,6,7$.

In recent years, many articles have been devoted to finding the upper bounds for the second-order Hankel determinant $H_{2,2}$, for various

subclasses of analytic functions and the upper bounds for the third and fourth-order Hankel determinants by many researchers [9,12,17,19,20]. Recently, Cho et al. [3] introduced the following function class $\mathcal{S}_s^*$

$$\mathcal{S}_s^* = \left\{ f \in \mathcal{A}: \frac{zf'(z)}{f(z)} \prec 1 + \sin z, (z \in D) \right\},$$

which implies that the quantity $\frac{zf'(z)}{f(z)}$ lies in an eight-shaped region in the right-half plane. The work investigates a subclass of starlike functions with respect to symmetric conjugate points associated with the sine function. The sine function is a classical transcendental function with rich analytic and geometric properties.

The study extends theoretical knowledge by deriving sharp estimates and properties of higher-order logarithmic coefficients, and by connecting classical functions to complex analysis by associating the sine function with a subclass of starlike functions.

The article opens up new directions for analyzing function classes that are both geometrically meaningful and analytically rich.

Although the study is primarily theoretical, it has potential indirect applications in areas such as:

- Control theory and analytic transforms
- Signal and image analysis
- Complex differential equations
- Approximation theory and numerical analysis

2. Preliminary results

In this section, we give some lemmas to prove our main results.

Lemma 2.1. ([4]) For a function $p \in P$ of the form $p(z) = 1 + \sum_{n=1}^{\infty} c_n z^n, z \in D$

the sharp inequality $|c_n| \leq 2$ holds for each $n \geq 1$ and

$$\left| c_2 - \frac{c_1^2}{2} \right| \leq 2 - \frac{|c_1|^2}{2}.$$

Equality holds for the function $p(z) = \frac{1+z}{1-z}$.

Lemma 2.2. ([5]) Let $p \in P$ of the form $p(z) = 1 + \sum_{n=1}^{\infty} c_n z^n, z \in D$ and $\mu \in \mathbb{C}$. Then

$|c_n - \mu c_k c_{n-k}| \leq 2 \max\{1, |2\mu - 1|\}, 1 \leq k \leq n - 1.$

If $|2\mu - 1| \geq 1$, then the inequality is sharp for the function $p(z) = \frac{1+z}{1-z}$ or its rotations.

If $|2\mu - 1| < 1$, then the inequality is sharp for the function $p(z) = \frac{1+z^n}{1-z^n}$ or its rotations.

Lemma 2.3. ([2]) Let $p \in P$ of the form $p(z) = 1 + \sum_{n=1}^{\infty} c_n z^n, z \in D$ and $\alpha, \beta, \delta \in \mathbb{R}$. Then

$$|\alpha c_1^3 - \beta c_1 + \gamma c_3| \leqslant 2|\alpha| + 2|\beta - 2\alpha| + 2|\alpha - \beta + \delta|.$$

Lemma 2.4. [13] If $p \in P$ of the form $p(z) = 1 + \sum_{n=1}^{\infty} c_n z^n, z \in D$, then $|c_2 - \mu c_1^2| \leq \begin{cases} -4\mu + 2 \ if \ \mu \leq 0 \\ 2 \ if \ 0 \leq \mu \leq 1 \\ 4\mu - 2 \ \text{if} \ \mu \geq 1 \end{cases}$

When $\mu < 0$ or $\mu > 1$, the equality holds if and only if $p(z)$ is $\frac{1+z}{1-z}$ or one of its rotations. If $0 < \mu < 1$, then equality holds if and only if $p(z)$ is $\frac{1+z^2}{1-z^2}$ or one of its rotations. If $\mu = 0$, the equality holds if and only if

$$p(z) = \left(\frac{1}{2} + \frac{1}{2}\lambda\right)\frac{1+z}{1-z} + \left(\frac{1}{2} - \frac{1}{2}\lambda\right)\frac{1-z}{1+z} \ (0 \leq \lambda \leq 1)$$

Or one of its rotations. If $\mu = 1$, the equality holds if and only if p is the reciprocal of one of the functions such that the equality holds in the case of $\mu = 0$.

3. Taylor coefficients and Fekete-Szegö inequality for $f \in \mathcal{S}_{SC}^*(\sin z)$

Theorem 3.1. If f is of the form (1.1) belongs to $\mathcal{S}_{SC}^*(\sin z)$, then

$$|a_2| \leq \frac{1}{2}, |a_3| \leq \frac{1}{2},$$

$$|a_4| \leq \frac{1}{4}, |a_5| \leq \frac{1}{2}$$

$$|a_6| \leq \frac{1009}{1440}, |a_7| \leq \frac{31}{9},$$

and

$$|a_3 - \mu a_2^2| \leq \frac{1}{4}\begin{cases} -4v + 2 \ if \ v \leq 0 \\ 2 \ if \ 0 \leq v \leq 1 \\ 4v - 2 \ \text{if} \ v \geq 1 \end{cases},$$

where $v = \frac{1}{2}\left(1 + \frac{\mu}{2}\right)$.

Proof. Since $f \in \mathcal{S}_{SC}^*(\sin z)$, from the definition of subordination, there exists a Schwarz function w with $w(0) = 0$ and $|w(z)| < 1$, and from (1.3) we have

$$\frac{zf'(z)}{h(z)} = 1 + \sin w(z), z \in D. \tag{3.1}$$

Assuming that

$$p(z) = \frac{1 + w(z)}{1 - w(z)} = 1 + \sum_{n=1}^{\infty} c_n z^n,$$

$$1 + w(z) = p(z)(1 - w(z)) \Rightarrow w(z)(1 + p(z)) = p(z) - 1.$$

This leads to

$$\begin{aligned} w(z) = \frac{p(z)-1}{p(z)+1} &= \frac{c_1 z + c_2 z^2 + c_3 z^3 + c_4 z^4 + \cdots}{2 + c_1 z + c_2 z^2 + c_3 z^3 + c_4 z^4 + \cdots} \\ &= \frac{1}{2}c_1 z + \frac{1}{2}\left(c_2 - \frac{1}{2}{c_1}^2\right) z^2 \\ &+ \frac{1}{2}\left(c_3 - c_1 c_2 + \frac{1}{4}{c_1}^3\right) z^3 \\ &+ \frac{1}{2}\left(c_4 - c_1 c_3 - \frac{1}{2}{c_2}^2 + \frac{3}{4}{c_1}^2 c_2 - \frac{1}{8}{c_1}^4\right) z^4 \\ &+ \frac{1}{2}\left(c_5 - c_1 c_4 - c_2 c_3 - \frac{1}{2}c_2 {c_1}^3 \right. \\ &\left. + \frac{3}{4}{c_2}^2 c_1 + \frac{3}{4}c_3 {c_1}^2 + \frac{1}{16}{c_1}^5\right) z^5 \\ &+ \frac{1}{2}\left(c_6 - c_1 c_5 - c_2 c_4 - \frac{1}{2}{c_3}^2 \right. \\ &+ \frac{3}{2}c_1 c_2 c_3 + \frac{3}{4}c_4 {c_1}^2 + \frac{1}{4}{c_2}^3 - \frac{3}{4}{c_1}^2 {c_2}^2 \\ &\left. + \frac{5}{16}{c_1}^4 c_2 - \frac{1}{32}{c_1}^6\right) z^6 + \cdots. \end{aligned}$$

Hence, from the right-hand side of (3.1), we obtain

$$\begin{aligned} 1 + \sin w(z) &= 1 + w(z) - \frac{(w(z))^3}{3!} + \frac{(w(z))^5}{5!} - \cdots \\ &= 1 + \frac{1}{2}c_1 z + \left(\frac{1}{2}c_2 - \frac{1}{4}{c_1}^2\right) z^2 \\ &+ \left(\frac{5{c_1}^3}{48} - \frac{c_1 c_2}{2} + \frac{c_3}{2}\right) z^3 \\ &+ \left(\frac{c_4}{2} + \frac{5{c_1}^2 c_2}{16} - \frac{{c_2}^2}{4} - \frac{c_1 c_3}{2} - \frac{{c_1}^4}{32}\right) z^4 \\ &+ \left(\frac{c_5 - c_1 c_4 - c_2 c_3}{2} - \frac{1}{8}c_2 {c_1}^3 \right. \\ &\left. + \frac{5{c_2}^2 c_1 + 5c_3 {c_1}^2}{16} + \frac{1}{3840}{c_1}^5\right) z^5 \\ &+ \left(\frac{c_6 - c_1 c_5 - c_2 c_4}{2} - \frac{1}{4}{c_3}^2 + \frac{5}{8}c_1 c_2 c_3 + \frac{5}{48}{c_2}^3 \right. \\ &+ \frac{1}{32}{c_1}^4 c_2 - \frac{1}{8}c_2 {c_1}^3 + \frac{5}{16}{c_1}^2 c_4 - \frac{3}{16}{c_1}^2 {c_2}^2 \\ &\left. + \frac{1}{96}{c_1}^6\right) z^6 + \cdots. \end{aligned}$$

On the other hand, since f of the form (1.1), this gives

$$zf'(z) = z + 2a_2 z^2 + 3a_3 z^3 + 4a_4 z^4 + 5a_5 z^5 + \cdots,$$

and

$$h(z) = \frac{2z + \sum_{n=2}^{\infty}(1 - (-1)^n)a_n z^n}{2} = z + a_3 z^3 + a_5 z^5 + a_7 z^7 + \cdots.$$

Further, we have from (3.1) that

$$zf'(z) = h(z)(1 + \sin w(z)),$$

$$z + 2a_2 z^2 + 3a_3 z^3 + 4a_4 z^4 + 5a_5 z^5 + 6a_6 z^6 + 7a_7 z^7 + \cdots$$

$$= (z + a_3z^3 + a_5z^5 + a_7z^7 + \cdots)$$
$$\cdot\left[1 + \frac{1}{2}c_1z + \left(\frac{1}{2}c_2 - \frac{1}{4}{c_1}^2\right)z^2 + \left(\frac{5{c_1}^3}{48} - \frac{c_1c_2}{2} + \frac{c_3}{2}\right)z^3 + \frac{1}{2}\left(c_4 - c_1c_3 - \frac{1}{2}{c_2}^2 + \frac{5}{8}{c_1}^2c_2 - \frac{1}{16}{c_1}^4\right)z^4 + \left(\frac{c_5 - c_1c_4 - c_2c_3}{2} - \frac{1}{8}c_2{c_1}^3 + \frac{5{c_2}^2c_1 + 5c_3{c_1}^2}{16} + \frac{1}{3840}{c_1}^5\right)z^5 + \left(\frac{c_6 - c_1c_5 - c_2c_4}{2} - \frac{1}{4}{c_3}^2 + \frac{5}{8}c_1c_2c_3 + \frac{5}{48}{c_2}^3 + \frac{1}{32}{c_1}^4c_2 - \frac{1}{8}c_2{c_1}^3 + \frac{5}{16}{c_1}^2c_4 - \frac{3}{16}{c_1}^2{c_2}^2 + \frac{1}{96}{c_1}^6\right)z^6 + \cdots\right]. \quad (3.2)$$

Expanding the series and comparing the coefficients of z^n, n = 1, 2, 3, 4, 5,6,7 on both sides of (3 2) yields

$$2a_2 = \frac{1}{2}c_1 \Rightarrow a_2 = \frac{c_1}{4}, \quad (3.3)$$

$$\frac{c_2}{2} - \frac{{c_1}^2}{4} + a_3 = 3a_3$$

$$\Rightarrow a_3 = \frac{1}{8}(2c_2 - {c_1}^2), \quad (3.4)$$

$$\frac{5{c_1}^3}{48} - \frac{c_1c_2}{2} + \frac{c_3}{2} + \frac{c_1a_3}{2} = 4a_4 \Rightarrow a_4 = \frac{{c_1}^3}{96} - \frac{3c_1c_2}{32} + \frac{c_3}{8}$$

$$\Rightarrow a_4 = \frac{1}{96}({c_1}^3 - 9c_1{c_2} + 12c_3), \quad (3.5)$$

$$a_5 + \frac{c_4}{2} + \frac{5{c_1}^2c_2}{16} - \frac{{c_2}^2}{4} - \frac{c_1c_3}{2} - \frac{{c_1}^4}{32} + a_3\left(\frac{c_2}{2} - \frac{{c_1}^2}{4}\right) = 5a_5$$

$$\Rightarrow a_5 = \frac{c_4}{8} + \frac{3{c_1}^2c_2}{64} - \frac{{c_2}^2}{32} - \frac{c_1c_3}{8}$$

$$\Rightarrow a_5 = \frac{1}{64}(8c_4 + 3{c_1}^2c_2 - 2{c_2}^2 - 8c_1c_3), \quad (3.6)$$

$$6a_6 = \frac{c_5 - c_1c_4 - c_2c_3}{2} - \frac{1}{8}c_2{c_1}^3 + \frac{5{c_2}^2c_1 + 5c_3{c_1}^2}{16} + \frac{1}{3840}{c_1}^5 + a_3\left(\frac{5{c_1}^3}{48} - \frac{c_1c_2}{2} + \frac{c_3}{2}\right) + \frac{1}{2}a_5c_1, \quad (3.7)$$

Substituting (3.4) and (3.6) in (3.7), then we get

$$6a_6 = \frac{1}{2}c_5 - \frac{7}{16}c_1c_4 - \frac{3}{8}c_2c_3 + \frac{3}{16}c_3{c_1}^2 - \frac{5}{384}c_2{c_1}^3 + \frac{11}{64}{c_1}^2c_2 - \frac{49}{3840}{c_1}^5$$

$$\Rightarrow a_6 = \frac{1}{12}c_5 - \frac{7}{96}c_1c_4 - \frac{1}{16}c_2c_3 + \frac{3}{96}c_3{c_1}^2 - \frac{5}{2304}c_2{c_1}^3 + \frac{11}{384}{c_1}^2c_2 - \frac{49}{23040}{c_1}^5$$

$$\Rightarrow a_6 = \frac{1}{23040}(1920c_5 - 1680c_1c_4 - 1440c_2c_3 + 720c_3{c_1}^2 - 50c_2{c_1}^3 + 660{c_2}^2c_1 - 49{c_1}^5)$$
$$= \frac{1}{23040}\left[1920\left(c_5 - \frac{7}{8}c_1c_4\right) - 50c_2\left({c_1}^3 - \frac{66}{5}c_1c_2 + \frac{144}{5}c_3\right) - 720{c_1}^2\left(\frac{49}{720}{c_1}^3 - c_3\right)\right], \quad (3.8)$$

and

$$7a_7 = \frac{c_6 - c_1c_5 - c_2c_4}{2} - \frac{1}{4}{c_3}^2 + \frac{5}{8}c_1c_2c_3 + \frac{5}{48}{c_2}^3 + \frac{1}{32}{c_1}^4c_2 - \frac{1}{8}c_3{c_1}^3 + \frac{5}{16}{c_1}^2c_4 - \frac{3}{16}{c_1}^2{c_2}^2 + \frac{1}{96}{c_1}^6 + a_3\left(\frac{c_4}{2} + \frac{5{c_1}^2c_2}{16} - \frac{{c_2}^2}{4} - \frac{c_1c_3}{2} - \frac{{c_1}^4}{32}\right) + a_5\left(\frac{1}{2}c_2 - \frac{1}{4}{c_1}^2\right) + a_7, \quad (3.9)$$

Substituting (3.4) and (3.6) in (3.9), then we get

$$6a_7 = \frac{c_6 - c_1c_5}{2} - \frac{5}{16}c_2c_4 - \frac{1}{4}{c_3}^2 + \frac{7}{16}c_1c_2c_3 + \frac{5}{192}{c_2}^3 + \frac{113}{256}{c_1}^4c_2 - \frac{1}{32}c_3{c_1}^3 + \frac{7}{32}{c_1}^2c_4 - \frac{3}{64}{c_1}^2{c_2}^2 + \frac{11}{768}{c_1}^6$$

$$\Rightarrow a_7 = \frac{1}{6}\left(\frac{c_6 - c_1c_5}{2} - \frac{5}{16}c_2c_4 - \frac{1}{4}{c_3}^2 + \frac{7}{16}c_1c_2c_3 + \frac{5}{192}{c_2}^3 + \frac{113}{256}{c_1}^4c_2 - \frac{1}{32}c_3{c_1}^3 + \frac{7}{32}{c_1}^2c_4 - \frac{3}{64}{c_1}^2{c_2}^2 + \frac{11}{768}{c_1}^6\right)$$

$$\Rightarrow a_7 = \frac{1}{6}\left[\frac{1}{2}(c_6 - c_1c_5) - \frac{1}{32}c_3(c_1{}^3 - 14c_1c_2 + 8c_3) + \frac{7}{32}{c_1}^2\left(c_4 - \frac{3}{14}{c_2}^2\right) + \frac{113}{256}{c_1}^4\left(c_2 + \frac{11}{339}{c_1}^2\right) - \frac{5}{16}c_2\left(c_4 - \frac{1}{12}{c_2}^2\right)\right]. \quad (3.10)$$

Using triangle inequality and Lemma 2.1 in (3.3), we get

$$|a_2| \le \frac{1}{2}.$$

Now, applying Lemma 2.4 in (3.4) and Lemma 2.3 in (3.5), respectively, implies that

$$|a_3| = \frac{1}{8}|2c_2 - {c_1}^2| = \frac{1}{4}\left|c_2 - \frac{{c_1}^2}{2}\right| \le \frac{1}{2},$$

where $\mu = \frac{1}{2}$.

$$|a_4| = \frac{1}{96}|{c_1}^3 - 9c_1c_2 + 12c_3| \le \frac{1}{96}[2|1| + 2|9 - 2(1)| + 2|1 - 9 + 12|] \le \frac{1}{4},$$

where $\alpha = 1, \beta = 9, \delta = 12$.

Rearranging the terms in (3.6), we can rewrite it as

$$a_5 = \frac{1}{64}\left(8(c_4 - c_1c_3) - 2c_2\left(c_2 - \frac{3}{2}{c_1}^2\right)\right),$$

$$|a_5| = \frac{1}{64}|8(c_4 - w_1c_1c_3) - 2c_2(c_2 - w_2{c_1}^2)|,$$

where $w_1 = 1$ and $w_2 = \frac{3}{2}$.

Consequently, by applying Lemma 2.1, Lemma 2.2, and Lemma 2.4 as well as the triangle inequality, we obtain

$$|a_5| \le \frac{1}{64}\left[8 \cdot 2\max\{1,1\} + 16\right] = \frac{1}{2}.$$

Using triangle inequality and Lemmas 2.1, 2.2, and 2.3 in (3. 8), we get

$$|a_6| \le \frac{1}{23040}\left[1920 \cdot 2\max\left\{1, \left|2 \cdot \frac{7}{8} - 1\right|\right\} + 50 \cdot 2\left(2|1| + 2\left|\frac{66}{5} - 2\right| + 2\left|1 - \frac{66}{5} + \frac{144}{5}\right|\right) + 720 \cdot 4\left(2\left|\frac{49}{720}\right| + 2\left|(-2) \cdot \frac{49}{720}\right| + 2\left|\frac{49}{720} - 1\right|\right)\right]$$
$$= \frac{1}{23040}\left[3840 + 100\left(2 + \frac{112}{5} + \frac{166}{5}\right) + 2880\left(\frac{49}{360} + \frac{49}{180} + \frac{671}{360}\right)\right]$$
$$= \frac{1}{23040}(3840 + 5760 + 6544) = \frac{16144}{23040} = \frac{1009}{1440},$$

where $\mu = \frac{7}{8}, \alpha_1 = 1, \beta_1 = \frac{66}{5}, \delta_1 = \frac{144}{5}, \alpha_2 = \frac{49}{720}, \beta_2 = 0, \delta_2 = -1.$

Using triangle inequality and Lemma 2.1, Lemma 2.2, Lemma 2.3, and Lemma 2.4 in (3. 10), we get

$$|a_7| \le \frac{1}{6}\left[\frac{1}{2}(2) + \frac{1}{32} \cdot 2(2 + 2|14 - 2| + 2|1 - 14 + 8|) + \frac{7}{32} \cdot 4 \cdot 2\max\left\{1, \left|2 \cdot \frac{3}{14} - 1\right|\right\} + \frac{113}{256} \cdot 16 \cdot 2\max\left\{1, \left|2\left(-\frac{11}{339}\right) - 1\right|\right\} + \frac{5}{16} \cdot 2\max\left\{1, \left|2 \cdot \frac{1}{12} - 1\right|\right\}\right]$$
$$= \frac{1}{6}\left(1 + \frac{9}{4} + \frac{7}{4} + \frac{5}{8} + \frac{361}{24}\right) = \frac{496}{144} = \frac{31}{9},$$

where $\mu_1 = 1, \alpha_1 = 1, \beta_1 = 14, \delta_1 = 8, \mu_2 = \frac{3}{14}, \mu_3 = -\frac{11}{339}, \mu_4 = \frac{1}{12}.$

$$a_3 - \mu a_2^2 = \frac{1}{8}(2c_2 - {c_1}^2) - \mu\frac{{c_1}^2}{16} = \frac{1}{4}\left\{c_2 - \frac{1}{2}\left(1 + \frac{\mu}{2}\right){c_1}^2\right\},$$

where $v = \frac{1}{2}\left(1 + \frac{\mu}{2}\right)$.

Using Lemma 2.4, we get

$$|a_3 - \mu a_2^2| \le \frac{1}{4}\begin{cases} -4v + 2 \ if \ v \le 0 \\ 2 \ if \ 0 \le v \le 1 \\ 4v - 2 \ \text{if} \ v \ge 1 \end{cases}.$$

This completes the proof of Theorem 3.1.

4. Hankel determinant for the Logarithmic coefficients of $f \in \mathcal{S}^*_{SC}(\sin z)$

Theorem 4.1. If f is of the form (1.1) belongs to $\mathcal{S}^*_{SC}(\sin z)$, then

$$|\gamma_1| \le \frac{1}{4}\ , |\gamma_2| \le \frac{1}{4}\ , |\gamma_3| \le \frac{1}{8}\ ,$$
$$|\gamma_4| \le \frac{7}{16}\ , |\gamma_5| \le \frac{9937}{5760}\ , |\gamma_6| \le \frac{23}{9}.$$

Proof. Putting (3.3) - (3.6) in (1.11) - (1.14), we obtain

$$\gamma_1 = \frac{a_2}{2} = \frac{c_1}{8}, \tag{4.1}$$

$$\gamma_2 = \frac{1}{2}\left(a_3 - \frac{1}{2}{a_2}^2\right) = \frac{1}{2}\left[\frac{1}{8}(2c_2 - {c_1}^2) - \frac{1}{2}\left(\frac{c_1}{4}\right)^2\right] = \frac{1}{2}\left(\frac{c_2}{4} - \frac{5{c_1}^2}{32}\right)$$
$$= \frac{1}{8}\left(c_2 - \frac{5}{8}{c_1}^2\right), \tag{4.2}$$

$$\begin{aligned}\gamma_3 = \frac{1}{2}\left(a_4 - a_2a_3 + \frac{1}{3}{a_2}^3\right) &= \frac{1}{2}\left[\frac{1}{96}({c_1}^3 - 9c_{\ 2} + 12c_3) - \left(\frac{c_1}{4}\right)\left(\frac{1}{8}(2c_2 - {c_1}^2)\right)\right.\\ &\left. + \frac{1}{3}\left(\frac{c_1}{4}\right)^3\right]\\ &= \frac{1}{2}\left(\frac{{c_1}^3}{96} - \frac{3c_1c_2}{32} + \frac{c_3}{8} - \frac{c_1c_2}{16} + \frac{{c_1}^3}{32} + \frac{{c_1}^3}{192}\right)\\ &= \frac{1}{2}\left(\frac{3{c_1}^3}{64} - \frac{5c_1c_2}{32} + \frac{c_3}{8}\right) = \frac{3{c_1}^3}{128} - \frac{5c_1c_2}{64} + \frac{c_3}{16}\\ &= \frac{1}{128}(3{c_1}^3 - 10c_1c_2 + 8c_3),\end{aligned} \tag{4.3}$$

$$\begin{aligned}\gamma_4 = \frac{1}{2}\left[\frac{1}{64}\right.&(8c_4 + 3{c_1}^2c_2 - 2{c_2}^2 - 8c_1c_3) - \frac{c_1}{4}\left(\frac{1}{96}({c_1}^3 - 9c_1c_2 + 12c_3)\right)\\ &+ \left(\frac{c_1}{4}\right)^2\left(\frac{1}{8}(2c_2 - {c_1}^2)\right) - \frac{1}{2}\left(\frac{1}{8}(2c_2 - {c_1}^2)\right)^2\\ &\left. - \frac{1}{4}\left(\frac{c_1}{4}\right)^4\right]\end{aligned}$$
$$= \frac{1}{2}\left(\frac{11{c_1}^2c_2}{128} + \frac{c_4}{8} - \frac{{c_{\ 2}}^2}{32} - \frac{5c_1c_3}{32} - \frac{4{c_1}^4}{384} - \frac{{c_1}^4}{1024} - \frac{{c_2}^2}{32} + \frac{{c_1}^2c_2}{32} - \frac{{c_1}^4}{128}\right)$$
$$\begin{aligned}&= \frac{c_4}{16} + \frac{15{c_1}^2c_2}{256} - \frac{{c_2}^2}{32} - \frac{5c_1c_3}{64} - \frac{59{c_1}^4}{6144}\\ &= \frac{1}{6144}(384c_4 - 192{c_2}^2 - 480c_1c_3 + 360{c_1}^2c_2\\ &\quad - 59{c_1}^4),\end{aligned} \tag{4.4}$$

$$\begin{aligned}\gamma_5 = \frac{1}{2}\left(a_6 - a_2a_5 - a_3a_4 + a_2^2a_4 + a_2a_3^2 - a_3a_2^3 + \frac{1}{5}a_2^5\right)&\\ = \frac{1}{2}\left[\frac{1}{23040}\right.&(1920c_5 - 1680c_1c_4 - 1440c_2c_3\\ &+ 720c_3{c_1}^2 - 50c_2{c_1}^3 + 660{c_2}^2c_1 - 49{c_1}^5)\\ &- \frac{1}{256}(8c_1c_4 + 3{c_1}^3c_2 - 2c_1{c_2}^2 - 8{c_1}^2c_3)\\ &- \frac{1}{768}(2{c_1}^3c_2 - 18{c_2}^2c_1 + 24c_2c_3 - {c_1}^5 + 9{c_1}^3c_2\\ &- 24c_3{c_1}^2) + \frac{1}{1536}({c_1}^5 - 9{c_1}^3c_2 + 12c_3{c_1}^2)\\ &+ \frac{1}{256}(4{c_2}^2c_1 + {c_1}^5 - 4{c_1}^3c_2)\\ &\left. - \frac{1}{512}(2{c_1}^3c_2 - {c_1}^5) + \frac{1}{5120}{c_1}^5\right]\end{aligned}$$
$$\begin{aligned}&= \frac{1}{2}\left(\frac{1}{12}c_5 - \frac{13}{32}c_1c_4 - \frac{19}{96}c_2c_3 + \frac{47}{640}c_3{c_1}^2 - \frac{33}{512}c_2{c_1}^3 + \frac{41}{640}{c_2}^2c_1\right.\\ &\quad \left. - \frac{271}{46080}{c_1}^5\right)\\ &= \frac{1}{2}\left[\frac{1}{12}\left(c_5 - \frac{39}{8}c_1c_4\right) - \frac{33}{512}c_2\left({c_1}^3 - \frac{164}{165}c_1c_2 + \frac{304}{99}c_3\right)\right.\\ &\quad \left. - \frac{271}{46080}{c_1}^2\left({c_1}^3 - \frac{3384}{271}c_3\right)\right],\end{aligned} \tag{4.5}$$

$$\begin{aligned}\gamma_6 = \frac{1}{2}\Big(a_7 - a_2a_6 - a_3a_5 + a_2^2a_5 - \frac{3}{2}a_2^2a_3^2&\\ - a_4a_2^3 - \frac{1}{2}a_4^2 + 2a_2a_3a_4 + \frac{1}{3}a_3^3 + a_3a_2^4 - \frac{1}{6}a_2^6\Big)&\\ = \frac{1}{2}\Big[\frac{1}{6}\Big(\frac{c_6 - c_1c_5}{2} - \frac{5}{16}c_2c_4 - \frac{1}{4}{c_3}^2 + \frac{7}{16}c_1c_2\,c_3&\\ + \frac{5}{192}{c_2}^3&\\ + \frac{113}{256}{c_1}^4c_2 - \frac{1}{32}c_3{c_1}^3 + \frac{7}{32}{c_1}^2c_4 - \frac{3}{64}{c_1}^2{c_2}^2&\\ + \frac{11}{768}{c_1}^6\Big)&\\ - \frac{1}{92160}(1920c_1c_5 - 1680{c_1}^2c_4 - 1440c_1c_2c_3&\\ + 720c_3{c_1}^3 - 50c_2{c_1}^4 + 660{c_2}^2{c_1}^2 - 49{c_1}^6)&\\ - \frac{1}{512}(16c_2c_4 + 8{c_1}^2{c_2}^2 - 4{c_2}^3 - 16c_1c_2\,c_3&\\ - 8{c_1}^2c_4 - 3{c_1}^4c_2 + 8c_3{c_1}^3)&\\ + \frac{1}{1024}\Big(8c_4{c_1}^2 + 3{c_1}^4c_2 - 2{c_1}^2{c_2}^2 - 8{c_1}^3c_3\Big)&\\ - \frac{3}{2048}(4{c_1}^2{c_2}^2 + {c_1}^6 - 4{c_1}^4c_2)&\\ - \frac{1}{6144}\,({c_1}^6 - 9{c_1}^4c_2 + 12c_3{c_1}^3)&\\ - \frac{1}{18432}\Big({c_1}^6 + 144{c_3}^2 + 81{c_1}^2{c_2}^2 - 216c_1c_2\,c_3&\\ + 24c_3{c_1}^3 - 18{c_1}^4c_2\Big)&\\ + \frac{1}{1536}\Big(11{c_1}^4c_2 + 24c_1c_2\,c_3 - 18{c_1}^2{c_2}^2 - {c_1}^6&\\ - 12c_3{c_1}^3\Big)&\\ + \frac{1}{1536}\Big(8{c_2}^3 - 12{c_1}^2{c_2}^2 + 6{c_1}^4c_2 - {c_1}^6\Big)&\\ + \frac{1}{2048}(2{c_1}^4c_2 - {c_1}^6) - \frac{1}{24576}{c_1}^6\Big]&\end{aligned}$$
$$\begin{aligned}= \frac{1}{2}\Big(\frac{1}{12}c_6 - \frac{5}{48}c_1c_5 - \frac{1}{12}c_2c_4 + \frac{113}{768}c_1c_2\,c_3 + \frac{5}{288}{c_2}^3 - \frac{19}{384}{c_3}^2&\\ + \frac{1903}{18432}{c_1}^4c_2 - \frac{73}{1536}c_3{c_1}^3 + \frac{5}{64}{c_1}^2c_4&\\ - \frac{383}{6144}{c_1}^2{c_2}^2 + \frac{107}{122880}{c_1}^6\Big)&\\ = \frac{1}{2}\Big[\frac{1}{12}\Big(c_6 - \frac{5}{4}c_1c_5\Big) - \frac{73}{1536}c_3\Big({c_1}^3 - \frac{226}{73}\,c_1c_2 + \frac{76}{73}c_3\Big)&\\ + \frac{5}{64}{c_1}^2\Big(c_4 - \frac{383}{480}{c_2}^2\Big)&\\ + \frac{1903}{18432}{c_1}^4\Big(c_2 + \frac{321}{38060}{c_1}^2\Big)&\\ - \frac{1}{12}c_2\Big(c_4 - \frac{5}{24}{c_2}^2\Big)\Big].&\end{aligned} \tag{4.6}$$

The bounds of $|\gamma_1|$, $|\gamma_2|$, $|\gamma_3|$, $|\gamma_4|$, $|\gamma_5|$ *and* $|\gamma_6|$ follow from Lemma 2.1, Lemma 2.2, Lemma 2.3, and Lemma 2.4. On the other hand, rearranging the terms in (4.1), (4.2), (4.3), (4.4), (4.5), and (4.6) we get

$$|\gamma_1| = \left|\frac{c_1}{8}\right| \le \frac{2}{8} = \frac{1}{4},$$

$$|\gamma_2| = \frac{1}{8}\left|c_{\ 2} - \frac{5}{8}{c_1}^2\right| \le \frac{1}{8}\cdot 2 = \frac{1}{4},$$

where $\mu = \frac{5}{8}$.

$$|\gamma_3| = \frac{1}{128}|3{c_1}^3 - 10c_1c_2 + 8c_{\ 3}|$$
$$\le \frac{1}{128}[2|3| + 2|10 - 6| + 2|3 - 10 + 8|] = \frac{16}{128} = \frac{1}{8},$$

where $\alpha = 3, \beta = 10\ , \delta = 8$.

$$|\gamma_4| = \frac{1}{6144}|384c_4 - 192{c_2}^2 - 480c_1c_3 + 360{c_1}^2c_2 - 59{c_1}^4|$$
$$= \frac{1}{6144}\left|384\left(c_4 - \frac{1}{2}{c_2}^2\right) - c_1(480c_{\ 3} - 360c_1c_{\ 2} + 59c_{\ 1}^{\ 3})\right|$$
$$\begin{aligned}\le \frac{1}{6144}\Big[384\cdot 2\max\Big\{1, \Big|2\left(\frac{1}{2}\right) - 1\Big|\Big\}&\\ + 2(2|59| + 2|360 - 2(59)|&\\ + 2|59 - 360 + 480|)\Big] = \frac{1}{6144}(768 + 1920)&\\ = \frac{2688}{6144} = \frac{7}{16}\ ,&\end{aligned}$$

where $\mu = \frac{1}{2}\ , \alpha = 59, \beta = 360\ , \delta = 480$.

$$\begin{aligned}|\gamma_5| = \frac{1}{2}\Big|\Big[\frac{1}{12}\Big(c_5 - \frac{39}{8}c_1c_4\Big) - \frac{33}{512}c_2\Big({c_1}^3 - \frac{164}{165}\,c_1c_2 + \frac{304}{99}c_3\Big)&\\ - \frac{271}{46080}{c_1}^2\Big({c_1}^3 - \frac{3384}{271}c_3\Big)\Big]\Big|&\end{aligned}$$

$$\leq \frac{1}{2}\left[\frac{1}{12}\cdot 2\max\left\{1,\left|2\left(\frac{39}{8}\right)-1\right|\right\}+2\cdot\frac{33}{512}\left(2|1|+2\left|\frac{164}{165}-2(1)\right|+2\left|1-\frac{164}{165}+\frac{304}{99}\right|\right)+\frac{73}{15360}\cdot 4\left(2|1|+2|0-2(1)|+2\left|1-0-\frac{3384}{271}\right|\right)\right]$$

$$=\frac{1}{2}\left[\frac{1}{6}\cdot\frac{35}{4}+\frac{33}{256}\left(2+\frac{332}{165}+\frac{3046}{495}\right)+\frac{271}{11520}\left(2+4+\frac{6226}{271}\right)\right]$$

$$=\frac{1}{2}\left(\frac{35}{24}+\frac{33}{256}\cdot\frac{5032}{495}+\frac{271}{11520}\cdot\frac{7852}{271}\right)=\frac{1}{2}\left(\frac{35}{24}+\frac{629}{480}+\frac{1963}{2880}\right)=\frac{1}{2}\cdot\frac{9937}{2880}=\frac{9937}{5760},$$

where $\mu=\frac{39}{8}$, $\alpha_1=1,\beta_1=\frac{164}{165}$, $\delta_1=\frac{304}{99}$, $\alpha_2=1,\beta_2=0$, $\delta_2=-\frac{3384}{271}$.

$$|\gamma_6|=\frac{1}{2}\left|\left[\frac{1}{12}\left(c_6-\frac{5}{4}c_1c_5\right)-\frac{73}{1536}c_3\left({c_1}^3-\frac{226}{73}c_1c_2+\frac{76}{73}c_3\right)+\frac{5}{64}{c_1}^2\left(c_4-\frac{383}{480}{c_2}^2\right)+\frac{1903}{18432}{c_1}^4\left(c_2+\frac{321}{38060}{c_1}^2\right)-\frac{1}{12}c_2\left(c_4-\frac{5}{24}{c_2}^2\right)\right]\right|$$

$$\leq \frac{1}{2}\left[\frac{1}{12}\cdot 2\max\left\{1,\left|2\left(\frac{5}{4}\right)-1\right|\right\}+2\cdot\frac{73}{1536}\left(2|1|+2\left|\frac{226}{73}-2(1)\right|+2\left|1-\frac{226}{73}+\frac{76}{73}\right|\right)+\frac{5}{64}\cdot 4\cdot 2\max\left\{1,\left|2\left(\frac{383}{480}\right)-1\right|\right\}+\frac{1903}{18432}\cdot 16\cdot 2\max\left\{1,\left|2\left(\frac{-321}{38060}\right)-1\right|\right\}+\frac{1}{12}\cdot 2\cdot 2\max\left\{1,\left|2\left(\frac{5}{24}\right)-1\right|\right\}\right]$$

$$=\frac{1}{2}\left[\frac{1}{4}+\frac{73}{768}\left(2+\frac{160}{73}+\frac{154}{73}\right)+\frac{5}{8}+\frac{1903}{576}+\frac{1}{3}\right]=\frac{1}{2}\left[\frac{1}{4}+\frac{460}{768}+\frac{5}{8}+\frac{1903}{576}+\frac{1}{3}\right]=\frac{1}{2}\cdot\frac{46}{9}=\frac{23}{9},$$

where $\mu_1=\frac{5}{4}$, $\alpha_1=1,\beta_1=\frac{226}{73}$, $\delta_1=\frac{76}{73}$, $\mu_2=\frac{383}{480}$, $\mu_3=\frac{-321}{38060}$, $\mu_4=\frac{5}{24}$.

Theorem 4.2. If f is of the form (1.1) belongs to $\mathcal{S}_{SC}^{*}(\sin z)$, then

$$\left|H_{2,1}(F_f/2)\right|\leq\frac{75}{512}.$$

Proof: In view of (4.1), (4.2), (4.3), we have

$$H_{2,1}(F_f/2)=\gamma_1\gamma_3-{\gamma_2}^2=\frac{c_1}{8}\left(\frac{1}{128}(3{c_1}^3-10c_1c_2+8c_3)\right)-\left(\frac{1}{8}\left(c_2-\frac{5}{8}{c_1}^2\right)\right)^2$$

$$=\frac{1}{64}\left(\frac{3}{16}{c_1}^4-\frac{10}{16}{c_1}^2c_2+\frac{1}{2}c_1c_3-{c_2}^2+\frac{5}{4}{c_1}^2c_2-\frac{25}{64}{c_1}^4\right)$$

$$=\frac{1}{4096}(-13{c_1}^4+40{c_1}^2c_2+32c_1c_3-64{c_2}^2).\qquad(4.7)$$

Rearranging the terms in (4.7), it becomes

$$\gamma_1\gamma_3-{\gamma_2}^2=\frac{1}{4096}(-c_1(13{c_1}^3-40c_1\,c_2-32c_3)-64{c_2}^2),$$

where $\chi=13,\lambda=40$, and $\eta=-32$.

By applying the triangle inequality as well as Lemma 2.1 and Lemma 2.3, we get the desired inequality.

$$\left|\gamma_1\gamma_3-{\gamma_2}^2\right|\leq\frac{1}{4096}\left([2(2|13|+2|40-26|+2|13-40-32|)]+64(4)\right)$$

$$=\frac{1}{4096}\left(2(172)+64(4)\right)=\frac{600}{4096}\leq\frac{75}{512}.$$

Theorem 4.3. If f is of the form (1.1) belongs to $\mathcal{S}_{SC}^{*}(\sin z)$, then

$$\left|H_{2,2}(F_f/2)\right|\leq\frac{33}{256}.$$

Proof: In view of (4.2), (4.3), (4.4), we have

$$H_{2,2}(F_f/2)=\gamma_2\gamma_4-{\gamma_3}^2$$

$$=\left(\frac{1}{8}\left(c_2-\frac{5}{8}{c_1}^2\right)\right)\left(\frac{1}{6144}(384c_4-192{c_2}^2-480c_1c_3+360{c_1}^2c_2-59{c_1}^4)\right)-\left(\frac{1}{128}(3{c_1}^3-10c_1c_2+8c_3)\right)^2$$

$$=\frac{1}{49152}\left[\left(384c_4c_2-192{c_2}^3-480c_1c_2c_3+480{c_1}^2{c_2}^2-284{c_1}^4c_2-240{c_1}^2c_4+300{c_1}^3c_3+\frac{295}{8}{c_1}^6\right)-\frac{1}{16384}(9{c_1}^6-60{c_1}^4c_2+100{c_1}^2{c_2}^2+64{c_3}^2+48{c_1}^3c_3-160c_1c_2c_3)\right]$$

$$=\frac{1}{128}c_4c_2-\frac{1}{256}{c_2}^3+\frac{15}{4096}{c_1}^2{c_2}^2-\frac{13}{6144}{c_1}^4c_2-\frac{5}{1024}{c_1}^2c_4+\frac{13}{4096}{c_1}^3c_3+\frac{79}{393216}{c_1}^6-\frac{1}{256}{c_3}^2$$

$$=\left[\frac{1}{128}c_4\left(c_2-\frac{5}{8}{c_1}^2\right)-\frac{1}{256}{c_2}^2\left(c_2-\frac{15}{16}{c_1}^2\right)+\frac{79}{393216}{c_1}^3\left({c_1}^3-\frac{832}{79}c_1\,c_2+\frac{1248}{79}c_3\right)-\frac{1}{256}{c_3}^2\right],$$

$$\left|H_{2,2}(F_f/2)\right|\leq\frac{1}{128}\cdot 4+\frac{1}{256}\cdot 8+\frac{79}{393216}\cdot 8\left(2|1|+2\left|\frac{832}{79}-2(1)\right|+2\left|1-\frac{832}{79}+\frac{1248}{79}\right|\right)+\frac{1}{256}\cdot 4$$

$$=\frac{1}{16}+\frac{13}{256}+\frac{1}{64}=\frac{33}{256}.$$

5. Hankel determinant for the Taylor coefficients of $f\in\mathcal{S}_{SC}^{*}(\sin z)$

Corollary 5.1. If f is of the form (1.1) belongs to $\mathcal{S}_{SC}^{*}(\sin z)$, then

$$\left|H_{2,1}(f)\right|\leq\frac{1}{2}$$

Proof:

Putting $\mu=1$ In Theorem 3.1, we obtain

$$\left|H_{2,1}(f)\right|=|a_3-a_2^2|\leq\frac{1}{4}\cdot 2=\frac{1}{2},$$

where $v=\frac{1}{2}\left(1+\frac{1}{2}\right)=\frac{3}{4}$, $0<\frac{3}{4}<1$.

Theorem 5.2. If f is of the form (1.1) belongs to $\mathcal{S}_{SC}^{*}(\sin z)$, then

$$\left|H_{3,1}(f)\right|\leq\frac{29}{48}.$$

***Proof*:** In view of (3.3), (3.4), (3.5), we have

$$H_{2,2}(f)=a_2a_4-{a_3}^2=-\frac{5}{384}{c_1}^4+\frac{1}{32}c_1\,c_3+\frac{1}{128}{c_1}^2c_2-\frac{1}{16}{c_2}^2$$

$$=-\frac{5}{384}c_1\left({c_1}^3-\frac{3}{5}c_1\,c_2-\frac{12}{5}c_3\right)-\frac{1}{16}{c_2}^2.$$

Using the triangle inequality and Lemmas 2.1 and 2.3, we obtain

$$\left|H_{2,2}(f)\right|\leq\frac{5}{384}\cdot 2\left(2|1|+2\left|\frac{3}{5}-2(1)\right|+2\left|1-\frac{3}{5}-\frac{12}{5}\right|\right)+\frac{1}{16}\cdot 4$$

$$=\frac{11}{48}+\frac{1}{4}=\frac{23}{48}.\qquad(5.1)$$

$$|a_4-a_2a_3|=\frac{1}{24}\left|{c_1}^3-\frac{3}{4}c_1\,c_2+3c_3\right|\leq\frac{1}{24}\left(2|1|+2\left|\frac{3}{4}-2(1)\right|+2\left|1-\frac{3}{4}+3\right|\right)=\frac{11}{24}\qquad(5.2)$$

Using the triangle inequality, Theorem 4.3, Corollary 5.1, and (5.1), (5.2), we obtain

$$\left|H_{3,1}(f)\right|\leq|a_3|\left|H_{2,2}(f)\right|+|a_4||a_4-a_2a_3|+|a_5|\left|H_{2,1}(f)\right|$$

$$\leq\frac{1}{2}\cdot\frac{23}{48}+\frac{1}{4}\cdot\frac{11}{24}+\frac{1}{2}\cdot\frac{1}{2}=\frac{29}{48}.$$

Theorem 5.3. If f is of the form (1.1) belongs to $\mathcal{S}_{SC}^{*}(\sin z)$, then

$$\left|H_{4,1}(f)\right|\leq\frac{26759147}{8294400}.$$

***Proof*:** From (1.8) and using the triangle inequality, we obtain

$|H_{4,1}(f)| \le |a_7||H_{3,1}(f)| + |a_6||\rho_1| + |a_5||\rho_2| + |a_4||\rho_3|$.

We must find ρ_1, ρ_2 and ρ_3.

From (3.3), (3.4), (3.5), and (3.6) we will find $\rho_1$as follows:

i. $a_2a_5 - a_3a_4 = \frac{1}{256}c_1c_4 - \frac{1}{384}{c_1}^3c_2 + \frac{1}{64}{c_2}^2c_1 - \frac{1}{64}{c_1}^2c_3 - \frac{1}{32}c_2c_3 + \frac{1}{768}{c_1}^5$

$= \frac{1}{256}c_1(c_4 - 4c_1\,c_3) - \frac{1}{384}c_2({c_1}^3 - 6c_1\,c_2 + 12c_3) + \frac{1}{768}{c_1}^5$.

Using the triangle inequality and Lemmas 2.1, 2.2, and 2.3, we obtain

$$|a_2a_5 - a_3a_4| \le \frac{1}{256}\cdot 2\cdot 2\cdot 7 + \frac{1}{384}\cdot 2(2|1| + 2|6 - 2(1)| + 2|1 - 6 + 12|) + \frac{1}{768}\cdot 32$$
$$= \frac{7}{64} + \frac{1}{192}(2 + 8 + 14) + \frac{1}{24} = \frac{7}{64} + \frac{1}{8} + \frac{1}{24}$$
$$= \frac{53}{192}. \quad (5.3)$$

ii. $a_5 - a_2a_4 = \frac{1}{8}c_4 + \frac{9}{128}{c_1}^2c_2 - \frac{1}{32}{c_2}^2 - \frac{5}{32}c_1\,c_3 - \frac{1}{384}{c_1}^4$

$= -\frac{1}{384}c_1({c_1}^3 - 27c_1\,c_2 + 60c_3) + \frac{1}{8}\left(c_4 - \frac{1}{4}{c_2}^2\right)$

Using the triangle inequality and Lemmas 2.1, 2.2, and 2.3, we obtain

$$|a_5 - a_2a_4| \le \frac{1}{384}\cdot 2(2|1| + 2|27 - 2(1)| + 2|1 - 27 + 60|) + \frac{1}{8}\cdot 2$$
$$= \frac{1}{192}(2 + 50 + 68) + \frac{1}{4} = \frac{5}{8} + \frac{1}{4} = \frac{7}{8}. \quad (5.4)$$

From (3.3), (3.4), (3.5), and (3.6), we will find ρ_2.

$$a_3a_5 - a_4^2 = \frac{1}{32}c_2c_4 + \frac{7}{1024}{c_1}^2{c_2}^2 - \frac{1}{128}{c_2}^3 - \frac{1}{128}c_1\,c_2c_3 - \frac{1}{64}{c_1}^2c_4 - \frac{1}{256}{c_1}^4c_2 + \frac{5}{384}{c_1}^3c_3 - \frac{1}{9216}{c_1}^6 - \frac{1}{64}{c_3}^2$$
$$= \frac{1}{32}c_4\left(c_2 - \frac{1}{2}{c_1}^2\right) - \frac{1}{128}{c_2}^2\left(c_2 - \frac{7}{8}{c_1}^2\right) + \frac{5}{384}c_3\left({c_1}^3 - \frac{3}{5}c_1\,c_2 - \frac{6}{5}c_3\right) - \frac{1}{256}{c_1}^4\left(c_2 + \frac{1}{36}{c_1}^2\right).$$

Using the triangle inequality and Lemmas 2.1, 2.3, and 2.4, we obtain

$$|a_3a_5 - a_4^2| \le \frac{1}{32}\cdot 2\cdot 2 + \frac{1}{128}\cdot 4\cdot 2 + \frac{5}{384}\cdot 2\left(2|1| + 2\left|\frac{3}{5} - 2(1)\right| + 2\left|1 - \frac{3}{5} - \frac{6}{5}\right|\right) + \frac{1}{256}\cdot 16\cdot\frac{19}{9} = \frac{1}{8} + \frac{1}{16} + \frac{5}{192}\left(2 + \frac{22}{5}\right) + \frac{19}{144} = \frac{1}{8} + \frac{1}{16} + \frac{1}{6} + \frac{19}{144}$$
$$= \frac{35}{72}. \quad (5.5)$$

Using the triangle inequality and Theorem 3.1, Corollary 5.1, (5.3) and (5.4), then

$$|\rho_1| = |a_3(a_2a_5 - a_3a_4) - a_4(a_5 - a_2a_4) + a_6(a_3 - {a_2}^2)| \le |a_3||a_2a_5 - a_3a_4| + |a_4||a_5 - a_2a_4| + |a_6||H_{2,1}(f)| \le \frac{1}{2}\cdot\frac{53}{192} + \frac{1}{4}\cdot\frac{7}{8} + \frac{1009}{1440}\cdot\frac{1}{2}$$
$$= \frac{53}{384} + \frac{7}{32} + \frac{1009}{2880} = \frac{4073}{5760}. \quad (5.6)$$

Using the triangle inequality and Theorem 3.1, (5.2), (5.4), and (5.5), then

$$|\rho_2| = |a_3(a_3a_5 - a_4^2) - a_5(a_5 - a_2a_4) + a_6(a_4 - a_2a_3)| \le |a_3||a_3a_5 - a_4^2| + |a_5||a_5 - a_2a_4| + |a_6||a_4 - a_2a_3| \le \frac{1}{2}\cdot\frac{35}{72} + \frac{1}{2}\cdot\frac{7}{8} + \frac{1009}{1440}\cdot\frac{11}{24}$$
$$= \frac{35}{144} + \frac{7}{16} + \frac{11099}{34560} = \frac{34619}{34560}. \quad (5.7)$$

Using the triangle inequality and Theorem 3.1, (5.1), (5.3), and (5.5), then

$$|\rho_3| = |a_4(a_3a_5 - a_4^2) - a_5(a_2a_5 - a_3a_4) + a_6(a_2a_4 - {a_3}^2)| \le |a_4||a_3a_5 - a_4^2| + |a_5||a_2a_5 - a_3a_4| + |a_6||a_2a_4 - {a_3}^2| \le \frac{1}{4}\cdot\frac{35}{72} + \frac{1}{2}\cdot\frac{53}{192} + \frac{1009}{1440}\cdot\frac{23}{48}$$
$$= \frac{35}{288} + \frac{53}{384} + \frac{23207}{69120} = \frac{41147}{69120}. \quad (5.8)$$

Using Theorem 3.1, (5.6), (5.7), and (5.8), we obtain

$$|H_{4,1}(f)| \le |a_7||H_{3,1}(f)| + |a_6||\rho_1| + |a_5||\rho_2| + |a_4||\rho_3| \le \frac{31}{9}\cdot\frac{29}{48} + \frac{1009}{1440}\cdot\frac{4073}{5760} + \frac{1}{2}\cdot\frac{34619}{34560} + \frac{1}{4}\cdot\frac{41147}{69120}$$
$$= \frac{899}{432} + \frac{4109657}{8294400} + \frac{34619}{69120} + \frac{41147}{276480}$$
$$= \frac{26759147}{8294400}.$$

6. Conclusion

Several previous studies inspired this study. In this article, we have obtained the upper bounds of some coefficient problems for functions in the class $\mathcal{S}_{SC}^{*}(\sin z)$ including Taylor coefficients, logarithmic coefficients, and Hankel determinants of logarithmic coefficients. The results presented in this article may be the subject of further research on higher-order Hankel determinants of logarithmic coefficients and other coefficient problems, for instance, the Fekete-Szegö functional. Additionally, for another particular value of φ, several other classes of functions that are starlike with respect to symmetric conjugate points can also be studied.

Funding

This research received no specific grant from any funding agency in the public, commercial, or not-for-profit sectors.

Conflict of Interest

The authors declare that there are no conflicts of interest.

References

[1] Allu, V., Arora, V., Shaji, A. (2023) On the second Hankel determinant of logarithmic coefficients for certain univalent functions, *Mediterranean Journal of Mathematics* **20**: 81.

[2] Arif, M., Raza, M., Tang, H., Hussain, S., Khan, H. (2019) Hankel determinant of order three for familiar subsets of analytic functions related with sine function, *Open Mathematics* **17**: 1615-1630.

[3] Cho, N., Kumar, V., Kumar, S.S., Ravichandran, V. (2019) Radius problems for starlike functions associated with the sine function, *Bulletin of the Iranian Mathematical Society* **45**: 213-232.

[4] Duren, P.L. (2010) Univalent Functions, ed., *Springer Science & Business Media*, New York, USA, pp. 384.

[5] Efraimidis, I. (2016) A generalization of Livingston's coefficient inequalities for functions with positive real part, *Journal of Mathematical Analysis and Applications* **435**: 369-379.

[6] El-Ashwah, R.M., Thomas, D. (1987) Some subclasses of close-to-convex functions, *J. Ramanujan Math. Soc* **2**: 85-100.

[7] Janowski, W. (1973) Some extremal problems for certain families of analytic functions I, *Annales Polonici Mathematici* **28**: 297-326.

[8] Kayumov, I. (2005) On Brennan's conjecture for a special class of functions, *Mathematical Notes* **78**: 498-502.

[9] Khan, M.G., Ahmad, B., Sokol, J., Muhammad, Z., Mashwani, W.K., Chinram, R., Petchkaew, P. (2021) Coefficient problems in a class of functions with bounded turning associated with Sine function, *European Journal of Pure and Applied Mathematics* **14**: 53-64.

[10] Kowalczyk, B., Lecko, A. (2022) Second Hankel determinant of logarithmic coefficients of convex and starlike functions of order alpha, *Bulletin of the Malaysian Mathematical Sciences Society* **45**: 727-740.

[11] Lasode, A.O., Ajiboye, A.O., Ayinla, R.O. (2023) Some coefficient problems of a class of close-to-star functions of type α defined by means of a generalized differential operator, *International Journal of Nonlinear Analysis and Applications* **14**: 519-526.

[12] Lee, S.K., Khatter, K., Ravichandran, V. (2020) Radius of starlikeness for classes of analytic functions, *Bulletin of the Malaysian Mathematical Sciences Society* **43**: 4469-4493.

[13] Ma, W. (1992) A unified treatment of some special classes of univalent functions. Proceedings of the Conference on Complex Analysis, *International Press Inc.*, Tianjin, China, pp. 157-169.

[14] MacGregor, T.H. (1967) Majorization by univalent functions, *Duke Mathematical Journal* **34**: 95-102.

[15] Mohamad, D., Abdul Wahid, N.H.A., Hasni, N.N. (2023) Coefficient problems for star-like functions with respect to symmetric conjugate points connected to the sine function, *European Journal of Pure and Applied Mathematics* **16**: 1167-1179.

[16] Noonan, J., Thomas, D. (1976) On the second Hankel determinant of areally mean *Transactions of the American Mathematical Society* **223**: 337-346.

[17] Olatunji, S.O., Altinkaya, Ş. (2021) Generalized distribution associated with quasi-subordination in terms of error function and bell numbers, *Jordan Journal of Mathematics and Statistics* **14**: 97-109.

[18] Ping, L.C., Janteng, A. (2011) Subclass of starlike functions with respect to symmetric conjugate points, *International Journal of Algebra* **5**: 755-762.

[19] Shi, L., Arif, M., Rafiq, A., Abbas, M., Iqbal, J. (2022) Sharp bounds of Hankel determinant on logarithmic coefficients for functions of bounded turning associated with petal-shaped domain, *Mathematics* **10**: 1939.

[20] Thomas, D.K., Tuneski, N., Vasudevarao, A. (2018) Univalent Functions: A Primer, ed., *Walter de Gruyter GmbH & Co KG*, pp. 265.

TuJNaS

Original Article

Thamar University Journal of Natural & Applied Sciences 10(2) (2025) 9– 16

DOI: https://doi.org/10.59167/tujnas.v10i2.3012

Association between Diabetes Mellitus and Acute Coronary Syndrome in Adults: A Cross-Sectional Study in Dhamar City, Yemen

Bakeel A. Radman[1,2*†], Abdullah Ali Al-Alawi[3,†], Ziad Abdo Al-Bdash[4†], Moyed Alsaadawe[4], and Ibraheem B. A. Radman[5]

[1]Cancer Center, Integrated Hospital of Traditional Chinese Medicine, Southern Medical University, 510315 Guangzhou, China.

[2]Department of Biology, College of Science and Education, Albaydha University, Yemen.

[3]Department of Microbiology, Medical Research Institute, Southwest University, China.

[4]Department, Institute for Continuous Learning, Thamar University, Dhamar 87246, Yemen.

[5]Department of Pharmacy, Institute for Continuous Learning, Thamar University, Dhamar 87246, Yemen.

† **Equal contribution**: the Authors are equal contributors.

***Corresponding Author:** Bakeel A. Radman, Cancer Center, Integrated Hospital of Traditional Chinese Medicine, Southern Medical University, 510315 Guangzhou, China, and Department of Biology, College of Science and Education, Albaydha University, Yemen. E-mail: b-radman@qq.com

Received: 22 July 2025. Received (in revised form): 16 December 2025. Accepted: 17 December 2025. Published: 28 December 2025.

Abstract

Background: Diabetes mellitus is one of the most serious chronic diseases worldwide and greatly increases the risk of cardiovascular complications. Acute coronary syndrome (ACS) is a critical outcome of diabetes, resulting from sudden reductions in blood flow to the heart. When combined, diabetes and ACS pose major concerns for public health, especially in low-resource settings. This study explored the relationship between diabetes and ACS in adult patients in Dhamar City, Yemen. **Methods:** A cross-sectional study was carried out among 77 ACS patients admitted to several hospitals in Dhamar between February and May 2022. Sociodemographic characteristics, medical history, laboratory findings, and clinical outcomes were collected through interviews and patient records. Data were analyzed using SPSS version 23. **Results:** Of the participating ACS patients, 74.03% were male and 67.5% had diabetes, with 51.9% diagnosed with type 2 diabetes. Most patients were between 40 and 60 years old, overweight, uneducated, and hypertensive. Troponin was positive in 94.8% of cases. STEMI accounted for 36.4% of ECG findings, while NSTEMI represented 57.1%. Diabetic patients showed higher LDL and lower HDL levels than non-diabetics, and significantly higher blood glucose indices. The hospital mortality rate was 9.1%. **Conclusion:** The findings indicate a strong association between diabetes and ACS among adults in Dhamar City. Poor lipid control, elevated blood glucose levels, hypertension, and overweight may contribute to ACS development in diabetic patients. Routine follow-up, improved screening, and early detection are important to reduce ACS-related complications in this population.

Keywords: Diabetes Mellitus; Acute Coronary Syndrome; Dhamar; Yemen

1. Introduction

Diabetes mellitus (DM) is the seventh leading cause of death globally and a major cause of costly and debilitating complications such as heart attacks, strokes, kidney failure, blindness, and lower limb amputations [1-3]. More than 420 million people live with diabetes, and this number is estimated to rise to 570 million by 2030 and to 700 million by 2045, according to the World Health Organization .The Middle East has the highest prevalence of diabetes in the world with Egypt (17.2%), United Arab Emirates (16.3%), Saudi Arabia (15.8%), Qatar and Bahrain (15.6%), (Syria 13.5%), Jorden (12.7%), Kuwait (12.2%), Iran (9.6%) and Yemen (5.4%) [4, 5].

Diabetes is a significant global cause of death, mostly because of its vascular consequences. According to the International Diabetes Federation (IDF), diabetes claimed the lives of four million people in 2017 and was the primary cause of 10.7% of all deaths worldwide among persons aged 20 to 79 [6]. Hypertension, dyslipidemias, pro-inflammatory and pro-thrombotic effects of hyperglycemia, and hyperinsulinemia that impair vascular autoregulation are some of the mechanisms by which vascular diseases develop. These include glycosylation of serum and tissue proteins with the formation of advanced glycation end products (AGEs), superoxide production, activation of protein kinase C, accelerated hexamine biosynthetic and polyol pathways, and. Insulin resistance and

hyperglycemia are the mediators of all of the aforementioned pathways [7-11]. Two important and related risk factors for atherosclerotic cardiovascular disease, which include acute ACS [12, 13]. Diabetes and hypertension are. Because of common pathogenic processes like inflammation, insulin resistance, and obesity, they commonly co-occur [14]. However, when they appear together, their combined risk for cardiovascular events is higher than the sum of their separate effects; this phenomenon is known as synergistic [15].

The complications of DM can be divided into two main types. The microvascular complication that affects small vessels in the retina, peripheral nerves, and kidneys, leading to retinopathy, neuropathy, and nephropathy, respectively [16, 17]. And macro-vascular complications that affect large vascular, including: peripheral artery disease, coronary artery disease (CAD), and cerebrovascular disease [18]. Diabetes-associated cardiovascular autonomic neuropathy (CAN) damages autonomic nerve fibers that innervate the heart and blood vessels, in turn causing abnormalities in heart rate and vascular dynamics. It is known to affect multiple organ systems and is a major cause of morbidity and mortality in patients with diabetes [19-22].

Diabetes is a growing pandemic and a leading cause of morbidity and mortality. About 18 million people die every year from cardiovascular disease (CVD), for which diabetes and hypertension are major predisposing factors [23, 24]. People with diabetes have a cardiovascular risk that is 2–4 times higher than that of individuals without the disease, and the risk increases as glycemic control deteriorates. Diabetes has been associated with a 75% increase in mortality rate in adults. People with diabetes remain at significantly higher cardiovascular risk compared with people without diabetes, and CVD is a major cause of comorbidity and death among people with diabetes [24, 25].

Ischemic heart disease (IHD) is the main global cause of death, accounting for >9 million deaths in 2016 according to the World Health Organization (WHO) estimates [26, 27]. Patients with diabetes, especially those with type 2 diabetes mellitus (T2DM), frequently have silent myocardial ischemia, which is likely caused by cardiac autonomic dysfunction. In our research population, the prevalence of silent cardiac ischemia is strongly influenced by age, history of smoking, history of hypertension, fasting blood sugar (FBS) level, body weight, and body mass index (BMI) [28, 29].

The main cause of death in the United States is still coronary artery disease (CAD) [30], in which atherosclerotic plaque accumulates inside the coronary arteries and inhibits blood flow, hence decreasing oxygen supply to the heart. Despite the time and money invested in educating doctors and the public on its risk factors, symptoms, and treatment, one woman or man encounters a coronary artery disease episode every 25 seconds. Acute coronary syndrome (ACS), a disorder characterized by signs and symptoms of abrupt myocardial ischemia—a rapid decrease in blood supply to the heart—can develop as a result of coronary artery disease (CAD) [31]. Because it was thought that the name ACS better represented the illness course associated with myocardial ischemia, it was chosen. According to the American Heart Association (AHA), 785,000 People will encounter a myocardial infarction (MI) this year, and roughly 500,000 of them will experience another one the following year. These two conditions are both included under the ACS umbrella [32]. In 2006, almost 1.4 million patients were released from the hospital with either a primary or secondary diagnosis of ACS, including 537,000 with Unstable Angina (UA) and 810,000 with a non-ST-segment-elevated myocardial infarction (N-STEMI) or an ST-segment-elevated myocardial infarction (STEMI). Some patients also had both UA and MI [32, 33].

The International Committee of the Red Cross (ICRC) reported that more than 80% of Yemen's population lacks food, fuel, drinking water, and access to health care services, which makes it particularly vulnerable to chronic diseases like diabetes. Economic crises, reduced health services, and increased costs made most of the people in Yemen unable to discover most of the chronic diseases until a long time after they occur, which also made diabetic patients incompetent to make a regular investigation for treating and managing their disease [34]. Despite this alarming trend, we have observed an increased prevalence of diabetes mellitus compared to previous years, and an increase in the incidence of ACS, where there is a relationship between diabetes and CVD. Furthermore, there is limited data regarding ACS, and the factors linked to its increase among DM patients remain poorly understood in Yemen. Additionally, no study has addressed the extent of diabetes's effect on ACS occurrence or the relationship between diabetes and ACS patients in the government of Dhamar, Yemen.

This study aimed to investigate the association between diabetes and ACS in Dhamar City, Yemen. Determination of the prevalence of ACS in a patient with/without diabetes according to (gender, marital status, employment, residence, occupation, income level, age, and education) in Dhamar City, Yemen. 2. To evaluate the risk factors (habitus and body mass index) in ACS patients in Dhamar, Yemen. To evaluate the clinical manifestations and hospital course of ACS in diabetic and non-diabetic patients in Dhamar City, Yemen. Estimation of biomarker tests (cardiac enzymes, lipid profile, HbA1c, FBS, and RBS) and Echo and ECG.

2. Materials and Methods

2.1 Study Design, Setting, and Period

This study was conducted in Dhamar City, Yemen Figure 1. Dhamar City is located in the central part of Dhamar province, 100 km south of the capital Sana`a (about 130 km south of the capital Sana`a airport. Ibb governorate of the south, Al-Bida province, and part of Sana`a in the east, Al-Hudaydah governorate, and part of Sana`a (the capital of Yemen), and a governorate to the west. The area of the governorate is about 7586 km2, and the population of the governorate, according to the results of the general census of population, housing, and establishments for 2004, is about 1330108 (https://yemen-nice.info/gover/thamar/classoff).

A Cross-sectional study conducted between February 2022 and May 2022 involved patients with ACS, with or without diabetes, at various health facilities, including Al-Riyada International Hospital, Taiba Consulting Hospital, Dar Al-Shifa Hospital, and Dhamar General Hospital Authority.

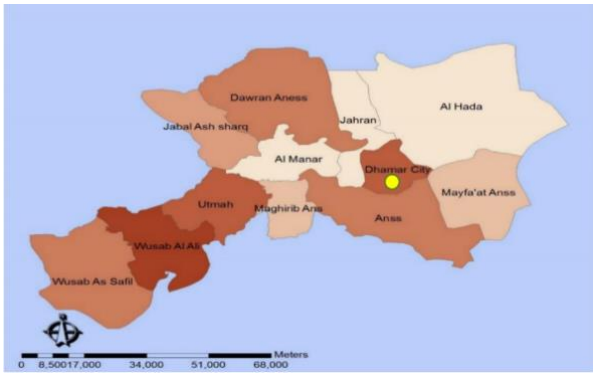

Figure 1: Dhamar city, Yemen (https://yemen-nice.info/gover/thamar/classoff).

2.2. Participant Recruitment and Eligibility Criteria

Upon the treatment of the physician identifying an eligible patient, a member of the research team approached the patient (or their next of kin in cases where the patient was critically ill or unable to communicate). The study's purpose, procedures, potential risks, benefits, and the voluntary nature of participation were explained verbally in Arabic. Written informed consent was obtained from all participants (or their legally authorized representatives) prior to data collection.

ACS patients who agreed to participate in this study. Patients were enrolled consecutively upon hospital presentation. The Study included both sexes, adults aged 77, ACS patients, and diabetic and non-diabetic patients. Some ACS inpatients were excluded who refused to participate in this study, and some who had not completed answering the questionnaire questions, who did not have the required investigation in this study, or were non-adults. This study deals with the city of Dhamar in Yemen under very difficult circumstances. It was performed during a period when there were no cardiology departments in local hospitals, and choosing a sample size was practical and necessary. These limitations, coupled with the difficulty of collecting data in such an environment, limit the scope of the study but are justified under the circumstances. Despite these challenges, the study provides valuable local insights into a critical health issue within this specific context. It is a laudable effort, and it lays the foundation for future research in more stable conditions. The criteria for classifying diabetes (history, medication, or HbA1c > 6.5%) and the classic triad for diagnosing ACS (symptoms ECG abnormalities, and troponin elevation) were established as diagnostic criteria.

2.3 Operational Definitions

Based on the combination of the following, the attending physician diagnosed ACS: Clinical Presentation (typical signs of acute myocardial ischemia, such as pressure, dyspnea, or chest pain); Electrocardiographic (ECG) Findings (new or suspected new significant ST-segment-T wave

changes (ST-elevation, ST-depression, or T-wave inversion) at least two consecutive leads. Biochemical Evidence (an increase or decrease in cardiac troponin levels, with at least one value above the assay's 99th percentile upper reference. The diagnosis was based on troponin tests performed in emergency rooms at all participating institutions, using ECG machines and basic laboratory capabilities.

2.4 Data Collection Procedures

2.4.1 Questionnaire Interview

A pre-tested questionnaire was used in a face-to-face interview to collect data on sociodemographics, medication use, medical history (diabetes, hypertension), and lifestyle choices (smoking, khat use, physical activity).

2.4.2 Biochemical Tests and Blood Samples Collection

Standard commercial assays were used for on-site analysis of blood samples at the collaborating hospital laboratories. The blood samples collected by the laboratory department in Al-Riyadh International Hospital, Taiba Consulting Hospital, Dar Al-Shifa Hospital, and Dhamar General Hospital Authority were used to check the following investigations: Fast blood sugar (FBS), Random blood sugar (RBS), HbA1c, Lipid Profile (total cholesterol, high-density lipoprotein (HDL), and LDL), and cardiac enzymes (CK-MB and troponin).

2.4.3 Anthropometric Measurements

The height of all patients was measured using tape in centimeters while the participant stood still without shoes, and the weight of all patients was measured with an electronic weight scale in kilograms, with the participant lightly clothed. The body mass index (BMI) is calculated by using the following formula:

$$BMI = \text{weight (kg)}/[Hight\ (m)]^2$$

2.4.4 Specific Investigation of Acute Coronary Syndrome

All ACS patients underwent investigations that confirmed the diagnosis of ACS, including an ECG and an echocardiogram (Echo). For the hospital management section, this section included Condition improved with medication, such as PCI (patients recommended a PCI, patients performed a PCI, and recommended the Type of PCI).

2.6 Data Analysis

Data were analyzed using the Statistical Package for Social Sciences (SPSS Version 23), and descriptive statistics were reported using relative frequencies (percentages) for categorical data. The differences in biochemical parameters between the different glycemic status groups were assessed using a t-test or one-way ANOVA, depending on data distribution. The relationship of biomarker tests with DM was evaluated using the Chi-square test. Statistical significance was set at a p-value of ≤0.05.

3. Results

Statistical analysis of 77 individuals who participated showed that, the majority of the study population most likely to of ACS, 57 (74.03%) male, 71 (92.2%) married, 66 (85.7%) non-employed, 56 (72.7%) rural residents, 49 (63.6%) farmer, 45 (58.4%) mid-income level, 36 (46.8%) ages between 40-60-year-old and 40 (51.9%) non-educated and 36 (46.75%) over-weight as in the following Figures (2.A-I). (A–I) Distribution by sex, marital status, employment status, residence, occupation, monthly income level, age group, education level, and body mass index.

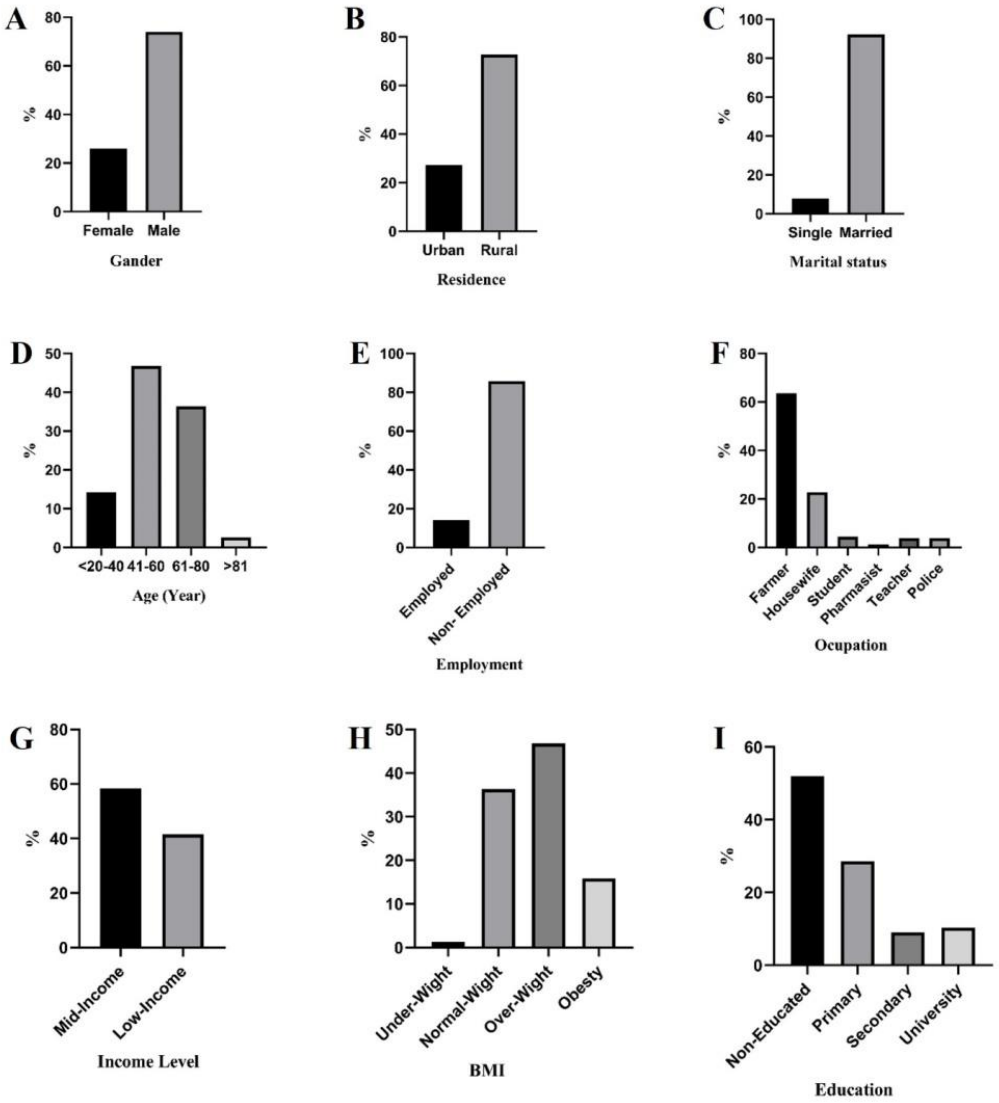

Figure 2: Sociodemographic characteristics of ACS patients with and without diabetes.

Regarding lifestyle habits. About 39 (50.6 %) of ssmokers patients, while 38 (49.4%) of patients are not smokers, 40 (51.9%) chew Khat (Yemeni plant) daily, 26 (33.77%) do not do anybody activities (sport), 41 (53.2%) do insufficient sport for less than 30 minutes and 44 (57.1%) do not follow a diet system, Table 1.

Table 1. Lifestyle characteristics of ACS patients, including smoking status, khat chewing, physical activity, and dietary habits.

Habits		Frequency	%
Smoking	Yes	39	50.6
	No	38	49.4
Type of smoking	Cigarettes	32	41.55
	Meekness	7	9.1
	Non-smoker	38	49.35
Chewing Khat (Yemeni plant)	Daily	40	51.9
	Sometimes	24	31.2
	Never	13	16.9
Body activities (sport)	Yes	29	37.66
	No	26	33.77
	Sometimes	22	28.57
Sports time	Less than 30 minutes	41	53.2
	More than 30 minutes	10	13.0
	Does not exercise	26	33.8
Diet system	Yes	33	42.9
	No	44	57.1

According to ACS patient's historical characteristics of DM which are shown in Table 2, out of 77 ACS patients, 61 (79.2%) had DM, 40 (51.9%) diabetes patients had T2DM and 14 (18.2%) do not know what type of diabetes they have, 28 (36.36%) had diabetes duration less than 3 years, 33 (42.85%) had a family history of DM, 54 (70.1%) numbness and 40 (51.9%) had a recurrent infection. Regarding treatment, 49 (59.7%) patients were receiving oral Anti-hyperglycaemic drugs, 6 (7.8%) patients were on insulin and tablets, and 38 (49.4 %) were not measuring their blood sugar regularly. Of the 77 ACS patients, 42 (54.5%) had hypertension. Twenty of them (25.97% of the group as a whole) had experienced hypertension for less than three years. Only 15 (19.5%) of the hypertensive patients reported routinely checking their blood pressure, even though all of them were on medication. 22 individuals (28.6%) had a family history of cardiac disease (Table 2).

Data analysis of the clinical manifestations of ACS showed that, in this sample, the presentation was often abnormal. All 77 patients complained of chest discomfort; however, only 23 (29.9%) said it was painful. Among individuals who were in pain, the most prevalent characteristics were burning 9, 11.7%) or heaviness 14, 18.2%). Interestingly, 54 patients (70.1%) reported no chest pain, suggesting that non-painful chest discomfort is the most common presentation. Dyspnea was associated with all patients, 35 (45.5%) were associated with nausea and vomiting, and 13 (16.9%) were associated with loss of consciousness, Table 3.

As for the investigation to confirm the diagnosis of ACS shown in Table 4, regarding cardiac enzymes, 73 (94.8%) had troponin-positive results, and 70 (90.9%) had CK-MB-positive results. Regarding ECG, 28 (36.4%) had ST-segment elevation (STEMI) in at least two leads, 44 (57.1%) had Flat or inverted T wave (N-STEMI) in at least two leads, and 5 (6.5%) had a normal ECG in all 12 leads. Regarding the echocardiogram, 32(41.6%) had IHD, and 42 (54.5%) had IHD and HTN. Based on clinical management of ACS, Table 4 showed that, regarding treatment, 32 (41.5%) did not improve their condition with medication, 50 (64.93%) needed PCI, 36 (46.75%) did not undergo PCI, and 27 (35.06%) underwent PCI for therapeutic purposes. The total of those who have performed PCI and will do it later is 41(53.24%), which matches the recommended type of PCI 41 (53.24%) (Diagnostic 8 (10.39%), Therapeutic 24 (31.17%), and both types, diagnostic and therapeutic 9 (11.68%).

Table 2. History of diabetes and hypertension among ACS patients, including disease duration, medication use, monitoring habits, and family history.

Characteristics		Frequency	%
History of DM:			
Diabetes	Diabetic	61	79.2
	Non-Diabetic	16	20.8
Type of Diabetes	T1DM	7	9.1
	T2DM	40	51.9
	I don't know	14	18.2
	Non-diabetic	16	20.8
Period Diabetes	Less than 3 years	28	36.36
	4-6 Years	14	18.18
	7-10 Years	13	16.88
	More than 10 years	6	7.8
	Non-diabetic	16	20.78
Family history of diabetes	Yes	33	42.85
	No	31	40.25
	I don't know	13	16.9
Numbness in the extremities	Yes	54	70.1
	No	23	29.9
Recurrent infection	Yes	40	51.9
	No	37	48.1
Measurement of Sugar	Always	14	18.2
	Sometimes	38	49.4
	No	25	32.5
Ant-hyperglycemic drugs	Insulin	6	7.8
	Tablets	46	59.7
	Both (Insulin and Tablets)	6	7.8
	Do not use	3	3.9
	Non-diabetic	16	20.8
History of Hypertension:			
Hypertension	Yes	42	54.5
	No	23	29.9
	I don't know	12	15.6
Hypertension Duration	Less than 3 years	20	25.97
	4-6 Years	10	12.98
	7-10 Years	5	6.5
	More than 10 years	7	9.1
	Normal blood pressure	35	45.45
Regularity Measurement for Blood Pressure	Always	15	19.5
	Sometimes	34	44.1
	No	28	36.4
Family History of Heart Disease	Yes	22	28.6
	No	55	71.4
Anti-hypertensive Drugs	Yes	42	54.5
	No	22	28.6
	Normal blood pressure	13	16.9

Table 3. Clinical manifestations reported by ACS patients, including chest discomfort, radiation of pain, associated symptoms, and frequency and duration of episodes.

Clinical Manifestation		Frequency	%
Feel Chest Discomfort	Yes	77	100.0
	No	0	0
Chest Discomfort in The Form of Pain	Yes	23	29.9
	No	54	70.1
Character of Pain	Heaviness	14	18.2
	Burning	9	11.7
	There is no pain	54	70.1
Pain Radiated	Left arm	23	29.9
	There is no pain	54	70.1
Chest Discomfort or Pain Related to	Muscular effort	26	33.8
	Nervous excitement	20	26.0
	With rest	31	40.2
Chest Discomfort or Pain Occur	Frequently	4	5.2
	For first time	73	94.8
Period of Chest Discomfort or Pain	Less than 15 minutes	2	2.6
	More than 15 minutes	75	97.4
Use Pills to Expand the Blood Vessels Under the tongue is the Pain	It disappears in less than 15 minutes	2	2.6
	The pain persists for more than 15 minutes	75	97.4
Pain Accompanied by Difficulty Breathing	Yes	77	100.0
	No	0	0
Pain Accompanied by Nausea And Vomiting	Yes	35	45.5
	No	42	54.5
Lost Consciousness	Yes	13	16.9
	No	64	83.1

Table 4. Diagnostic and hospital management findings among ACS patients, including cardiac enzyme results, ECG interpretation, echocardiography findings, and PCI recommendations.

Investigation for a confirmed diagnosis			Frequency	%
Cardiac Enzyme	CK-MB	Positive	70	90.9
		Negative	7	9.1
	Troponin	Positive	73	94.8
		Negative	4	5.2
ECG	ST segment elevated		28	36.4
	Flat or inverted T wave		44	57.1
	Normal ECG		5	6.5
Echo.	IHD		32	41.6
	IHD and HTN		42	54.5
	Not done		3	3.9
Hospital management:				
Condition improved with medication	Yes, greatly		16	20.77
	Yes, moderately		29	37.66
	Not getting better		32	41.55
Recommended PCI	Yes		50	64.93
	No		27	35.06
Performed the PCI	Yes		27	35.06
	No		36	46.75
	later		14	18.18
Recommended Type of PCI	Diagnostic		8	10.39
	Therapeutic		24	31.17
	Both		9	11.68
	There is no PCI		36	46.75

P.C.I. = Percutaneous Coronary Intervention. CK-MB = MB Fraction of Creatine Kinase. Ech= Echocardiogram. E.C.G.= Electrocardiogram. IHD = Ischemic heart disease. H.T.N = Hypertension.

According to Table 5's biochemical analytical tests, individuals with diabetes had greater total cholesterol than those without the disease (239.80±33.86 and 226.39±37.31, respectively), although this difference was not statistically significant. Furthermore, those with diabetes had greater LDL than those without the disease (157.40±7.16) and 138.60±16.60, respectively, with a P value of 0.017. Furthermore, HDL is lower in diabetic patients than in non-diabetic patients (40.40±2.61 and 41.24±7.45, respectively), although this difference is not significant. Patients with diabetes have higher RBS than those without the disease (225.02±90.99 vs. 170.56±120.18, respectively), but the difference is not statistically significant. Furthermore, FBS is greater in diabetic patients than in non-diabetic individuals (155.60±11.94 and 117.80±3.26, respectively) without statistical significance. Also, with 0.031 p-values, the HbA1c in diabetics is greater than in non-diabetics (8.42±2.40) and 5.60±0.49, respectively. CK-MB is positive in 58 (75.3%) of ACS patients with DM, according to cardiac enzyme biochemical tests. But only 12 (15.6%) of the individuals did not have diabetes. Additionally, 60 individuals (77.9%) with DM had Troponin enzyme levels.

Table 5. Comparison of biochemical test results between diabetic and non-diabetic ACS patients, including lipid profile, blood glucose indices, and cardiac enzyme patterns.

Relationship between lipid profile and diabetes in ACS patients:

Lipid profile	T. cholesterol Mean ± S.D	HDL Mean ± S.D	LDL Mean ± S.D
Diabetic	239.80±33.86	40.40±2.61	157.40±7.16
Non-Diabetic	226.39±37.31	41.24±7.45	138.60±16.60
P value	No-Sig.	Non-Sig.	0.017

Relationship between blood glucose and diabetes in ACS patients:

Diabetes	RBS Mean ± S. D	FBS Mean ± S.D	HbA1c Mean ± S.D
Diabetic	225.02±90.99	155.60±11.94	8.42±2.40
Non-Diabetic	170.56±120.18	117.80±3.26	5.60±0.49
P value	No-Sig.	Non-Sig.	0.031

Patterns of cardiac enzymes and diabetes in ACS patients:

Diabetes	CKMB		P-Value	Troponin		P-Value
	Positive	Negative		Positive	Negative	
Diabetic	58 (75.3)	3 (3.9)	0.013	60 (77.9%)	1 (1.3)	0.006
Non-Diabetic	12 (15.6)	4 (5.2)		13 (16.9%)	3 (3.9)	

CE = Cardiac Enzyme. CK-MB = MB Fraction of Creatine Kinase. T. cholesterol = Total Cholesterol. HDL = High-Density Lipoprotein. LDL = Low-Density Lipoprotein. RBS = Random Blood Sugar. F.B.S. = Fasting blood sugar. H.b.A1c= Hemoglobin A1c

According to Table 6, the evaluation findings for ACS Diabetic and Non-Diabetic Patients showed 7 (9.1%) deaths.

Table 6. Clinical outcomes of ACS patients with and without diabetes during hospitalization.

Diabetes	Get better	Death	Not recorded	P-Value
Diabetic	52 (67.5)	7 (9.1)	2 (2.6)	/
Non-Diabetic	16 (20.8)	0 (0.0)	0 (0.0)	

4. Discussion

Diabetes mellitus is a medical concern and a broad field of research that plays a key role in the development of many serious and fatal complications. The present study was conducted on ACS patients presenting with diabetes and non-diabetic patients. In this study, we enrolled 77 ACS patients, 57 (74.03%) male and 20 (25.97%) female, and more than half of the study population, 47 (61.04%), were aged <60 years. This is in agreement with [35] on 331 ACS patients, 225 (68.0%) male and 106 (32.0%) female, and 221 (66.8) aged < 60 years. Regarding residence, the study revealed that rural residents are more likely to have ACS than urban residents, and this is not in agreement with [35]. The reasons and justifications may be due to differences in sample size and the period in which you are studying or may be due to the differences in race or environment between countries of the world. The current study showed that the uneducated group with diabetes is more likely to have heart attacks, constituting 51% (95%), while the educated group of people with diabetes constitutes a percentage of 10- 39 %. The proportion of people with diabetes who are principally educated is 28.57%, whereas the percentage of people with diabetes who are secondary educated is 9.09%. This study coincided with the study [36], which took place in China. Those with diabetes who were less educated had a 70% chance of having a heart attack, compared to 30% for those with diabetes who were better educated.

The results of the current study show that the number of individuals in the sample who chewed Khat was more prone to heart attacks by 51.9, and this is consistent with the study [37]. Conducted in Sana`a, the number of

individuals who chewed Khat was 54.5%. Also, 40 (51.9%) chew Khat daily, 26 (33.8%) do not exercise, 41 (53.2%) do not exercise adequately for less than 30 minutes, and 44 (57.1%) do not follow a diet. Which agreement with [38] reported on type 2 diabetes in Dhamar Governorate, and the percentage of those who used Khat was reported (at 63.6%) and those who do not use Khat (36.4%), while the percentage of smokers was (27.3 %) and non-smokers (72.77%).

Diabetes is significant, according to this study's comparison of the mean and standard deviation of ACS between patients with and without diabetes, and HbA1c with Mean±S.D (8.42 ±2.40) (p value = 0.031). This result is consistent with [4]in the United Arab Emirates for the lipid profile with Mean ± SD. (157.40±7.16) (p value=0.017). The study's findings indicated that individuals with diabetes had high levels of cholesterol (mean and standard deviation of 239.80±33.86), high-density lipoprotein (40.40±2.61), and low-density lipoprotein (157.40±7.16), whereas patients without diabetes had higher levels of cholesterol (226.39±37.31), high-density lipoprotein (41±7.45), and low-density lipoprotein (138.60±16.60) [39].. The difference may be justified by the size of the study sample, where the number of cases in the study was 77 cases, while the number of cases in the study of them was 738790 cases.

The results of the study showed that people with diabetes and high blood pressure are more likely to suffer a myocardial infarction, 54.5% of the total, than people without diabetes, who are only 29.9% at risk. This result is consistent with a different research [39] in Poland. Where the percentage of people with high blood pressure was represented (87.4%).

As for the extent of health awareness among the study samples, especially those with diabetes, 18.2% of them are interested in measuring and checking their diabetes continuously, while 49.4% of them follow up on measuring their sugar sometimes. Our findings align with the results recorded by Saghir et al. (2019) in Al-Hodeida. That study showed that diabetics measured regularly (23.6%, irregularly (76.4%), and 7.8 %. The study sample used insulin, while 70% of the patients used anti-diabetic pills such as metformin and others, where metformin was proven to be effective in regulating sugar and burning fat, and it matches this result is in line with the result of the study [38] In Dhamar, Yemen, 68.5% use tablets, while 24% use insulin.

As for the clinical manifestations of acute coronary syndrome, 29.9% suffer from chest discomfort in the form of pain, and in the same percentage, the results show that 29.9% of those who suffer from left arm pain, only because they are affected by an acute case of coronary syndrome. Also, the use of vasodilator pills and clotting drugs contributed to the disappearance of pain 15 minutes before, and the answer rate was 35.1%. For those who felt nausea and vomiting accompanied by chest pain amounted to 45.5%, and the death percentage from acute coronary syndrome among diabetic patients is 7 cases of acute coronary syndrome among 77 diabetic patients, 370 cases of acute coronary syndrome among 7323 diabetic patients. This result is consistent with the results of the study conducted in Poland by [39].

According to our research, those with diabetes had greater LDL than people without the disease. Furthermore, patients with diabetes have lower HDL than people without the disease. Numerous studies have connected diabetes mellitus to a reduction in the activity of the antioxidant system, as well as an increase in reactive oxygen species production[40, 41]. Increased oxidative stress hastens the development of atherosclerosis and raises the risk of cardiovascular events by triggering inflammatory responses, endothelial dysfunction, thrombogenic propensity, plaque instability, and the migration, proliferation, and transformation of smooth muscle cells [42]. Elevated plasma cholesterol, TG, or both are signs of dyslipidemia, as are low HDL or LDL levels. A well-known possible risk factor for atherosclerotic cardiovascular disease, which includes ischemic heart disease and cerebrovascular illnesses like strokes, is dyslipidemia [43].

We find that RBS in diabetes patients is higher than in non-diabetic patients. FBS in diabetes patients is higher than in non-diabetic patients. HbA1c in diabetes patients is higher than in non-diabetic patients. The HbA1c test measures chronic hyperglycemia levels, which are connected to the risk of diabetes complications. With the permission of many diabetic organizations throughout the world, this test may now be used to diagnose and screen for diabetes [44]. Through enhancing glycemic control and reducing the risk of cardiovascular disease (CVD), diabetes treatment primarily attempts to postpone the development of disease complications and slow down its course [45, 46].

This study's outcome showed that ACS Diabetic and Non-Diabetic Patients' outcomes recorded 7 (9.1%) deaths. CVD kills 50-80% of all diabetics, with cerebrovascular illness and renal failure also among the primary causes of mortality [47, 48]. T2DM is a well-known cause of disability and early mortality, mostly through CVD and other chronic consequences [49]. Some studies recorded that the significant co-prevalence of hypertension (54.5%) and diabetes mellitus in our ACS cohort underscores a critical cluster of synergistic cardio metabolic risk factors, a pattern consistently observed in other settings [50]. This concurrence is not merely additive; evidence suggests their combined pathological impact on vascular and renal systems is greater than the sum of their individual effects, accelerating atherosclerosis and complicating disease management [51, 52]. While hypertension is a potent risk factor, its high prevalence in our population is contextualized by local data indicating a substantial burden of hypertension among individuals with type 2 diabetes in Dhamar [53]. Therefore, the interaction between conditions needs integrated management strategies targeting this risk factor cluster in Yemen's resource-constrained setting.

5. Conclusions

This study concludes that there is a substantial correlation between Type 2 Diabetes Mellitus (T2DM) and Acute Coronary Syndrome (ACS), with a high incidence of T2DM in the studied group leading to higher mortality, increased healthcare costs, and systemic sequelae. Hyperlipidemia and poor glycemic control were found to be the most important modifiable factors for the development of ACS in diabetic patients. Other risk factors included age, male gender, hypertension, overweight, sedentary lifestyle, lower educational levels, and irregular diabetes monitoring. The unusual presentation of ACS in diabetic individuals is a major clinical problem that highlights how diabetes worsens the prognosis of ACS and increases the chance of misdiagnosis. Proactive management is therefore crucial, including routinely screening lipid profiles and HbA1c, maintaining a high clinical suspicion for ACS by carefully assessing the patient's history and any non-classical symptoms at the time of diagnosis, and providing regular medical follow-up for all diabetic patients.

List of Abbreviations

Term	The Meaning
ACS	Acute Coronary Syndrome
AGEs	Advanced Glycation End Products
AHA	American Heart Association
BMI	Body Mass Index
CAD	Coronary Artery Disease
CKMB	Mb Fraction of Creatine Kinase
CVD	Cardiovascular Disease
DM	Diabetes Mellitus
ECG	Electrocardiogram
FBS	Fasting Blood Sugar
HbA1c	Hemoglobin A1c
ICRC	International Committee of The Red Cross
IDF	International Diabetes Federation
IHD	Ischemic Heart Disease
MI	Myocardial Infarction
N-STEMI	Non-ST Segment Elevated Myocardial Infarction
PCI	Percutaneous Coronary Intervention
SPSS	Statistical Package for Social Sciences
STEMI	ST Segment Elevated Myocardial Infarction
T1DM	Type 1 Diabetes Mellitus
T2DM	Type 2 Diabetes Mellitus
UA	Unstable Angina
WHO	World Health Organization

Ethical Approval

Ethical approval was obtained from the deanship of the Thamar University Institute for Continuing Education (2021-12-25), in addition to obtaining approval from human resources in health facilities.

Subject Consent

Verbally informed consent was obtained from the parents or legal guardians of all participating children after a full explanation of the study's purpose and procedures. Participation was voluntary, and consent was reaffirmed prior to data collection. All collected data were anonymized and used solely for research purposes.

Data Availability

The datasets used and analyzed during the current study are available from the corresponding author upon reasonable request.

Funding

This research received no specific grant from any funding agency in the public, commercial, or not-for-profit sectors.

Conflict of Interest

The authors declare that there are no conflicts of interest.

References

[1] Bauer, U.E., Briss, P.A., Goodman, R.A., Bowman, B.A. (2014) Prevention of chronic disease in the 21st century: elimination of the leading preventable causes of premature death and disability in the USA, *The Lancet* **384**: 45-52.

[2] Durstine, J.L., Gordon, B., Wang, Z., Luo, X. (2013) Chronic disease and the link to physical activity, *Journal of Sport and Health Science* **2**: 3-11.

[3] Tocantins, C., Diniz, M.S., Grilo, L.F., Pereira, S.P. (2022) The birth of cardiac disease: Mechanisms linking gestational diabetes mellitus and early onset of cardiovascular disease in offspring, *WIREs Mechanisms of Disease* **14**: e1555.

[4] Saeedi, P., Petersohn, I., Salpea, P., Malanda, B., Karuranga, S., Unwin, N., Colagiuri, S., Guariguata, L., Motala, A.A., Ogurtsova, K. (2019) Global and regional diabetes prevalence estimates for 2019 and projections for 2030 and 2045: Results from the International Diabetes Federation Diabetes Atlas, *Diabetes Research and Clinical Practice* **157**: 107843.

[5] Zhang, M., Zhang, H., Zhu, R., Yang, H., Chen, M., Wang, X., Li, Z., Xiong, Z. (2023) Factors affecting the willingness of patients with type 2 diabetes to use digital disease management applications: a cross-sectional study, *Frontiers in Public Health* **11**: 1-10.

[6] Cho, N.H., Shaw, J., Karuranga, S., Huang, Y., da Rocha Fernandes, J., Ohlrogge, A., Malanda, B. (2018) IDF Diabetes Atlas: Global estimates of diabetes prevalence for 2017 and projections for 2045, *Diabetes Research and Cinical Practice* **138**: 271-281.

[7] Andreeva–Gateva, P.A., Mihaleva, I.D., Dimova, I.I. (2020) Type 2 diabetes mellitus and cardiovascular risk; what the pharmacotherapy can change through the epigenetics, *Postgraduate Medicine* **132**: 109-125.

[8] Bikbov, B., Purcell, C.A., Levey, A.S., Smith, M., Abdoli, A., Abebe, M., Adebayo, O.M., Afarideh, M., Agarwal, S.K., Agudelo-Botero, M. (2020) Global, regional, and national burden of chronic kidney disease, 1990–2017: a systematic analysis for the Global Burden of Disease Study 2017, *The lancet* **395**: 709-733.

[9] Dutta, S., Singhal, A., Suryan, V., Chandra, N.C. (2023) Obesity: An Impact with Cardiovascular and Cerebrovascular Diseases, *Indian Journal of Clinical Biochemistry* **39**: 168–178.

[10] González, P., Lozano, P., Ros, G., Solano, F. (2023) Hyperglycemia and Oxidative Stress: An Integral, Updated and Critical Overview of Their Metabolic Interconnections, *International Journal of Molecular Sciences* **24**: 9352.

[11] Shen, Y., Dai, Y., Wang, X.Q., Zhang, R.Y., Lu, L., Ding, F.H., Shen, W.F. (2019) Searching for optimal blood pressure targets in type 2 diabetic patients with coronary artery disease, *Cardiovascular Diabetology* **18**: 1-13.

[12] Cheung, B.M., Li, C. (2012) Diabetes and hypertension: is there a common metabolic pathway?, *Current Atherosclerosis Reports* **14**: 160-166.

[13] Kamalumpundi, V., Shams, E., Tucker, C., Cheng, L., Peterson, J., Thangavel, S., Ofori, O., Correia, M. (2022) Mechanisms and pharmacotherapy of hypertension associated with type 2 diabetes, *Biochemical Pharmacology* **206**: 115304.

[14] Hezam, A.A.M., Shaghdar, H.B.M., Chen, L. (2024) The connection between hypertension and diabetes and their role in heart and kidney disease development, *Journal of Research in Medical Sciences* **29**: 22.

[15] Guang, Y., Yun-Tao, W.U., Xiao-Lan, R., Yan, D., Jie, T., Yao, Z., Chun-Peng, J.I., Xin-Ying, G., Shuo-Hua, C., Shou-Ling, W.U. (2014) The incidence and risk factors of cardiovascular events in diabetes and hypertension patients, *Chinese Journal of Hypertension* **22**: 1132-1138.

[16] Ergashev, U., Zokhirov, A., Minavarkhujaev, R. (2023) Study and treatment of changes in biochemical processes in complications of diabetes mellitus, *Obrazovanie i nauka v XXI veke* **1**: 1-11.

[17] Hamdan-Mansour, A.M., Dughmosh, R.A. (2023) Moderating effect of coping on the relationship between depression and chronic DM complications among patients with diabetes mellitus, *International Journal of Diabetes in Developing Countries* **43**: 12–19.

[18] Mezil, S.A., Abed, B.A. (2021) Complication of diabetes mellitus, *Annals of the Romanian Society for Cell Biology* **25**: 1546-1556.

[19] Vinik, A.I., Erbas, T., Casellini, C.M. (2013) Diabetic cardiac autonomic neuropathy, inflammation and cardiovascular disease, *Journal of Diabetes Investigation* **4**: 4-18.

[20] Wooton, A.K., Melchior, L. (2020) Diabetes-associated cardiac autonomic neuropathy, *The Nurse Practitioner* **45**: 24-31.

[21] Gad, H., Elgassim, E., Mohammed, I., Alhaddad, A.Y., Aly, H.A.H.Z., Cabibihan, J.-J., Al-Ali, A., Sadasivuni, K.K., Petropoulos, I.N., Ponirakis, G. (2023) Cardiovascular autonomic neuropathy is associated with increased glycemic variability driven by hyperglycemia rather than hypoglycemia in patients with diabetes, *Diabetes Research and Clinical Practice* **200**: 110670.

[22] Prakash, K.H., Parija, S., Kar, M. (2023) Assessment of the relationship of systemic vascular dysfunction and cardiac autonomic neuropathy (CAN) with diabetic retinopathy, *Journal of Family Medicine and Primary Care* **12**: 3236-3241.

[23] Tabish, S.A. (2007) Is diabetes becoming the biggest epidemic of the twenty-first century?, *International Journal of Health Sciences* **1**: V-VIII.

[24] Jyotsna, F., Ahmed, A., Kumar, K., Kaur, P., Chaudhary, M.H., Kumar, S., Khan, E., Khanam, B., Shah, S.U., Varrassi, G. (2023) Exploring the complex connection between diabetes and cardiovascular disease: analyzing approaches to mitigate cardiovascular risk in patients with diabetes, *Cureus* **15**: e4388.

[25] Dal Canto, E., Ceriello, A., Rydén, L., Ferrini, M., Hansen, T.B., Schnell, O., Standl, E., Beulens, J.W. (2019) Diabetes as a cardiovascular risk factor: An overview of global trends of macro and micro vascular complications, *European Journal of Preventive Cardiology* **26**: 25-32.

[26] World Health Organization (2017) *Global Diffusion of EHealth: Making Universal Health Coverage Achievable: Report of the Third Global Survey on EHealth*,

[27] Pirillo, A., Norata, G.D. (2023) The burden of hypercholesterolemia and ischemic heart disease in an ageing world, *Pharmacological Research* **193**: 106814.

[28] Zia, N., Aftab, S., Butt, N.I., Ashfaq, F., Anser, A., Saeed, S. (2021) Prevalence of Silent Cardiac Ischemia in Type II Diabetes Mellitus, *Pakistan Heart Journal* **54**: 162-166.

[29] Kaze, A.D., Fonarow, G.C., Echouffo-Tcheugui, J.B. (2023) Cardiac Autonomic Dysfunction and Risk of Silent Myocardial Infarction Among Adults With Type 2 Diabetes, *Journal of the American Heart Association* **12**: e029814.

[30] Natour, A.K., Shepard, A.D., Nypaver, T.J., Rteil, A., Corcoran, P., Tang, X., Kabbani, L. (2023) Impact of Preoperative Anemia on Hospitalization, Death, and Overall Survival in Patients With Peripheral Artery Disease Undergoing Endovascular Therapy: A Retrospective Cohort Study in the United States and Canada, *Journal of Endovascular Therapy* **31**: 1-9.

[31] Yong, J., Tian, J., Zhao, X., Yang, X., Xing, H., He, Y., Song, X. (2021) Optimal treatment strategies for coronary artery disease in patients with advanced kidney disease: a meta-analysis, *Therapeutic Advances in Chronic Disease* **12**: 1-17.

[32] Lloyd-Jones, D., Adams, R., Brown, T., Carnethon, M., Dai, S., De Simone, G., Ferguson, T., Ford, E., Furie, K., Gillespie, C., Go, A., Greenlund, K., Haase, N., Hailpern, S., Ho, P., Howard, V., Kissela, B., Kittner, S., Lackland, D., Lisabeth, L., Marelli, A., McDermott, M., Meigs, J., Mozaffarian, D., Mussolino, M., Nichol, G., Roger, V., Rosamond, W., Sacco, R., Sorlie, P., Stafford, R., Thom, T., Wasserthiel-Smoller, S., Wong, N., Wylie-Rosett, J. (2010) Heart disease and stroke statistics—2010 update: a report from the American Heart Association, *Circulation* **121**: e46-e215.

[33] Roger, V.L., Go, A.S., Lloyd-Jones, D.M., Adams, R.J., Berry, J.D., Brown, T.M., Carnethon, M.R., Dai, S., De Simone, G., Ford, E.S. (2011) Heart disease and stroke statistics—2011 update: a report from the American Heart Association, *Circulation* **123**: e18-e209.

[34] International Committee of the Red Cross (2019) *Health crisis in Yemen,* https://www.icrc.org/en/where-we-work/middle-east/yemen/health-crisis-yemen,

[35] Marwat, M., Ahmad, I., Ashiq, F., Ali, S., Zamir, S., Rehman, M.U., Farid, M., Rehman, B., Zahoor, H., Aman, Z. (2019) Frequency, distribution and

determinants of diabetes mellitus in adult acute coronary syndrome population of DI Khan Division, Pakistan, *Gomal Journal of Medical Sciences* **17**.

[36] Ansari, R.M. (2012) Applications of public health education and health promotion interventions, ed., *Trafford Publishing*, Singapore, pp. 140.

[37] Al Khawlani, A., Atef, Z., Al Ansi, A. (2010) Macrovascular complications and their associated risk factors in type 2 diabetic patients in Sana'a city, Yemen, *EMHJ-Eastern Mediterranean Health Journal, 16 (8), 851-858, 2010*.

[38] Al-Shammak, A., Ali, A., Jermozy, H.A. (2019) Prevalence of proteinuria among type 2 diabetic patients in Dhamar Governorate, Yemen, *International Journal of Diabetes and Clinical Research* **6**: 1-7.

[39] Niedziela, J.T., Hiczkiewicz, J., Kleinrok, A., Pączek, P., Leszek, P., Lelonek, M., Rozentryt, P., Parma, Z., Witkowski, A., Bartuś, S. (2020) Prevalence, characteristics, and prognostic implications of type 2 diabetes in patients with myocardial infarction: the Polish Registry of Acute Coronary Syndromes (PL-ACS) annual 2018 report, *Kardiologia Polska (Polish Heart Journal)* **78**: 243-246.

[40] Marco, E.D., Jha, J.C., Sharma, A., Wilkinson-Berka, J.L., Jandeleit-Dahm, K.A., de Haan, J.B. (2015) Are reactive oxygen species still the basis for diabetic complications?, *Clinical Science* **129**: 199-216.

[41] Giacco, F., Brownlee, M. (2010) Oxidative stress and diabetic complications, *Circulation Research* **107**: 1058-1070.

[42] Katakami, N. (2018) Mechanism of development of atherosclerosis and cardiovascular disease in diabetes mellitus, *Journal of Atherosclerosis and Thrombosis* **25**: 27-39.

[43] Holmes, M.V., Millwood, I.Y., Kartsonaki, C., Hill, M.R., Bennett, D.A., Boxall, R., Guo, Y., Xu, X., Bian, Z., Hu, R. (2018) Lipids, lipoproteins, and metabolites and risk of myocardial infarction and stroke, *Journal of The American College of Cardiology* **71**: 620-632.

[44] Sherwani, S.I., Khan, H.A., Ekhzaimy, A., Masood, A., Sakharkar, M.K. (2016) Significance of HbA1c test in diagnosis and prognosis of diabetic patients, *Biomarker insights* **11**: 95–104.

[45] Murray, A., Hsu, F., Williamson, J., Bryan, R., Gerstein, H., Sullivan, M., Miller, M., Leng, I., Lovato, L., Launer, L. (2017) Action to Control Cardiovascular Risk in Diabetes Follow-On Memory in Diabetes (ACCORDION MIND) Investigators. ACCORDION MIND: results of the observational extension of the ACCORD MIND randomised trial, *Diabetologia* **60**: 69-80.

[46] Agrawal, L., Azad, N., Bahn, G.D., Ge, L., Reaven, P.D., Hayward, R.A., Reda, D.J., Emanuele, N.V., Group, V.S. (2018) Long-term follow-up of intensive glycaemic control on renal outcomes in the Veterans Affairs Diabetes Trial (VADT), *Diabetologia* **61**: 295-299.

[47] Astrup, A., Finer, N. (2000) Redefining type 2 diabetes:'diabesity'or 'obesity dependent diabetes mellitus'?, *Obesity Reviews* **1**: 57-59.

[48] Torres, A., Blasi, F., Dartois, N., Akova, M. (2015) Which individuals are at increased risk of pneumococcal disease and why? Impact of COPD, asthma, smoking, diabetes, and/or chronic heart disease on community-acquired pneumonia and invasive pneumococcal disease, *Thorax* **70**: 984-989.

[49] Roglic, G., Unwin, N., Bennett, P.H., Mathers, C., Tuomilehto, J., Nag, S., Connolly, V., King, H. (2005) The Burden of Mortality Attributable to Diabetes: Realistic estimates for the year 2000, *Diabetes Care* **28**: 2130-2135.

[50] Jover, A., Corbella, E., Muñoz, A., Millán, J., Pintó, X., Mangas, A., Zúñiga, M., Pedro-Botet, J., Hernández-Mijares, A. (2011) Prevalence of Metabolic Syndrome and its Components in Patients With Acute Coronary Syndrome, *Revista Española de Cardiología* **64**: 579-586.

[51] Costa, M.C.D.B.G., Furtado, M.V., Borges, F.K., Ziegelmann, P.K., Suzumura, É.A., Berwanger, O., Devereaux, P.J., Polanczyk, C.A. (2021) Perioperative Troponin Screening Identifies Patients at Higher Risk for Major Cardiovascular Events in Noncardiac Surgery, *Current Problems in Cardiology* **46**: 100429.

[52] Shi, W., Wang, H., Zhou, Y., Sun, Y., Chen, Y. (2020) Synergistic interaction of hypertension and diabetes on chronic kidney disease: Insights from the National Health and Nutrition Examination Survey 1999-2006, *Journal of Diabetes and its Complications* **34**: 107447.

[53] Mareai, S.S., Gawli , K. (2023) Type 2 diabetes with obesity and hypertension: prevalence and sociodemographic risk factors in Yemen, *Diabetes Mellitus (Сахарный диабет)* **26**: 124–130.

TuJNaS

Original Article

Thamar University Journal of Natural & Applied Sciences 10(2) (2025) 17– 21

DOI: https://doi.org/10.59167/tujnas.v10i2.3013

Assessing the Potential for MRSA and VRSA Transmission among Food Handlers in Dhamar: A Critical Need for Intervention

Abdullah Ali Al-Alawi[1,2,*], Bakeel A. Radman[3], and Osman Esmail Al-Banaa[4]

[1]Department of Microbiology, Faculty of Medical Sciences, Thamar University, Dhamar 87246, Yemen.

[2]Medical Research Institute, Southwest University, Chongqing 400715, China.

[3]Cancer Center, Integrated Hospital of Traditional Chinese Medicine, Southern Medical University, Guangzhou 510315, China.

[4]Department of Medical Laboratory, Thamar University Institute for Continuous Education, Thamar University, Dhamar 87246, Yemen.

***Corresponding Author:** Abdullah Ali Al-Alawi, Department of Microbiology, Faculty of Medical Sciences, Thamar University, Dhamar 87246, Yemen, and Medical Research Institute, Southwest University, Chongqing 400715, China. Tel: 0086-17265376769 or 00967-772150893, E-mails: alalawisky@tu.edu.ye or alalawisky@yahoo.com

Received: 22 July 2025. Received (in revised form): 24 November 2025. Accepted: 26 November 2025. Published: 28 December 2025.

Abstract

Scientific background: Food handlers carrying *Staphylococcus aureus* on their noses mainly contribute to food contamination. Antibiotic resistance in *S. aureus* represents a significant public health concern. The drug of choice, Vancomycin, has become more popular as the rate of *MRSA* has increased. Consequently, *VRSA* has begun to emerge. This study aimed to assess the distribution of *S. aureus* nasal carriage and its antibiotic susceptibility patterns among food handlers at Dhamar restaurants in Yemen. **Method:** A cross-sectional study was conducted in Dhamar City, Yemen, between January and February 2023, collecting nasal swabs from 100 food handlers. Standard bacteriological techniques were applied to inoculate the collected swabs on mannitol salt agar to identify and isolate *S. aureus*. Researchers used the Kirby-Bauer disk diffusion method to test the antimicrobial susceptibility of methicillin and Vancomycin. **Results:** *S. aureus* colonized 44 (44%) of the 100 nasal food handlers working in Dhamar, Yemeni restaurants. Among the 44 *S. aureus* isolates, 6 (13.6%) were resistant to Vancomycin (*VRSA*), and 23 (52.3%) were resistant to methicillin (*MRSA*). A correlation was not observed between the nasal carriage rate of *S. aureus* and specific food handler variables. In **conclusion**, the high nasal carriage of *S. aureus*, including *MRSA* and *VRSA*, among food handlers poses significant risks to consumers, underscoring the need for strict policies, routine screening, and effective management to ensure food safety and control resistant bacteria.

Keywords: *S. aureus*; *MRSA*; *VRSA*; Nasal carriage

1. Introduction

Staphylococcus aureus is a Gram-positive bacterium that is often part of the normal human flora, especially in the anterior nares. It is an opportunistic pathogen widely recognized for its virulence factors, which cause a wide range of diseases, from mild symptoms to serious infections such as endocarditis and sepsis [1, 2]. As a major cause of both nosocomial and community-acquired infections, *S. aureus* represents a significant public health concern worldwide, with high morbidity and mortality rates [3, 4]. A significant concern with *S. aureus* is the production of enterotoxins, which are linked to food poisoning [5]. This risk is particularly pronounced among food handlers, who may inadvertently transmit the bacteria through respiratory secretions or manual contact, leading to gastrointestinal intoxication [6, 7].

The rise of methicillin-resistant *S. aureus* (*MRSA*) and vancomycin-resistant *S. aureus* (*VRSA*) highlights growing alarm about drug resistance in *S. aureus*. Once the go-to therapy, penicillins are no longer effective because *S. aureus* produces penicillinases, leading to resistance [8, 9]. The mortality rate of Methicillin-resistant *S. aureus* bacteremia (*MRSA*) is high [10], and its prevalence has steadily increased globally. In hospitals in Germany and Austria, *MRSA* was found in 20% and 10% of clinical isolates, respectively [11], the other study by Ahmed OB. (2020) found that the prevalence of *MRSA* among Sudanese food handlers was high [12]. In line with this, a study conducted in central Iran by Fooladvand S. *et al.* (2019) revealed a high prevalence of enterotoxin-positive and meticillin-resistant *S. aureus* among food handlers [13].

In addition to *MRSA*, *VRSA* represents an alarming development, as Vancomycin, a last-line treatment for Gram-positive bacterial infections, is

increasingly resistant [14, 15]. Consequently, *VRSA* poses a major global public health [16]. A study in Qena City, Egypt, by El-Zamkan, M. A. et al. (2019) found that food handlers transmit *MRSA* and *VRSA* to hospitalized patients [17].

As a result, the presence of *S. aureus* among food handlers remains a persistent public health concern. Asymptomatic workers are sources of staphylococcal food poisoning via contaminated food through respiratory secretions or manual contact, which leads to gastrointestinal intoxication [7]. In support of this, the study by El-Shenawy M. et al. (2014) highlighted the possibility that food handlers' skin may become colonized with enterotoxigenic strains of *S. aureus*, increasing the risk of food contamination [18]. Similarly, the study in Jimma Town, Southwest Ethiopia, by Beyene G. et al. (2019) found that the percent isolation of *S. aureus* from the nose and hands was 8.3% (nose) and 11.3%[19] (hands), respectively [19]. Another study found that the prevalence of *S. aureus* in the nose, hands, and both (nose and hands) was 19.8%, 11.1%, and 6.2%, respectively [20]. Strict hygienic measures and high standards of food handlers' hygiene are important for preventing the transmission of *MRSA* and *VRSA* [21, 22].

The widespread occurrence of endemic diseases in Yemen reflects its status as a developing country. Key contributing factors include population overcrowding, limited provision of safe drinking water, ineffective waste management, inadequate hygiene practices, and deficient environmental sanitation [23-25]. A lack of governmental oversight, reliance on poorly trained staff, and unhygienic food practices may increase the risk of staphylococcal food poisoning. As data on nasal carriage and antimicrobial resistance of *S.aureus* among Yemeni food handlers are scarce, this study provides the first assessment of these factors among restaurant workers in Dhamar city, Yemen.

2. Materials and Methods

2.1 Study area and period

A cross-sectional study was conducted among restaurant food handlers in Dhamar, Yemen, from January to February 2023 to determine the distribution of nasal *S. aureus* colonization and its susceptibility to methicillin and Vancomycin. Using random sampling, 100 food handlers involved in meal preparation, serving, and utensil cleaning in various restaurants were recruited as study participants.

2.2 Sociodemographic data and swab specimen collection

Data on each food handler's social and demographic characteristics (age, sex, occupation, and educational level) were collected using a pre-designed questionnaire. A nasal specimen was obtained using a sterile swab moistened with saline solution. The tips were inserted 1-2 cm inside each nostril's anterior nares, rotated six times, and transported to the Medical Laboratory of the Thamar University Institute for Continuous Education, Thamar University.

2.3 *S. aureus* isolation and identification

The nasal swab specimens were inoculated on Mannitol Salt Agar (LAB M, UK) [26]. Each plate was incubated for 24 hours under aerobic conditions at 37℃ [27]. Researchers followed standard procedures after isolating a pure colony, including Gram staining. Using standard protocols, confirmatory biochemical tests, such as the coagulase tube and catalase tests, were performed to identify suspected *S. aureus* [28, 29].

2.4. Antimicrobial susceptibility testing of *S. aureus*

Susceptibility testing was performed on Mueller-Hinton agar (LAB M, UK) using the Kirby-Bauer agar disc diffusion method, as recommended, according to the guidelines of the Clinical and Laboratory Standards Institute [26, 29]. Researchers tested the following antibiotics: Methicillin (MET, 5 µg) and Vancomycin (30 µg) (HiMedia Comp., India). Disks were used to assess resistance in *S. aureus* isolates. The resistance and sensitivity results were analyzed according to the Clinical and Laboratory Standards Institute (CLSI) protocol. Isolates showing resistance or intermediate to Vancomycin were classified as **"presumptive *VRSA*"**.

2.5. Data analysis procedures

The data were analyzed using Version 20 of the Statistical Package for the Social Sciences (SPSS). Chi-Square tests (Crosstabs), frequencies, and percentages were employed in the analysis. A p-value threshold of ≤ 0.05 was applied to determine statistical significance.

2. Results and Discussion

The majority of employees at the restaurant in Dhamar, Yemen, as shown in Table 1, are male (98% of the workforce), and 76% of the workers are under 35. Contrasting with Beyene et al. (2019), who found that 65.7% of the participants were female [19]. This gender disparity may be attributed to cultural and traditional norms that discourage women from working in restaurants or public spaces. The most common roles are cooks (37%) and waiters (22%), while 33% fall into the unspecified "Others" category. Education levels are generally low: 42% have only primary education, 13% are illiterate, and just 6% hold a university degree. The findings suggest that food handling jobs require minimal formal education, attract a young workforce, and have limited female participation. This highlights potential areas for workforce development, gender inclusion, and clarifying job roles.

Table 1: Distribution of Sociodemographic Characteristics of Food Handlers Working in Restaurants in Dhamar, Yemen (January–February 2023).

Characteristics	Category	Frequency (n = 100)	Percentage (%)
Sex	Male	98	98.0
	Female	2	2.0
Age (years)	15-25	41	41.0
	26-35	35	35.0
	36-45	16	16.0
	>45	8	8.0
Job Category	cook	37	37.0
	Assistant Cook	8	8.0
	Waiter	22	22.0
	Others (e.g., cleaners, cashiers…)	33	33.0
Educational Status	Literature	13	13.0
	Read and Write only	9	9.0
	Primary	42	42.0
	Secondary	30	30.0
	University	6	6.0

Figure 1 shows that S. aureus contamination among food handlers in Dhamar is 44%, representing a significant risk to food safety. This rate is notably higher than rates reported in Sana'a, Yemen (18.6%) [25], and in other regions, such as Kerbala, Iraq (30.1%) [30], Jimma, Ethiopia (28.7%) [19], and Sanliurfa, Turkey (23.1%) [31]. The discrepancy may stem from variations in hygiene practices, educational background, working conditions, and regulatory enforcement across different locations. These findings underscore a significant public health concern and emphasize the urgent need for targeted food safety interventions. Implementing hygiene training programs, enforcing stricter food safety regulations, and conducting routine health screenings are essential to reducing bacterial contamination and minimizing foodborne illness outbreaks. Additionally, promoting education among food handlers and raising awareness of hygiene best practices could significantly improve compliance with food safety standards. Beyond hygiene, addressing workforce challenges—such as gender inclusivity, job role clarity, and employment conditions—could contribute to a more regulated and professionalized food service sector, ultimately strengthening public health protection.

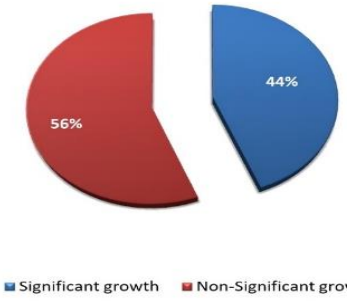

Figure 1: *S. aureus* carriage rate among nasal food handlers in hamar city, 2023.

Table 2: Association of Sociodemographic Characteristics with Nasal Carriage of *S. aureus* Among Food Handlers in Dhamar City, Yemen, from January to February 2023.

Characteristics		Significant Growth (No, %)	Non-Significant Growth (No, %)	P-value
Sex	Male	43 (%)	55 (%)	0.689
	Female	1 (%)	1 (%)	
Age	15-25	15 (%)	26 (%)	0.061
	26-35	16 (%)	19 (%)	
	36-45	6 (%)	10 (%)	
	>45	7 (%)	1 (%)	
Job Category	Cook	17 (%)	20 (%)	0.805
	Assistant Cook	3 (%)	5 (%)	
	Waiter	8 (%)	14 (%)	
	Others (e.g., cleaners, cashiers…)	16 (%)	17 (%)	
Educational Status	Literature	8 (%)	5 (%)	0.443
	Read and Write Only	3 (%)	6 (%)	
	Primary	20 (%)	22 (%)	
	Secondary	10 (%)	20 (%)	
	University	3 (%)	3 (%)	

Table 2 indicates no significant correlation between sociodemographic factors and nasal carriage of *S. aureus* among food handlers in Dhamar City. The study may not have sufficient power to detect smaller associations, so more research with larger sample sizes is needed to examine other factors, such as health or sanitary conditions. In this study, a significant portion had only primary education (42%) or were illiterate (13%), which may limit their understanding of hygiene and food safety regulations.

Table 3: Susceptibility pattern of *S. aureus* to methicillin and Vancomycin.

Antimicrobial agent	Resistance (No. %)	Intermediate (No. %)	Sensitive (No. %)
Methicillin	23 (52.3%)	2 (4.5%)	19 (43.2%)
Vancomycin	6 (13.6%)	6 (13.6%)	32 (72.8%)

The study revealed a high prevalence of *MRSA*, with 52.3% of *S. aureus* isolates showing methicillin resistance. This indicates a significant public health concern due to the difficulty in treating *MRSA* infections with standard antibiotics. This resistance underscores the urgent need for enhanced infection control measures, particularly in food-handling environments, where bacterial transmission can cause foodborne illnesses. Poor sanitation, improper handwashing, and inadequate handling of contaminated surfaces may facilitate the spread of MRSA among food handlers.

Globally, *S. aureus* has become increasingly resistant to vancomycin and β-lactam antibiotics, making it one of the most dangerous bacteria [32-34]. Several studies have identified *MRSA* as a causative agent of community-acquired infections worldwide [35-38]. The *MRSA* prevalence in this study (52.3%) is higher than reported in other countries, such as Egypt (32%) [39], Ghana (28%) [40], Nigeria (9.43%) [41], and Iran (38.14% and 31.31%) [42, 43], but lower than the study in Sana'a, Yemen (66.7%) [25]. The higher *MRSA* percentage in the present study may be attributed to antibiotic overuse and misuse, poor infection control practices, and limited healthcare infrastructure. Given these findings, it is crucial to implement strict antimicrobial stewardship, routine screening for *MRSA*, and comprehensive hygiene training programs to control its spread and ensure public health safety.

As seen in Table 3, identifying 13.6% of isolates with reduced susceptibility to Vancomycin and 13.6% exhibiting intermediate resistance raises significant public health concerns. These isolates should be considered as showing 'presumptive *VRSA*,' and the need for confirmatory testing is crucial to validate these findings. Although 72.8% of isolates remain sensitive, resistance detection indicates a potential risk of treatment failure, particularly in severe infections, since Vancomycin is one of the primary treatment options for *MRSA* infections. The emergence of resistance further limits available therapeutic strategies and poses a significant challenge to infection control efforts [44-46].

Globally, *VRSA* prevalence has risen dramatically, with data from Scopus, Embase, PubMed, and Web of Science showing a 3.5-fold increase between 2006 and 2020 [16]. Before 2006, *VRSA* prevalence was 2%, rising to 5% from 2006 to 2014 and further increasing to 7% between 2015 and 2020, reflecting the growing challenge of antibiotic resistance. In this study, the *VRSA* prevalence (13.6%) is comparable to rates reported in Egypt (13.8%) [47]. However, it is notably higher than in Ethiopia (7%) [19]and Iran (0%) [43]. The high rate of *VRSA* in Yemen may be linked to the high rate of *MRSA*, poor surveillance systems, and the wrong use of antibiotics, all of which could lead to antibiotic resistance. Nonetheless, additional research is required to validate these associations.

The detection of *VRSA* among food handlers also poses a significant risk of transmission to food products and consumers, increasing concerns over foodborne infections. Strict antimicrobial stewardship, enhanced monitoring, and stronger infection control measures must be implemented to prevent the further spread of *VRSA*. Addressing inappropriate antibiotic use, improving hygiene practices, and reinforcing infection prevention strategies are essential to curbing *VRSA* transmission and safeguarding public health.

3. Conclusions

The study reveals a high prevalence of *S. aureus* among food handlers in Dhamar, including MRSA (52.3%) and presumptive VRSA (13.6%), posing a significant food safety risk. Contributing factors include poor hygiene, low levels of education, and antibiotic misuse. To mitigate these risks, strengthening hygiene training, enforcing food safety regulations, promoting antimicrobial stewardship, and conducting regular health screenings are crucial for protecting public health.

Ethical Approval

Before this research project could be carried out, the Public Health and Population Office, Dhamar Branch, and the Institute for Continuous Education at Thamar University gave their approval. Data were gathered after each food handler provided written consent.

Subject Consent

Verbally informed consent was obtained from the parents or legal guardians of all participating children after a full explanation of the study's purpose and procedures. Participation was voluntary, and consent was reaffirmed before data collection. All collected data were anonymized and used solely for research purposes.

Data Availability

The datasets used and analyzed during the current study are available from the corresponding author upon reasonable request.

Funding

This research received no specific grant from any funding agency in the public, commercial, or not-for-profit sectors.

Conflict of Interest

The authors declare that there are no conflicts of interest.

Acknowledgment

The authors extend their sincere appreciation to the researchers who supported the project: Khadeeja Al-Nomery, Yahya Al-Ghashm, Balqis Al-Thejre, Najm Al-Razhy, Fatoom Mohammed, Ayman Al-Yemeni, Rehab Al-Qadadi, Riyad Al-Ziadi, Hakema Al-Saiady, and Najwa Abu-Hasan in the Department of Medical Laboratory, Institute for Continuous Education, Thamar University, Yemen.

References

[1] Pal, M., Gutama, K.P., Koliopoulos, T. (2021) *Staphylococcus aureus*, an important pathogen of public health and economic importance: A comprehensive review, *Journal of Emerging Environmental Technologies and Health Protection* **4**: 17-32.

[2] Kwiecinski, J.M., Horswill, A.R. (2020) *Staphylococcus aureus* bloodstream infections: pathogenesis and regulatory mechanisms, *Current Opinion in Microbiology* **53**: 51-60.

[3] Cheung, G.Y.C., Bae, J.S., Otto, M. (2021) Pathogenicity and virulence of *Staphylococcus aureus*, *Virulence* **12**: 547-569.

[4] Ahmad-Mansour, N., Loubet, P., Pouget, C., Dunyach-Remy, C., Sotto, A., Lavigne, J.P., Molle, V. (2021) Staphylococcus aureus Toxins: An Update on Their Pathogenic Properties and Potential Treatments, *Toxins (Basel)* **13**: 677.

[5] Grispoldi, L., Karama, M., Armani, A., Hadjicharalambous, C., Cenci-Goga, B.T. (2021) *Staphylococcus aureus* enterotoxin in food of animal origin and staphylococcal food poisoning risk assessment from farm to table, *Italian Journal of Animal Science* **20**: 677-690.

[6] Lv, G., Jiang, R., Zhang, H., Wang, L., Li, L., Gao, W., Zhang, H., Pei, Y., Wei, X., Dong, H., Qin, L. (2021) Molecular Characteristics of *Staphylococcus aureus* From Food Samples and Food Poisoning Outbreaks in Shijiazhuang, China, *Frontiers in Microbiology* **12**: 652276.

[7] Bencardino, D., Amagliani, G., Brandi, G. (2021) Carriage of *Staphylococcus aureus* among food handlers: An ongoing challenge in public health, *Food Control* **130**: 108362.

[8] Marques, V.F., Motta, C.C., Soares, B.D., Melo, D.A., Coelho, S.M., Coelho, I.D., Barbosa, H.S., Souza, M.M. (2017) Biofilm production and beta-lactamic resistance in Brazilian *Staphylococcus aureus* isolates from bovine mastitis, *Brazilian Journal of Microbiology* **48**: 118-124.

[9] Bush, K., Bradford, P.A. (2020) Epidemiology of β-Lactamase-Producing Pathogens, *Clinical Microbiology Reviews* **33**: e00047-19.

[10] Kim, T., Chong, Y.P., Park, K.H., Bang, K.M., Park, S.J., Kim, S.H., Jeong, J.Y., Lee, S.O., Choi, S.H., Woo, J.H., Kim, Y.S. (2019) Clinical and microbiological factors associated with early patient mortality from methicillin-resistant *Staphylococcus aureus* bacteremia, *The Korean Journal of Internal Medicine* **34**: 184-194.

[11] Hell, M., Bauer, J., Laimer, M. (2016) Molekulare Diagnostik von Methicillin-resistentem *Staphylococcus aureus*, *Hautarzt* **67**: 6-15.

[12] Ahmed, O.B. (2020) Prevalence of Methicillin-Resistant *Staphylococcus aureus* and Classical Enterotoxin Genes Among Sudanese Food Handlers, *Cureus* **12**: e12289.

[13] Fooladvand, S., Sarmadian, H., Habibi, D., van Belkum, A., Ghaznavi-Rad, E. (2019) High prevalence of methicillin resistant and enterotoxin gene-positive *Staphylococcus aureus* among nasally colonized food handlers in central Iran, *European Journal of Clinical Microbiology & Infectious Diseases* **38**: 87-92.

[14] Wijesekara, P.N.K., Kumbukgolla, W.W., Jayaweera, J., Rawat, D. (2017) Review on Usage of Vancomycin in Livestock and Humans: Maintaining Its Efficacy, Prevention of Resistance and Alternative Therapy, *Veterinary Sciences* **4**: 6.

[15] Silverman, S.M., Moses, J.E., Sharpless, K.B. (2017) Reengineering antibiotics to combat bacterial resistance: click chemistry [1, 2, 3]-triazole vancomycin dimers with potent activity against MRSA and VRE, *Chemistry–A European Journal* **23**: 79-83.

[16] Wu, Q., Sabokroo, N., Wang, Y., Hashemian, M., Karamollahi, S., Kouhsari, E. (2021) Systematic review and meta-analysis of the epidemiology of vancomycin-resistance *Staphylococcus aureus* isolates, *Antimicrobial Resistance & Infection Control* **10**: 101.

[17] El-Zamkan, M.A., Mubarak, A.G., Ali, A.O. (2019) Prevalence and phylogenetic relationship among methicillin-and vancomycin-resistant *Staphylococci* isolated from hospital's dairy food, food handlers, and patients, *Journal of Advanced Veterinary and Animal Research* **6**: 463–473.

[18] El-Shenawy, M., Tawfeek, M., El-Hosseiny, L., El-Shenawy, M., Farag, A., Baghdadi, H., Saleh, O., Ma, J., Soriano, J.M. (2014) Cross sectional study of skin carriage and enterotoxigenicity of *Staphylococcus aureus* among food handlers, *Open Journal of Medical Microbiology* **4**: 16-22.

[19] Beyene, G., Mamo, G., Kassa, T., Tasew, G., Mereta, S.T. (2019) Nasal and Hand Carriage Rate of *Staphylococcus aureus* among Food Handlers Working in Jimma Town, Southwest Ethiopia, *Ethiopian Journal of Health Sciences* **29**: 605-612.

[20] Castro, A., Santos, C., Meireles, H., Silva, J., Teixeira, P. (2016) Food handlers as potential sources of dissemination of virulent strains of *Staphylococcus aureus* in the community, *Journal of Infection and Public Health* **9**: 153-60.

[21] Mahros, M.A., Abd-Elghany, S.M., Sallam, K.I. (2021) Multidrug-, methicillin-, and vancomycin-resistant *Staphylococcus aureus* isolated from ready-to-eat meat sandwiches: An ongoing food and public health concern, *International Journal of Food Microbiology* **346**: 109165.

[22] Saber, T., Samir, M., El-Mekkawy, R.M., Ariny, E., El-Sayed, S.R., Enan, G., Abdelatif, S.H., Askora, A., Merwad, A.M.A., Tartor, Y.H. (2021) Methicillin- and Vancomycin-Resistant *Staphylococcus aureus* From Humans and Ready-To-Eat Meat: Characterization of Antimicrobial Resistance and Biofilm Formation Ability, *Frontiers in Microbiology* **12**: 735494.

[23] Al-Alousi, M., Al-Omary, T., Al-Shehari, A., Al-Alwi, A. (2010) Bacterial Contamination in Some Hospitals in Thamar, *Thamar University Journal of Natural & Applied Sciences* **2**: 23-34.

[24] Edrees, W.H., Anbar, A.A.M. (2021) Prevalence and antibiotic susceptibility of *Streptococcus pyogenes* isolated from schoolchildren in Sana'a City, Yemen, *PSM Veterinary Research* **6**: 22-30.

[25] Al-Aomary, N., Edrees, W., Al-Ofairi, B., Thabit, J. (2023) Nasal carriage of *Staphylococcus aureus* and its antibacterial susceptibility profiles among food handlers in Sana'a restaurants, Yemen, *Preprints* https://doi.org/10.20944/preprints202311.0495.v1.

[26] Khatri, S., Pant, N.D., Bhandari, R., Shrestha, K.L., Shrestha, C.D., Adhikari, N., Poudel, A. (2017) Nasal Carriage Rate of Methicillin Resistant *Staphylococcus aureus* among Health Care Workers at a Tertiary Care Hospital in Kathmandu, Nepal, *Journal of Nepal Health Research Council* **15**: 26-30.

[27] Bryant, R.E., Mazza, J.A. (1989) Effect of the abscess environment on the antimicrobial activity of ciprofloxacin, *The American Journal of Medicine* **87**: 23s-27s.

[28] Procop, G.W., Church, D.L., Hall, G.S., Janda, W.M. (2020) Koneman's Color Atlas and Textbook of Diagnostic Microbiology, ed., *Lippincott Williams & Wilkins*, Philadelphia, USA, pp. 1565

[29] Cheesbrough, M. (2005) District laboratory practice in tropical countries, part 2, ed., *Cambridge University Press*, Cambridge, UK, pp. 440

[30] Alhashimi, H.M.M., Ahmed, M.M., Mustafa, J.M. (2017) Nasal carriage of enterotoxigenic *Staphylococcus aureus* among food handlers in Kerbala city, *Karbala International Journal of Modern Science* **3**: 69-74.

[31] Simsek, Z., Koruk, I., Copur, A.C., Gürses, G. (2009) Prevalence of *Staphylococcus aureus* and intestinal parasites among food handlers in Sanliurfa, Southeastern Anatolia, *Journal of Public Health Management and Practice* **15**: 518-523.

[32] Tran, N., Rybak, M.J. (2018) β-Lactam Combinations with Vancomycin Show Synergistic Activity against Vancomycin-Susceptible *Staphylococcus aureus*, Vancomycin-Intermediate *S. aureus* (VISA), and Heterogeneous VISA, *Antimicrobial Agents and Chemotherapy* **62**: e00157-18.

[33] Loomba, P.S., Taneja, J., Mishra, B. (2010) Methicillin and Vancomycin Resistant *S. aureus* in Hospitalized Patients, *Journal of Global Infectious Diseases* **2**: 275-83.

[34] Mandal, S.M., Ghosh, A.K., Pati, B.R. (2015) Dissemination of antibiotic resistance in methicillin-resistant *Staphylococcus aureus* and vancomycin-resistant S aureus strains isolated from hospital effluents, *American Journal of Infection Control* **43**: e87-88.

[35] Vaidya, P., Pawar, G., Krishnamurthy, N. (2015) Community acquired MRSA infections—Three recent cases and an overview of CA MRSA infections, *Pediatric Infectious Disease* **7**: 8-12.

[36] Yamamoto, T., Nishiyama, A., Takano, T., Yabe, S., Higuchi, W., Razvina, O., Shi, D. (2010) Community-acquired methicillin-resistant *Staphylococcus aureus*: community transmission, pathogenesis, and drug resistance, *Journal of Infection and Chemotherapy* **16**: 225-254.

[37] Otter, J.A., French, G.L. (2011) Community-associated meticillin-resistant *Staphylococcus aureus* strains as a cause of healthcare-associated infection, *Journal of Hospital Infection* **79**: 189-193.

[38] Skov, R., Christiansen, K., Dancer, S.J., Daum, R.S., Dryden, M., Huang, Y.C., Lowy, F.D. (2012) Update on the prevention and control of

community-acquired meticillin-resistant *Staphylococcus aureus* (CA-MRSA), *International Journal of Antimicrobial Agents* **39**: 193-200.

[39] Eid, H.M., El-Mahallawy, H.S., Mohammed, S.R., Mohammed, N.E.Y., Eidaroos, N.H. (2022) Multidrug-resistant and enterotoxigenic methicillin-resistant *Staphylococcus aureus* isolated from raw milk of cows at small-scale production units, *Journal of Advanced Veterinary and Animal Research* **9**: 113-121.

[40] Saba, C.K.S., Naa-Inour, F., Kpordze, S.W. (2022) Antibiotic resistance pattern of methicillin-resistant *Staphylococcus aureus* and Escherichia coli from mobile phones of healthcare workers in public hospitals in Ghana, *Pan African Medical Journal* **41**: 259.

[41] Oginni, I.O., Olayinka, A.A. (2022) Distribution and Antibiotics Resistance Pattern of Community-Acquired Methicillin-Resistance *Staphylococcus aureus* in Southwestern Nigeria, in: Donelli, G., (Ed.), Advances in Microbiology, Infectious Diseases and Public Health. Advances in Experimental Medicine and Biology, *Springer*, Cham, Switzerland, pp. 81-91.

[42] Ying, H., Mahmudiono, T., Alghazali, T., Abdelbasset, W.K., Khadivar, P., Rahimi, S., Amini, A. (2022) Molecular Characterization, Virulence Determinants, and Antimicrobial Resistance Profile of Methicillin-Resistant *Staphylococcus aureus* in the North of Iran; a High Prevalence of ST239-SCC*mec* III/t037 Clone, *Chemotherapy* **67**: 37-46.

[43] Firouzi, F., Akhtari, J., Nasrolahei, M. (2016) Prevalence of MRSA and VRSA strains of *Staphylococcus aureus* in healthcare staff and inpatients, *Journal of Mazandaran University of Medical Sciences* **26**: 96-107.

[44] Tang, J., Hu, J., Kang, L., Deng, Z., Wu, J., Pan, J. (2015) The use of vancomycin in the treatment of adult patients with methicillin-resistant *Staphylococcus aureus* (MRSA) infection: a survey in a tertiary hospital in China, *International Journal of Clinical and Experimental Medicine* **8**: 19436-19441.

[45] Shimizu, K., Orizu, M., Kanno, H., Kitamura, S., Konishi, T., Soma, K., Nishitani, H., Noguchi, Y., Hasegawa, S., Hasegawa, H., Wada, K. (1996) Clinical studies on vancomycin in the treatment of MRSA infection, *The Japanese Journal of Antibiotics* **49**: 782-99.

[46] Giuliano, C., Haase, K.K., Hall, R. (2010) Use of vancomycin pharmacokinetic-pharmacodynamic properties in the treatment of MRSA infections, *Expert Review of Anti-infective Therapy* **8**: 95-106.

[47] ElSayed, N., Ashour, M., Amine, A.E.K. (2018) Vancomycin resistance among *Staphylococcus aureus* isolates in a rural setting, Egypt, *Germs* **8**: 134-139.

TUJNAS

Original Article

Thamar University Journal of Natural & Applied Sciences 10(2) (2025) 22– 26

DOI: https://doi.org/10.59167/tujnas.v10i2.3014

Phytochemical Screening of Some Medicinal Plants and Antibacterial Activity against Bacteria Isolated from Clinical Specimens - Dhamar City – Yemen

Hussein K. Salam[1,*], Morad G. S. Al-asbahi[1,2], Doa'a A. Omar[1], Jihad A. Alwashli[1], Huda H. Alqarni[1], Aseel M. Al-Jama'id[1], and Raoof Sultan[3]

[1]Biology Department, Faculty of Applied Science, Thamar University, Dhamar 87246, Yemen.

[2]Laboratory Department, Faculty of Medical Sciences, Al-Hikma University, Dhamar, Yemen.

[3]Biology Department, Faculty of Education, Taiz University, Taiz, Yemen.

***Corresponding Author:** Hussein K. Salam, Biology Department, Faculty of Applied Science, Thamar University, Dhamar 87246, Yemen. Email: sallam27@gmail.com

Received: 7 August 2025. Received (in revised form): 20 October 2025. Accepted: 30 October 2025. Published: 28 December 2025.

Abstract

Medicinal plants continue to play an important role in traditional healthcare systems, particularly in regions where access to modern medicine is limited. Many of these plants are known to contain bioactive compounds with antimicrobial properties. This study aimed to investigate the phytochemical composition and antibacterial activity of aqueous extracts from *Solanum incanum* (leaves and fruits), *Dodonaea viscosa* (leaves), and *Argemone mexicana* (leaves) against selected bacterial pathogens isolated from clinical specimens in Dhamar City, Yemen. Qualitative phytochemical screening was carried out using standard methods to detect major secondary metabolites, while antibacterial activity was evaluated using the agar well diffusion technique. The tested bacterial species included *Escherichia coli*, *Staphylococcus aureus*, *Klebsiella* spp., and *Salmonella* spp. The screening results revealed the presence of several bioactive compounds, including alkaloids, phenols, tannins, flavonoids, steroids, terpenoids, saponins, and glycosides, although their distribution varied among the extracts. Alkaloids, phenols, and tannins were consistently detected in all tested samples. Among the evaluated extracts, the aqueous fruit extract of *S. incanum* showed the strongest antibacterial activity, particularly at a concentration of 100 mg/mL. The largest zones of inhibition were observed against *E. coli* (22 ± 1.6 mm), followed by *Salmonella* spp. (18.6 ± 1.7 mm), *Klebsiella* spp. (17.7 ± 1.2 mm), and *S. aureus* (15 ± 0.8 mm). Overall, the findings highlight the antibacterial potential of *S. incanum*, especially its fruit extract, and support its traditional use as a medicinal plant. Further studies are recommended to isolate and characterize the active compounds and to evaluate their potential as alternative antimicrobial agents.

Keywords: Phytochemical screening; Antibacterial activity; Medicinal plants; *Solanum incanum*; Yemen

1. Introduction

Yemen is known for its rich plant biodiversity, with many species traditionally used for medicinal purposes. For generations, these plants have played an essential role in healthcare, particularly in rural communities where access to modern medical facilities remains limited. In such settings, traditional medicine continues to be the primary source of treatment for a wide range of illnesses, relying on local knowledge passed down through generations [1, 2]. This reliance on medicinal plants reflects both cultural practices and practical necessity.

Medicinal plants have long attracted scientific interest because they contain phytochemicals—naturally occurring bioactive compounds that contribute to their therapeutic properties. According to the World Health Organization, nearly 80% of the global population uses herbal remedies as part of primary healthcare, largely due to their accessibility, affordability, and perceived safety [3]. These phytochemicals include alkaloids, flavonoids, phenols, terpenoids, tannins, sterols, and glycosides, many of which exhibit antimicrobial, anti-inflammatory, and antioxidant activities [4, 5].

Among the medicinal plants widely used in traditional medicine, species belonging to the genus *Solanum* have received considerable attention for their antimicrobial potential. *Solanum incanum* L. (family Solanaceae) is one such species and is commonly used in folk medicine. Previous studies have reported that this plant contains solanine and other steroidal alkaloids that show activity against several pathogenic microorganisms [6, 7]. Similarly, *Dodonaea viscosa* L. (family Sapindaceae) has been investigated for its antibacterial properties, with reports indicating its effectiveness against *Staphylococcus aureus* and other Gram-positive bacteria, particularly in the treatment of skin infections [8-11].

Another plant of interest is *Argemone mexicana* L. (family Papaveraceae), commonly known as Ghamoya. Although native to South

America, it is now widely distributed in tropical and subtropical regions and has become well established in parts of Yemen. Traditionally, different parts of the plant—especially the leaves—have been used to treat wounds, skin infections, ulcers, cough, and itching. Because of its availability and ethnomedicinal importance, *A. mexicana* has been the subject of several studies exploring its antimicrobial and antifungal activities [12-14].

In recent years, the growing problem of antibiotic resistance has intensified the search for new antimicrobial agents. The misuse and overuse of antibiotics in both clinical practice and agriculture have contributed significantly to the emergence of multidrug-resistant bacteria [15, 16]. These resistant pathogens are increasingly responsible for both hospital-acquired and community-acquired infections [17, 18]. Common bacterial species such as *Escherichia coli*, *Klebsiella pneumoniae*, *Salmonella* spp., *Staphylococcus aureus*, and *Pseudomonas aeruginosa* have developed resistance to many commonly used antibiotics, posing serious challenges to public health worldwide [17, 19]. Recent estimates suggest that antibiotic-resistant infections are responsible for millions of illnesses and tens of thousands of deaths each year [20, 21].

Despite Yemen's long history of traditional medicine and its wide variety of medicinal plants, scientific studies evaluating the antimicrobial potential of native plant species remain limited. In particular, there is a lack of laboratory-based evidence supporting the use of commonly used plants against clinically relevant bacterial pathogens. Therefore, the present study aimed to evaluate the phytochemical composition and antibacterial activity of aqueous extracts from the leaves of *S. incanum*, *D. viscosa*, and *A. mexicana*, as well as the fruits of *S. incanum*. The antibacterial activity of these extracts was assessed against selected bacterial isolates (*E. coli*, *S. aureus*, *Klebsiella* spp., and *Salmonella* spp.) obtained from clinical specimens in Dhamar City, Yemen, with the goal of identifying potential plant-based alternatives for antimicrobial therapy.

2. Materials and Methods

2.1 Plant Collection

Leaves of *Solanum incanum*, *Dodonaea viscosa*, and *Argemone mexicana*, as well as fruits of *S. incanum* (Figure 1), were collected from different locations within Dhamar City, Yemen, between August and September 2024. Fresh plant materials were selected to avoid contamination or degradation. Botanical identification was carried out by specialists from Thamar University, and voucher specimens were authenticated to ensure correct species identification before laboratory analysis.

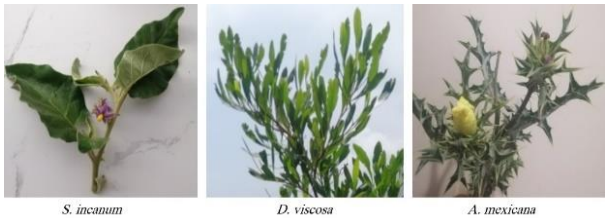

Figure 1: Medicinal plants used in the study collected from Dhamar City, Yemen: *Solanum incanum* (leaves and fruits), *Dodonaea viscosa* (leaves), and *Argemone mexicana* (leaves).

2.2 Preparation of Extracts

Fresh plant materials were washed, air-dried in the shade, and then pulverized using a laboratory blender. Approximately 10 grams of the dried and powdered plant material were extracted twice by maceration in 100 mL of distilled water. The mixtures were agitated continuously for three days using an orbital shaker. After maceration, the solutions were filtered through Whatman No. 1 filter paper. The resulting crude aqueous extracts were concentrated by evaporation in a water bath at 50°C, then weighed and stored in sterile, airtight containers at 4 °C for subsequent use within two weeks [22]. Three concentrations of plant extracts were used, each at 100 mg/ml, 50 mg/ml, and 25 mg/ml. These extracts were subsequently subjected to phytochemical screening [23].

2.3 Phytochemical Screening

Standard qualitative methods were used to detect the presence of major phytochemicals, including alkaloids, flavonoids, phenols, tannins, saponins, terpenoids, steroids, and glycosides. Procedures were adapted from established protocols [24, 25] as described in Table 1.

Table 1: Qualitative phytochemical screening tests used for the detection of major secondary metabolites in aqueous plant extracts.

Phytoconstituents	Test	Observation
Alkaloids	Mayer's test	Creamy or white precipitate
Phenols	Ferric chloride test	Blue-black coloration
Flavonoids	Alkaline reagent test	Yellow color and colorless on the addition of 3 drops of HCl
Tannin	Braymer's Test	Green precipitate
Glycosides	Killer Killiani test	Reddish brown at the junction
Saponins	Froth test	Layer of foam
Steroids	Liebermann-Burchard test	Brown ring at the junction
Terpenoids	Salhowski test	Reddish brown coloration

2.4 Antibacterial Activity

2.4.1 Sample Collection

Clinical bacterial isolates were obtained from patients at Taiba Hospital and Al-Dubai Specialized Laboratories between September and November 2024. Samples were transported to microbiology laboratories at Thamar University and Al-Hikma University (Dhamar) for analysis. Isolates were cultured on nutrient agar and incubated at 37°C for 24 hours. Identification of bacterial strains—*Escherichia coli*, *Klebsiella* spp., *Salmonella* spp., and *Staphylococcus aureus*—was performed using standard biochemical techniques [26].

2.4.2 Inoculum Preparation

Three to four well-isolated colonies of each bacterial strain were selected and inoculated into peptone water, followed by incubation at 35°C for three hours. The resulting turbidity was adjusted to match the 0.5 McFarland standard, ensuring a uniform bacterial concentration suitable for sensitivity testing.

2.4.3 Assessment of Antibacterial Activity

Antibacterial efficacy of the plant extracts was evaluated using the agar well diffusion method, as described by [27]. A standardized bacterial suspension (10^8 CFU/mL) was spread evenly across sterile Mueller-Hinton Agar (MHA) plates using sterile cotton swabs. After allowing the surface to dry, wells of 6 mm diameter were created using a sterile cork borer. Each well was filled with 20 µL of the respective plant extract using a sterile syringe, and a positive control (Amoxicillin 10 mcg) was added. Plates were incubated at 37 ± 2°C for 24 hours. Following incubation, zones of inhibition were measured in millimeters using a digital caliper. All experiments were conducted in triplicate to ensure reliability and reproducibility.

2.5 Data Analysis

All data were expressed as mean ± standard deviation. Statistical analysis was performed using one-way analysis of variance (ANOVA) via SPSS software (version 21, 2006). Differences among means were analyzed using the Student–Newman–Keuls post hoc test, with statistical significance accepted at $p < 0.05$.

3. Results and Discussion

3.1 Phytochemical Screening

Qualitative phytochemical screening revealed the presence of several secondary metabolites across the tested plant extracts, although their distribution varied among species and plant parts (Table 2). Alkaloids, phenols, and tannins were consistently detected in all extracts, suggesting that these compounds are common constituents of the selected medicinal plants. Flavonoids were present in most extracts but were not detected in the leaves of *Solanum incanum*. Saponins were absent in *Dodonaea viscosa*, while steroids and terpenoids were mainly confined to the fruit extract of *S. incanum*.

These findings are in agreement with previous studies. For instance, Karanja et al. (2021)[28] Reported that *S. incanum* fruits contain alkaloids, glycosides, steroids, tannins, flavonoids, phenols, saponins, and terpenoids. Similar results were found by Akanmu et al. (2019) [29], who observed the presence of cardiac glycosides, flavonoids, terpenoids, and steroids in *S. incanum* extracts. Jepkoech and Gakunga (2017) [21] also identified alkaloids as dominant compounds, followed by saponins and steroid glycosides, with terpenoids, flavonoids, and cardiac glycosides detected in lesser amounts.

Table 2: Phytochemical constituents detected in aqueous extracts of *Solanum incanum* (leaves and fruits), *Dodonaea viscosa* (leaves), and *Argemone mexicana* (leaves).

Phyto \ Plants	*Solanum incanum* leaves	*Solanum incanum* fruit	*Dodonaea viscosa*	*Argemone mexicana*
Alkaloids	+ve	+ ve	+ ve	+ ve
Phenols	+ ve	+ ve	+ ve	+ ve
Flavonoids	- ve	+ ve	+ ve	+ ve
Tannin	+ ve	+ ve	+ ve	+ ve
Glycosides	+ ve	+ ve	- ve	- ve
Saponins	+ ve	+ ve	- ve	+ ve
Steroids	- ve	+ ve	- ve	- ve
Terpenoids	- ve	+ ve	- ve	- ve

(+ve indicates presence; −ve indicates absence)

The presence of glycosides and saponins in several extracts is pharmacologically significant, as these compounds are known for their ability to combat microbial infections [24]. Their identification in this study further supports the medicinal value of these plants and their potential application in the development of novel antibacterial formulations.

3.2 Susceptibility of Bacterial Isolates to Plant Extracts

The antibacterial activity of each plant extract was assessed against three isolates of each bacterial species using the well-diffusion method. These species are known pathogens commonly implicated in human infections. Results indicated that all tested plant extracts exhibited antibacterial activity, though to varying degrees. This supports the concept that medicinal plants are rich reservoirs of bioactive compounds with antimicrobial potential [30].

Notably, the fruit extract of *S. incanum* displayed the strongest antibacterial effect across all bacterial isolates at a concentration of 100 mg/mL (Table 3), followed by its leaf extract. In contrast, the aqueous leaf extract of *D. viscosa* exhibited comparatively lower antibacterial efficacy. The enhanced activity of *S. incanum* extracts may be attributed to the higher concentration and diversity of phytochemicals present in its tissues [28]. As highlighted by Femi-Adepoju (2023) [31], the antimicrobial activity of plant-derived extracts is closely linked to the nature and abundance of their phytochemical constituents.

3.3 Antibacterial Activity Assessed by the Well Diffusion Method

This study evaluated the antibacterial properties of aqueous extracts from *S. incanum* (leaves and fruits), *D. viscosa* (leaves), and *Argemone mexicana* (leaves) against four clinically significant bacterial species: *Escherichia coli*, *Salmonella* spp., *Klebsiella* spp., and *Staphylococcus aureus*. Antibacterial activity was determined by measuring the zones of inhibition around the wells.

Among all extracts tested, the aqueous fruit extract of *S. incanum* exhibited the highest antibacterial activity. This can be attributed to its diverse range of phytochemical constituents—including alkaloids, glycosides, steroids, tannins, flavonoids, phenols, saponins, and terpenoids—which are known for their antimicrobial mechanisms [32, 33]. The solubility of these secondary metabolites in water may further enhance their bioactivity in aqueous extracts.

Each major class of phytochemicals contributes to antibacterial activity via specific mechanisms: Alkaloids act through various pathways, including inhibiting bacterial DNA replication, interfering with respiratory enzymes, disrupting membrane integrity, and modulating virulence gene expression. Phenolic compounds, including flavonoids and simple phenols, exhibit antimicrobial effects by forming stable complexes with bacterial proteins, inhibiting essential enzymes, and disrupting microbial membranes [34, 35].

Flavonoids contribute via direct interaction with bacterial membranes and oxidative disruption. Their activity is influenced by molecular structure; some studies report greater activity with increased hydroxylation [36], while others suggest higher membrane permeability in flavonoids lacking hydroxyl groups on the B-ring [37].

Overall, the extracts demonstrated differential efficacy against the bacterial strains, with *E. coli* showing the most significant susceptibility, followed by *Klebsiella* spp., *Salmonella* spp., and *S. aureus*.

In Tables 4 and 5, significant differences were observed between the plant extract and the bacteria used, except for *S.aureus* bacteria with Solanum leaves.

Previous studies support these findings. For instance, methanolic extracts of *A. mexicana* showed significant inhibition against *E. coli* and *Klebsiella* spp. at 100 mg/mL[38]. However, Sbhatu and Abraha (2020) [39] reported that *S. incanum* fruit extracts showed particularly high activity against Salmonella typhi. Similarly, Al-Haj et al. (2019)[40] found that methanolic extracts of *D. viscosa* produced inhibition zones of 8–9 mm against *S. aureus*. Importantly, our findings support a dose-dependent relationship, as greater inhibition was observed with higher extract concentrations—a trend consistent with other studies [41-43].

Table 3: Susceptibility of clinical bacterial isolates to different concentrations of aqueous plant extracts, expressed as number and percentage of responsive isolates.

Plants	Concentration of the plant extract	Bacteria							
		E. coli No = 3		*Salmonella* spp. No = 3		*Klebsiella* spp. No = 3		S. aureus No = 3	
		No.	%	No.	%	No.	%	No.	%
***Solanum incanum* leaves**	25 mg	1	33.3	0	0	0	0	1	33.3
	50 mg	2	66.7	2	66.7	1	33.3	1	33.3
	100 mg	3	100	2	66.7	2	66.7	2	66.7
***Solanum incanum* Fruit**	25 mg	3	100	2	66.7	3	100	2	66.7
	50 mg	3	100	3	100	3	100	3	100
	100 mg	3	100	3	100	3	100	3	100
***Dodonaea viscosa* leaves**	25 mg	0	0	0	0	0	0	0	0
	50 mg	1	33.3	1	33.3	2	66.7	1	33.3
	100 mg	2	66.7	2	66.7	2	66.7	2	66.7
***Argemone mexicana* leaves**	25 mg	0	0	0	0	0	0	0	0
	50 mg	1	33.3	2	66.7	2	66.7	1	33.3
	100 mg	2	66.7	2	66.7	3	100	2	66.7

Table 4: Antibacterial activity of aqueous plant extracts against selected bacterial species, measured as zones of inhibition (mm) using the agar well diffusion method.

Plants	Bacteria	Inhibition Zone (mm) (mean ± SD of 3 isolates			Control positive
		25 mg	50 mg	100 mg	
Solanum incanum leaves	*S. aureus*	10.3 ± 1.2	11.3 ± 1.7	13.3 ± 1.2	10 ± 0.8
	E. coli	7.3 ± 0.46	10.7 ± 0.46	14.3 ± 1.2	23.6 ± 1.2
	Salmonella spp.	0	10 ± 1.6	14.6 ± 0.46	22 ± 1.4
	Klebsiella spp.	0	8.7 ± 0.46	10.7 ± 0.94	11 ± 0.8
Solanum incanum Fruit	*S. aureus*	11 ± 1.6	13.3 ± 0.46	15 ± 0.8	10 ± 0.8
	E. coli	15.3 ± 1.2	18.6 ± 1.2	22 ± 1.6	23.6 ± 1.2
	Salmonella spp.	14.3 ± 1.7	16.3 ± 1.2	18.6 ± 1.7	22 ± 1.4
	Klebsiella spp.	8 ± 0.8	13.6 ± 1.2	17.7 ± 1.2	11 ± 0.8
Dodonaea viscosa leaves	*S. aureus*	0	7.3 ± 0.46	9.6 ± 0.46	10 ± 0.8
	E. coli	0	8.3 ± 1.2	12.3 ± 1.2	23.6 ± 1.2
	Salmonella spp.	0	7	8.3 ± 1.2	22 ± 1.4
	Klebsiella spp.	0	8 ± 0.8	10.3 ± 0.46	11 ± 0.8
Argemone mexicana leaves	*S. aureus*	0	9.6 ± 1.2	12 ± 0.8	10 ± 0.8
	E. coli	0	7.3 ± 0.46	8.3 ± 0.46	23.6 ± 1.2
	Salmonella spp.	0	8.6 ± 0.9	9	22 ± 1.4
	Klebsiella spp.	0	10 ±1.6	12.3 ± 1.2	11 ± 0.8

Values are presented as mean ± standard deviation (n = 3). Amoxicillin (10 µg) was used as a positive control.

Table 5: Statistical significance (p-values) of antibacterial activity between plant extracts and tested bacterial species.

Plants ex. / Bacteria sp.	*Solanum incanum* leaves	*Solanum incanum* fruit	*Dodonaea viscosa*	*Argemone mexicana*
S. aureus	0.23^{ns}	0.0029^{**}	$<0.0001^{***}$	$<0.0001^{***}$
E. coli	$<0.0001^{***}$	$<0.0001^{***}$	$<0.0001^{***}$	$<0.0001^{***}$
***Salmonella* spp.**	$<0.0001^{***}$	0.0011^{**}	$<0.0001^{***}$	$<0.0001^{***}$
***Klebsiella* spp.**	$<0.0001^{***}$	$<0.0001^{***}$	$<0.0001^{***}$	$<0.0001^{***}$

Significance levels: ns = not significant ($p > 0.05$), ** = significant ($p < 0.01$), *** = highly significant ($p < 0.001$).

4. Conclusion

This study demonstrated that aqueous extracts from selected medicinal plants commonly used in Yemen possess measurable antibacterial activity against clinically relevant bacterial pathogens. Among the tested plants, the fruit extract of *Solanum incanum* showed the strongest and most consistent antibacterial effect, which may be attributed to its rich and diverse phytochemical composition. The observed dose-dependent inhibition supports the role of plant-derived secondary metabolites as contributors to antimicrobial activity. These findings provide scientific support for the traditional use of *S. incanum*, *Dodonaea viscosa*, and *Argemone mexicana* in the treatment of infectious diseases. Although the results are limited to in vitro conditions, they highlight the potential of these plants—particularly *S. incanum*—as accessible sources of antibacterial agents. Further studies are warranted to isolate active compounds, evaluate their mechanisms of action, and assess safety and efficacy in vivo, with the aim of developing cost-effective alternatives to conventional antibiotics.

Data Availability

The datasets used and analyzed during the current study are available from the corresponding author upon reasonable request.

Funding

This research received no specific grant from any funding agency in the public, commercial, or not-for-profit sectors.

Conflict of Interest

The authors declare that there are no conflicts of interest.

References

[1] Al-Dubai, A., Al-Khulaidi, A. (2005) Medicinal and aromatic plants in Yemen: Deployment-components of effective-uses, ed., *Ebadi Center for Studies and Publishing*, Sana'a, Yemen, pp. 127.

[2] Chhetri, B.K., Awadh Ali, N.A., Setzer, W.N. (2015) A survey of chemical compositions and biological activities of Yemeni aromatic medicinal plants, *Medicines* **2**: 67-92.

[3] Sahle, T., Okbatinsae, G. (2017) Phytochemical investigation and antimicrobial activity of the fruit extract of *Solanum incanum* grown in Eritrea, *Ornamental and Medicinal Plants* **1**: 15-25.

[4] Dahiru, D., Onubiyi, J., Umaru, H.A. (2006) Phytochemical screening and antiulcerogenic effect of *Moringa oleifera* aqueous leaf extract, *African Journal of Traditional, Complementary and Alternative Medicines* **3**: 70-75.

[5] Mayekar, V.M., Ali, A., Alim, H., Patel, N. (2021) A review: Antimicrobial activity of the medicinal spice plants to cure human disease, *Plant Science Today* **8**: 629-646.

[6] Britto, S.J., Senthilkumar, S. (2001) Antibacterial activity of *Solanum incanum* L. leaf extracts, *Asian Journal of Microbiology, Biotechnology & Environmental Sciences* **3**: 65-66.

[7] Owino, J., Omundi, J., Ngoci, N. (2015) Antibacterial activity of methanolic crude extract of *Solanum incanum*: Kenyan traditional medicinal plant, *International Journal of Science and Research* **4**: 560-563.

[8] Lemus, C., Smith-Ravin, J., Marcelin, O. (2021) *Mammea americana*: A review of traditional uses, phytochemistry and biological activities, *Journal of Herbal Medicine* **29**: 100466.

[9] Lima, L.G.B., Montenegro, J., Abreu, J.P.d., Santos, M.C.B., Nascimento, T.P.d., Santos, M.d.S., Ferreira, A.G., Cameron, L.C., Ferreira, M.S.L., Teodoro, A.J. (2020) Metabolite profiling by UPLC-MSE, NMR, and antioxidant properties of Amazonian fruits: Mamey Apple (*Mammea americana*), Camapu (*Physalis angulata*), and Uxi (*Endopleura uchi*), *Molecules* **25**: 342.

[10] Mothana, R.A., Abdo, S.A., Hasson, S., Althawab, F.M., Alaghbari, S.A., Lindequist, U. (2010) Antimicrobial, antioxidant and cytotoxic activities and phytochemical screening of some yemeni medicinal plants, *Evidence-Based Complementary and Alternative Medicine* **7**: 323-330.

[11] Rajamanickam, V., Rajasekaran, A., Anandarajagopal, K., Sridharan, D., Selvakumar, K., Rathinaraj, B.S. (2010) Anti-diarrheal activity of *Dodonaea viscosa* root extracts, *International Journal of Pharma and Bio Sciences* **1**: 185.

[12] Andleeb, S., Alsalme, A., Al-Zaqri, N., Warad, I., Alkahtani, J., Bukhari, S.M. (2020) In-vitro antibacterial and antifungal properties of the organic solvent extract of *Argemone mexicana* L, *Journal of King Saud University-Science* **32**: 2053-2058.

[13] Ibrahim, H., Ibrahim, H. (2009) Phytochemical screening and toxicity evaluation on the leaves of *Argemone mexicana* Linn. (Papaveraceae), *International Journal of Applied Sciences* **3**: 39-43.

[14] Muinat, A.A., Mbang, F.-O.N., Lateef, B.G., Temionu, E.O., Oluyemisi, B.A. (2015) Antimicrobial studies of the leaf extract of *Argemone mexicana* and its ointment formulation, *West African Journal of Pharmacy* **26**: 33-40.

[15] Al-Gazi, Z., Al-Snafi, A., Al-Abady, F. (2016) Effect of toxoplasmosis and/or its treatment (sulpadiazine and pyrimetamine) on female rats reproductive performance, *Indian Journal of Pharmaceutical Science & Research* **6**: 35-40.

[16] Serwecińska, L. (2020) Antimicrobials and antibiotic-resistant bacteria: a risk to the environment and to public health, *Water* **12**: 3313.

[17] Bharadwaj, A., Rastogi, A., Pandey, S., Gupta, S., Sohal, J.S. (2022) Multidrug-resistant bacteria: their mechanism of action and prophylaxis, *BioMed research international* **2022**: 1-17.

[18] Othman, L., Sleiman, A., Abdel-Massih, R.M. (2019) Antimicrobial activity of polyphenols and alkaloids in middle eastern plants, *Frontiers in Microbiology* **10**: 911.

[19] Vivas, R., Barbosa, A.A.T., Dolabela, S.S., Jain, S. (2019) Multidrug-resistant bacteria and alternative methods to control them: an overview, *Microbial Drug Resistance* **25**: 890-908.

[20] Femi-Adepoju, A., Oluyori, A., Fatoba, P., Adepoju, A. (2021) Phytochemical and antimicrobial analysis of *Dryopteris filix-mas* (L.) Schott, *Rasayan Journal of Chemistry* **14**: 616-621.

[21] Jepkoech, K.E., Gakunga, N.J. (2016) Antimicrobial activity and phytochemical screening of *Solanum incanum* fruit extract against clinical samples of *Staphylococcus aureus* collecting from Nakuru Provincial General Hospital Laboratory, Kenya, *The International Research Journal of Medicine and Biomedical Sciences* **2**: 1-8.

[22] Adepoju, A., Fadiji, A., Femi-Adepoju, A., Akinyemi, A., Durodola, F. (2021) Comparative antimicrobial, phytochemical, nutritional and GC-MS profiling of methanolic extracts of Solanum Sect, *Melongena: International Journal of Agricultural and Biological Sciences* **4**: 82-91.

[23] Almaqtari, M.A., Mubarak, A.Y. (2024) Antioxidant and antimicrobial of three extracts of *Caralluma deflersiana* Laver, *Sana'a University Journal of Applied Sciences and Technology* **2**: 154-157.

[24] Al-Mekhlafi, N.A., Al-Badaii, F., Al-Ezzi, M.S., Al-Yamani, A., Almakse, E., Alfaqeeh, R., Al-Hatar, G., Al-Twity, M., Al-Masadi, M., Abdullah, M. (2023) Phytochemical Analysis and Antibacterial Studies of Some Yemeni Medicinal Plants against Selected Common Human Pathogenic Bacteria, *Thamar University Journal of Natural & Applied Sciences* **8**: 14–18.

[25] Kumar, K., Henry, D.C., Sivakumar, K. (2019) Bioprofiling of phytochemicals and phytonutritional potentials of *Solanum incanum* L, *World Scientific News* **128**: 328-347.

[26] De la Maza, L.M., Pezzlo, M.T., Bittencourt, C.E., Peterson, E.M. (2020) Color Atlas of Medical Bacteriology, 3rd ed., *ASM Press*, Washington, USA, pp. 464

[27] Rani, J.M.J., Chandramohan, G., Kumaravel, S. (2012) Evaluation of antimicrobial activity of some garden plant leaves against *Lactobacillus Sp, Streptococcus mitis, Candida albicans* and *Aspergillus niger*, *African Journal of Basic & Applied Sciences* **4**: 139-142.

[28] Karanja, L.N., K'Owino, I.O., Wangila, P.T., Ramkat, R.C. (2021) Phytochemical Composition and Antibacterial Activity of Fruit Extract of *Solanum incanum* L. against *Ralstonia solanacearum*, *Asian Journal of Applied Chemistry Research* **9**: 1-16.

[29] Akanmu, A.O., Bulama, Y.A., Balogun, S.T., Musa, S. (2019) Antibacterial activities of aqueous and methanol leaf extracts of *Solanum incanum* Linn. (Solanaceae) against multi-drug resistant bacterial isolates, *African Journal of Microbiology Research* **13**: 70-76.

[30] Pérez-Narváez, O.A., Castillo Hernández S, S.L., Leos-Rivas, C., Pérez-Hernández, R.A., Chávez-Montes, A., Verduzco-Martínez, J.A., Sánchez-García, E. (2023) Antibacterial Effect of Ethanolic Extracts of *Dodonaea viscosa* L. *Jacq.* and *Mammea americana* L. against *Staphylococci* Isolated from Skin Lesions, *BioMed Research International* **2023**: 5584412.

[31] Femi-Adepoju, A., Adepoju, A., Fadiji, A.E. (2023) Antimicrobial Potential and Biochemical Profile of Methanolic Extracts of Common *Solanum* Species in Nigeria, *Dhaka University Journal of Pharmaceutical Sciences* **22**: 163–172.

[32] Bansal, A., Priyadarsini, C. (2022) Medicinal Properties of Phytochemicals and Their Production, in: El-Shemy, H.A., (Ed.), Natural Drugs from Plants, *IntechOpen*, London, UK, pp. 151.

[33] Indhumathi, T., Mohandass, S. (2014) Efficacy of ethanolic extract of *Solanum incanum* fruit extract for its antimicrobial activity, *International Journal of Current Microbiology and Applied Sciences* **3**: 939-949.

[34] Mason, T.L. (1987) Inactivation of red beet β-glucan synthase by native and oxidized phenolic compounds, *Phytochemistry* **26**: 2197-2202.

[35] Cowan, M.M. (1999) Plant Products as Antimicrobial Agents, *Clinical Microbiology Reviews* **12**: 564-582.

[36] Sato, M., Fujiwara, S., Tsuchiya, H., Fujii, T., Iinuma, M., Tosa, H., Ohkawa, Y. (1996) Flavones with antibacterial activity against cariogenic bacteria, *Journal of Ethnopharmacology* **54**: 171-176.

[37] Chabot, S., Bel-Rhlid, R., Chenevert, R., Piche, Y. (1992) Hyphal growth promotion *in vitro* of the VA mycorrhizal fungus, *Gigaspora margarita* Becker & Hall, by the activity of structurally specific flavonoid compounds under CO_2-enriched conditions, *New Phytologist* **122**: 461-467.

[38] Haruna, Y., Ukamaka (2018) Anti-Microbial and Anti-Fungal Activities of Methanol Extract of *Argemone mexicana* and its Potential Anti-Hepatitis Promises, *Journal of Clinical and Experimental Pharmacology* **8**: 1000251.

[39] Sbhatu, D.B., Abraha, H.B. (2020) Preliminary antimicrobial profile of *Solanum incanum* L.: A common medicinal plant, *Evidence-based Complementary and Alternative Medicine* **2020**: 1-6.

[40] Al-Haj, N., Reem, A., Al-Shamahy, H., Al-Moyed, K., Bahaj, S.S., Jaber, A. (2019) Antimicrobial activity of five Yemeni medicinal plants against selected human pathogenic bacteria and fungi, *American Journal of Plant Sciences* **10**: 1699-1707.

[41] Abdel Gadir, I., Abdalgadir, E., El-Shabasy, A.E. (2024) Antimicrobial potential of some medicinal plants in Saudi Arabia and Jazan region, *Egyptian Journal of Botany* **64**: 1-15.

[42] Ateshim, B., Tekle, F., Tesfay, M., Tekleab, M., Tekie, R., Weldemariam, S., Achila, O.O., Mengistu, S.T., Hamida, M.E. (2022) Antimicrobial Activity evaluation and phytochemical screening of *Silene macrosolen* and *Solanum incanum*: A common medicinal plants in Eritrea, *Preprints* https://doi.org/10.21203/rs.3.rs-1288153/v1 1-19.

[43] Mawia, K.J., Muthuka, J.K., Wambura, F.M., Muthui, J. (2020) Antibacterial Activity of *Solanum incanum* Roots and Fruits Methanol Extracts Against Gastrointestinal Bacteria Causing Food Poisoning, *Journal of Pharmacy and Biological Sciences* **15**: 53-59.

TuJNaS

Original Article

Thamar University Journal of Natural & Applied Sciences 10(2) (2025) 27– 30

DOI: https://doi.org/10.59167/tujnas.v10i2.3015

Hematological Parameters Changes in Albino Rats Vaccinated with Bacilli Calmette-Guerin

Abdullah Ali Al-Alawi[1,2,*], and Fuad Ahmed Ali Saad[3]

[1]Department of Medical Laboratory, Faculty of Medical Sciences, Thamar University, Dhamar 87246, Yemen.

[2]Medical Research Institute, Southwest University, Chongqing 400715, China.

[3]Department of Biology (Microbiology Division), Faculty of Applied Science, Thamar University, Dhamar 87246, Yemen.

***Corresponding Author:** Abdullah Ali Al-Alawi, Department of Microbiology, Faculty of Medical Sciences, Thamar University, Dhamar 87246, Yemen, and Medical Research Institute, Southwest University, Chongqing 400715, China. Tel: 0086-17265376769 or 00967-772150893, E-mails: alalawisky@tu.edu.ye or alalawisky@yahoo.com

Received: 20 April 2024. Received (in revised form): 22 October 2025. Accepted: 23 October 2025. Published: 28 December 2025.

Abstract

Scientific background: The Bacillus Calmette-Guérin vaccine (BCG) against tuberculosis (TB) has beneficial protection against TB. This study investigated changes in hematological parameters in albino rats following BCG vaccination. **Method:** An experimental study on the freeze-dried BCG strain (Danish 1331) was carried out between November and December 2019. The experimental rats were randomly divided into three groups (control group and groups receiving 0.05 ml and 0.1 ml of BCG, respectively). To evaluate the effect of BCG on WBC differential count (total leucocytes and lymphocytes), RBC count (RBC count and PCV), and platelet count. **Results:** The results revealed a statistically significant variation among the groups, particularly in body weight and erythrocyte count. Rats administered 0.05 ml of BCG exhibited a significant increase in body weight (223.00 ± 9.5 g) compared to the control (195.50 ± 32.9 g) and the 0.1 ml BCG group (176.60 ± 11.6 g). Although total leukocyte counts did not differ significantly among groups, erythrocyte counts were significantly elevated in the 0.1 ml BCG group (8.1800 ± 0.49 $\times 10^6/mm^3$), indicating enhanced erythropoietic activity. Furthermore, lymphocyte percentages were highest in the 0.05 ml group (82.600 ± 4.0%), suggesting a dose-responsive immunostimulatory effect. However, a reduction in thrombocyte levels was noted with increasing BCG dosage, with the 0.1 ml group showing the lowest count (404.20 ± 121.3/mm^3). **Conclusion:** These findings suggest that a 0.05 mL dose of BCG may positively influence body weight gain and immune cell activity.

Keywords: BCG, Rats; Hematological parameters; Vaccine; Tuberculosis

1. Introduction:

Bacillus Calmette–Guérin (BCG) is one of the oldest vaccines still in widespread use and remains a cornerstone of tuberculosis (TB) prevention programs worldwide. Developed from an attenuated strain of *Mycobacterium bovis*, the BCG vaccine has been administered for nearly a century and is given to more than 160 million individuals annually, particularly in countries with a high burden of tuberculosis [1]. Although BCG provides inconsistent protection against adult pulmonary TB, it is highly effective in preventing severe and disseminated forms of the disease in infants and young children, including miliary TB and tuberculous meningitis [2].

The protective efficacy of BCG against pulmonary tuberculosis varies widely, ranging from no measurable protection to approximately 80%, depending on geographic region, population characteristics, and environmental factors [2]. Despite this variability, BCG vaccination has been shown to elicit strong cellular immune responses, particularly in neonates and young children. Several studies have demonstrated that BCG induces T-helper 1 (Th1) immune responses characterized by the production of interferon-gamma, which plays a critical role in host defense against mycobacterial infections [3].

Tuberculosis continues to pose a major global health challenge. Each year, *Mycobacterium tuberculosis* causes millions of new infections and remains one of the leading causes of death from infectious diseases worldwide [4]. The World Health Organization estimates that more than 10 million new TB cases occur annually, with approximately 1.5–1.8 million deaths reported each year [5, 6]. Despite advances in diagnosis and treatment, gaps in healthcare access, delayed case detection, and the emergence of drug-resistant strains have hindered global TB control efforts [7]. These challenges underscore the ongoing importance of vaccination strategies and the need to better understand the biological effects of existing vaccines, such as BCG.

Beyond its role in TB prevention, BCG vaccination has been associated with broader immunological effects, including modulation of both innate and adaptive immune responses. Hematological parameters, such as red and white blood cell counts and platelet levels, are closely linked to immune function and can provide valuable insight into systemic immune activation. In vertebrates, red blood cells have been shown to participate in immune responses to pathogens, while leukocytes play a central role in host defense against bacterial and viral infections. Platelets, traditionally associated with

hemostasis, are now recognized as active participants in innate immunity and inflammatory processes [8].

Changes in hematological parameters following vaccination may therefore reflect underlying immunostimulatory effects. Experimental animal models, including albino rats, provide a controlled setting for examining these changes and allow for detailed assessment of vaccine-related physiological responses. However, data on the hematological effects of BCG vaccination remain limited, particularly in experimental settings relevant to developing countries.

To date, no published studies from Yemen have examined the impact of BCG vaccination on hematological parameters in animal models. This represents an important gap in the regional scientific literature. Accordingly, the present study aimed to evaluate the effects of different doses of the BCG vaccine on selected hematological parameters in albino rats. Specifically, the study assessed changes in red blood cell count, packed cell volume, white blood cell count, lymphocyte percentage, platelet count, and body weight following vaccination.

In addition to contributing experimental data, this study seeks to address common misconceptions within the community, particularly concerns that vaccines may negatively affect growth, blood health, or immune function. By providing evidence from a controlled laboratory study, the findings may help strengthen public confidence in vaccination and support the continued use of BCG as a safe and effective immunization tool.

2. Materials and methods

2.1 Experimental Animals

The study was performed on eighteen male albino rats. The rats were 6 to 8 weeks old and obtained from the animal house of the Faculty of Applied Sciences at Sana'a University, Yemen. The rats were housed individually in stainless steel cages. The rats were kept in a temperature-controlled room (21 ± 2 °Ċ), and a 12-hour light/dark cycle was maintained [9]. Rats are fed a standard diet and water during the adaptation period and experimentation [10].

2.2 Animal Feeding

The diet formula consists of corn 30%, soybean meal 8%, wheat bran 7%, wheat 25%, dried fish (called Wazef locally) as a source of animal protein 10%, Sorghum Stover 20%, and 1 teaspoon (3.5 kg) of the above stock of vegetable oil. The ingredients were ground, mixed together, and supplemented with multivitamins and minerals (0.5 g per 5 L). The yielded paste was rolled into cylindrical pellets and dried. Each rat received approximately 100 g/day of dried pellets. Water was supplied [11, 12]. All rats were allowed to access water and diet freely [13].

2.3 BCG Vaccine

Freeze-dried (Danish 1331) was obtained from the branch of the Public Health and Population Office in Dhamar district, Dhamar governorate. BCG is a live, attenuated vaccine (Bacillus Calmette-Guérin strain) that is reconstituted with sodium chloride injection. **(Serum Institute of India Pvt. Ltd.).** The freeze-dried vaccine (each 0.1 ml contains between 2×10^5 and 8×10^5 C.F.U.) was reconstituted in diluents immediately before vaccination [14].

2.4 Methods

2.4.1 Experimental Design

The study was performed on 18 male albino rats, which were rested and allowed to adapt for 7–10 days before the experiment. The rats were divided into three groups, with equal random assignment to each group (6 rats per group). Body weights were recorded for all rats at the beginning and at the end of the experimental period to monitor any changes associated with the treatment. The experimental rats were divided randomly into three groups, and the hematological tests were as follows:

- **Control group: 6** male albino rats were given equal volumes of normal saline.
- **Immunized group of 0.05 ml of BCG vaccine: 6** male albino rats were submitted for hematological tests after receiving 0.05 ml of BCG vaccine. BCG was injected intradermally in the back with 50 µl/rat of BCG suspension containing 10^5 colony-forming units (CFU) according to a previously described procedure.
- **Immunized group of 0.1 ml of BCG vaccine:** 6 male albino rats were submitted for hematological tests after being immunized with 0.1 ml of BCG vaccine.

2.4.2 Specimens' Collection

Specimen collection during 2-3 weeks after vaccination. Blood specimens were collected using disposable syringes. The amount of blood collected with EDTA tubes, with gentle mixing for the hematological parameters assay, was analyzed within 2 hours of collection.

2.4.3 Assay

Hematological parameters

Total red and leucocyte counts were analyzed using an automated hematological analyzer (Nihon Kohden, Jaban). Parameters reported included erythrocytes, packed cell volume (PCV), leukocyte totals (TLC), lymphocytes, and platelets. The hematological parameters were analyzed at Dubai Specialized Labs, Dhamar City, Yemen.

2.4.4 Data Analysis

The data was analyzed by normal distribution using Kolmogorov-Smirnov. The results showed that the data were distributed normally, and then after that, the data were analyzed by one-way ANOVA. The results are expressed as means ± SD. The comparison between the control and the groups. The means were compared using Duncan's method in SAS 9.1.3. program.

3. Results

Tables 1 and 2 show the pre-experiment and post-treatment body weights (in grams) of rats in three groups: control, 0.05 ml BCG, and 0.1 ml BCG. In Table 1, there are no significant differences in pre-experiment weights, with the control group averaging Mean ± SD 129.50 ± 32.0 g, the 0.05 ml BCG group 128.00 ± 15.7 g, and the 0.1 ml BCG group 136.20 ± 17.4 g, as indicated by the same superscript (a). However, there is a significant difference in post-treatment, with the 0.05 ml BCG group showing the highest weight gain (Mean ± SD 223.00 ± 9.5 g), significantly higher than the 0.1 ml BCG group (Mean ± SD 176.60 ± 11.6 g) and the control group (Mean ± SD 195.50 ± 32.9 g), as indicated by different superscripts. These findings suggest that the 0.05 ml BCG dose leads to the most significant weight increase.

Table 1: Mean ± SD of Pre-Experiment and Post-Treatment Body Weights in Rats Following BCG Vaccine Administration.

Groups	N	Pre-experiment Mean ± SD (g)	Post-treatment Mean ± SD (g)
Control group	6	129.50 ± 32[a]	195.50 ± 32.9[ab]
0.05 ml of the BCG group	6	128.00 ± 15.7[a]	223.00 ± 9.5[a]
0.1 ml of the BCG group	6	136.20 ± 17.4[a]	176.60 ± 11.6[b]

(The values with different letters mean significant differences)

Table 2 summarizes the hematological parameters (%) in rats after BCG vaccination, with statistical significance indicated by the superscript letters. The 0.1 ml BCG group had the highest RBC count (8.1800 ± 0.49 × 10^6/mm^3), followed by the control group (7.6650 ± 0.81 × 10^6/mm^3). The 0.05 ml BCG group had a significantly lower RBC count (7.2280 ± 0.67 × 10^6/mm^3), marked by superscript b. For packed cell volume (PCV), no significant differences were observed across the groups. Platelet counts were highest in the control group (Mean ±STD 520.83 ± 53.7 × 10^3/mm^3), and the 0.05 ml BCG group (Mean ±STD 461.60 ± 57.3 × 10^3/mm^3), but the 0.1 ml BCG group had a significantly lower platelet count (Mean ±STD 404.20 ± 121.3 × 10^3/mm^3), marked by superscript b. White blood cell (WBC) counts showed no significant differences between the groups. Finally, lymphocytes, the 0.05 ml BCG group (Mean ± STD 82.600 ± 4.0%) had a significantly higher percentage than the control group (Mean ± STD 73.833 ± 5.1%). In contrast, the 0.1 ml BCG group (Mean ±STD 74.800 ± 3.3%) showed no significant difference from the control group. The results of this study show that the BCG vaccine, at varying doses, leads to dose-dependent alterations in hematological parameters, with significant differences in RBC count, platelet count, and lymphocyte percentage.

Table 2: Mean hematological parameters (%) in rats following treatment with the BCG vaccine.

Groups	N	RBC ($\times 10^6/mm^3$) ± STD	PCV (%) ± STD	Platelets ($\times 10^3/mm^3$) ± STD	WBC ($\times 10^9/L$) ± STD	Lymphocytes (%) ± STD
Control group	6	7.6650 ± 0.81^{ab}	49.850 ± 4.7^{a}	520.83 ± 53.7^{a}	8.73±3.0^{a}	73.833 ± 5.1^{b}
0.05 ml of the BCG group	6	7.2280 ± 0.67^{b}	46.900 ± 4.3^{a}	461.60 ± 57.3^{ab}	9.180 ±3.2^{a}	82.600 ± 4.0^{a}
0.1 ml of the BCG group	6	8.1800 ± 0.49^{a}	52.080 ± 3.7^{a}	404.20 ±121.3^{b}	10.0 ±2.1^{a}	74.800± 3.3^{b}

(The values with different letters mean significant differences)

4. Discussion

The highest weight gain was observed with the administration of 0.05 ml of BCG vaccine, indicating that this dose is the most effective for promoting weight increase. This study was in agreement with Fisker et al. (2011), whose results showed that administering the BCG vaccine at birth appears to be beneficial for boys' growth. Perhaps the BCG vaccine played a significant role in weight gain, as this study has demonstrated [15]. This may suggest that the 0.05 ml dose is optimal for stimulating the immune system and activating metabolic pathways that promote weight gain, while effectively balancing immune activation with more efficient nutrient utilization.

Among all groups, the 0.1 ml (100 µl) BCG group showed the highest mean red blood cell (RBC) count of 8.1800 ± 0.49, and this concentration was associated with a significantly greater increase in RBC count than the 50 µl BCG group. This effect may be due to the negative impact of the higher BCG vaccine dose, which could lead to loss of appetite and decreased fluid intake, resulting in dehydration. According to Pagana K and Pagana T (2014), dehydration can significantly increase RBC counts [16]. This study aligns with the findings of Silitonga M and Silitonga PM (2017), which indicate that RBC counts tend to increase in all AEP treatments but may also rise again when BCG is administered [8]. No statistically significant difference in mean packed cell volume was observed across groups, indicating that the treatment conditions did not have a measurable impact on this parameter. Similar to these findings by Silitonga M and Silitonga PM (2017), who found no significant difference in AEP and BCG in rats with control, all of them were in the normal range [8].

Platelet counts were highest in the control group, followed by the 0.05 ml BCG group, with the lowest counts observed in the 0.1 ml BCG group. Another study supports this finding, where the dose of BCG administered appears to correlate with the severity of thrombocytopenia (low platelet count). They found that a high dose of BCG (5×10^8 viable organisms) resulted in severe thrombocytopenia in two patients, with platelet counts falling below 2,000 and persisting for two weeks [17]. This study was in disagreement with the study by Silitonga M and Silitonga PM (2017), who indicated that the PLT increased significantly in all treatments compared to the controls [8].

The study revealed that the mean total white blood cell count was comparable across all groups. The reason may be that the difference was in the differential count and not in the TLC. This finding aligns with Jensen SK *et al.* (2020), who reported no significant differences in WBC counts between the BCG and control groups, suggesting that BCG does not affect WBC levels in healthy infants [18] . On the other hand, this study disagreed with the study by Silitonga M, Silitonga PM (2017), who found that white blood cells increased significantly in treatment AEP (31.5 g/kg body weight, 31.5 g AEP/kg body weight + BCG) [8].

The analysis identified significant variations in lymphocyte counts, with the 0.05 ml BCG group showing a marked increase compared to both the control and 0.1 ml BCG groups. The elevated lymphocyte levels may be attributed to a cellular immune response triggered by the BCG vaccine. These findings are consistent with previous research demonstrating that BCG vaccination of low-birth-weight neonates in West Africa increased in vitro cytokine responses to both specific and nonspecific stimuli. BCG vaccination enhanced Th1-polarizing cytokine responses (IFN-γ), shifted the TNF-α: IL-10 ratio toward more pro-inflammatory responses, and stimulated greater production of cytokines. Furthermore, BCG was found to be particularly effective in stimulating CD4+ T lymphocytes [19]. Our study supports a trial on neonatal BCG, which found limited effects on lymphocyte subsets, including an increase in effector memory cells [20]. However, disagree with the study by Jensen SK *et al.* (2020), who found no significant differences in WBC differential counts between the BCG and control groups [18].

5. Conclusions and Recommendations

In conclusion, the administration of BCG at varying doses elicited notable hematological responses in rats. The 0.05 ml dose was associated with favorable physiological and immunological outcomes, including increased body weight and a significant rise in lymphocyte percentages, suggesting enhanced immune activation without adverse hematological effects. Conversely, the 0.1 ml dose, although effective in elevating erythrocyte count, resulted in decreased thrombocyte levels and body weight, which may indicate dose-dependent hematotoxicity or systemic stress. These findings underscore the critical importance of dose optimization to prevent adverse systemic effects.

Based on the study's findings, we recommend the following: prioritizing the BCG vaccine for its proven immune response; conducting further research on its components, adjuvants, and varying doses' effects on platelet indices; ensuring the provision of necessary resources for studies on cell-mediated and humoral immunity, as well as cytokine changes; investigating other vaccines entering the country; and conducting comparative studies on BCG vaccines from different manufacturers to assess efficacy variations.

Ethical Approval

The animal protocol in this study complied with the Guide for the Care and Use of Laboratory Animals. The BCG vaccine was obtained from the Public Health and Population Office branch in Dhamar, Dhamar Governorate. The BCG vaccine is stored at the proper temperature. The study was conducted after obtaining approval from the Biology/Microbiology Department of the Faculty of Applied Science at Thamar University.

Data Availability

The datasets used and analyzed during the current study are available from the corresponding author upon reasonable request.

Funding

This research received no specific grant from any funding agency in the public, commercial, or not-for-profit sectors.

Conflict of Interest

The authors declare that there are no conflicts of interest.

Acknowledgment

The author extends their sincere appreciation to the researchers supporting the project and to Thamar University, Faculty of Applied Science, Dhamar, Yemen.

References

[1] Nieuwenhuizen, N.E., Kulkarni, P.S., Shaligram, U., Cotton, M.F., Rentsch, C.A., Eisele, B., Grode, L., Kaufmann, S.H.E. (2017) The Recombinant Bacille Calmette-Guérin Vaccine VPM1002: Ready for Clinical Efficacy Testing, *Frontiers in Immunology* **8**: 1147.

[2] Monteiro-Maia, R., Pinho, R.T. (2014) Oral bacillus Calmette-Guérin vaccine against tuberculosis: why not?, *Memórias do Instituto Oswaldo Cruz* **109**: 838-845.

[3] Schepers, K., Dirix, V., Mouchet, F., Verscheure, V., Lecher, S., Locht, C., Mascart, F. (2015) Early cellular immune response to a new candidate mycobacterial vaccine antigen in childhood tuberculosis, *Vaccine* **33**: 1077-83.

[4] Moliva, J.I., Turner, J., Torrelles, J.B. (2017) Immune Responses to Bacillus Calmette-Guérin Vaccination: Why Do They Fail to Protect against *Mycobacterium tuberculosis*?, *Frontiers in Immunology* **8**: 407.

[5] Bloom, B.R., Atun, R., Cohen, T., Dye, C., Fraser, H., Gomez, G.B., Knight, G., Murray, M., Nardell, E., Rubin, E., Salomon, J., Vassall, A., Volchenkov, G., White, R., Wilson, D., Yadav, P. (2017) Tuberculosis, in: Holmes, K.K., Bertozzi, S., Bloom, B.R., Jha, P., (Ed.), Major Infectious Diseases, *World Bank Publications*, Washington, USA, pp. 506

[6] Zhang, L., Ru, H.W., Chen, F.Z., Jin, C.Y., Sun, R.F., Fan, X.Y., Guo, M., Mai, J.T., Xu, W.X., Lin, Q.X., Liu, J. (2016) Variable Virulence and Efficacy of BCG Vaccine Strains in Mice and Correlation With Genome Polymorphisms, *Molecular Therapy* **24**: 398-405.

[7] Floyd, K., Glaziou, P., Zumla, A., Raviglione, M. (2018) The global tuberculosis epidemic and progress in care, prevention, and research: an overview in year 3 of the End TB era, *The Lancet Respiratory Medicine* **6**: 299-314.

[8] Silitonga, M., Silitonga, P.M. (2017) Haematological profile of rats (Rattus norvegicus) induced BCG and provided leaf extract of Plectranthus amboinicus Lour Spreng. AIP Conference Proceedings, **1868**: *AIP Publishing LLC*, Yogyakarta, Indonesia, pp. 090008.

[9] Abdel-Hamid, M., Osman, A., El-Hadary, A., Romeih, E., Sitohy, M., Li, L. (2020) Hepatoprotective action of papain-hydrolyzed buffalo milk protein on carbon tetrachloride oxidative stressed albino rats, *Journal of Dairy Science* **103**: 1884-1893.

[10] Najeeb Ur, R., Mehmood, M.H., Alkharfy, K.M., Gilani, A.H. (2011) Prokinetic and laxative activities of Lepidium sativum seed extract with species and tissue selective gut stimulatory actions, *Journal of Ethnopharmacology* **134**: 878-883.

[11] Al-Hashem, F. (2009) Camel's milk protects against aluminum chloride-induced toxicity in the liver and kidney of white albino rats, *American Journal of Biochemistry and Biotechnology* **5**: 98-109.

[12] Radman, B.A., Al-Khatib, B.Y., Alaizeri, Z.M., Al-Tamimi, A.S., Al-Thahibi, W.E., Mohan, R., Alhadlaq, H.A., Ahamed, M. (2022) Histology and radiography studies of effects of Lepidium sativum seeds on bone healing in male albino rats, *Journal of King Saud University-Science* **34**: 102062.

[13] Wang, W., Dong, Z., Zhang, J., Zhou, X., Wei, X., Cheng, F., Li, B., Zhang, J. (2019) Acute and Subacute Toxicity Assessment of Oxyclozanide in Wistar Rats, *Frontiers in Veterinary Science* **6**: 294.

[14] McFarland, C.T., Ly, L., Jeevan, A., Yamamoto, T., Weeks, B., Izzo, A., McMurray, D. (2010) BCG vaccination in the cotton rat (*Sigmodon hispidus*) infected by the pulmonary route with virulent *Mycobacterium tuberculosis*, *Tuberculosis* **90**: 262-267.

[15] Fisker, A.B., Benn, C.S., Diness, B.R., Martins, C., Rodrigues, A., Aaby, P., Bibby, B.M. (2011) The Effect of 50 000 IU Vitamin A with BCG Vaccine at Birth on Growth in the First Year of Life, *Journal of Tropical Medicine* **2011**: 1-9.

[16] Pagana, K., Pagana, T. (2014) Mosby's Canadian Manual of Diagnostic and Laboratory(fifth edition), 5th ed., *Elsevier Canada*, North York, Canada, pp. 1200

[17] Norton, J.A., Shulman, N.R., Corash, L., Smith, R.L., Au, F., Rosenberg, S.A. (1978) Severe thrombocytopenia following intralesional BCG therapy, *Cancer* **41**: 820-826.

[18] Jensen, S.K., Jensen, T.M., Birk, N.M., Stensballe, L.G., Benn, C.S., Jensen, K.J., Pryds, O., Jeppesen, D.L., Nissen, T.N. (2020) Bacille Calmette-Guérin vaccination at birth and differential white blood cell count in infancy. A randomised clinical trial, *Vaccine* **38**: 2449-2455.

[19] Jensen, K.J., Larsen, N., Biering-Sørensen, S., Andersen, A., Eriksen, H.B., Monteiro, I., Hougaard, D., Aaby, P., Netea, M.G., Flanagan, K.L., Benn, C.S. (2015) Heterologous immunological effects of early BCG vaccination in low-birth-weight infants in Guinea-Bissau: a randomized-controlled trial, *The Journal of Infectious Diseases* **211**: 956-967.

[20] Birk, N.M., Nissen, T.N., Kjærgaard, J., Hartling, H.J., Thøstesen, L.M., Kofoed, P.E., Stensballe, L.G., Andersen, A., Pryds, O., Netea, M.G., Benn, C.S., Nielsen, S.D., Jeppesen, D.L. (2017) Effects of Bacillus Calmette-Guérin (BCG) vaccination at birth on T and B lymphocyte subsets: Results from a clinical randomized trial, *Scientific Reports* **7**: 12398.

TuJNaS

Thamar University Journal of Natural & Applied Sciences 10(2) (2025) 31– 35

DOI: https://doi.org/10.59167/tujnas.v10i2.3016

Original Article

Protective Effect of Testosterone against Gentamicin's Toxicity in Adult Male Rabbits

Fahmi S Moqbel[1], Nada M. H. Al Hamdani[2,*], Elham A. S. Al-Shaibani[2], Fadhl A. M. Qasem[3], Mohammad Ahmed Ali Qasim[1], Ahlam Al-Salami[1], Ameera Al-Kawli[1], Eman Al-Kawli[1], and Ola'a Al-Awadi[1]

[1]Biology Department, Faculty of Applied Science, Thamar University, Dhamar 87246, Yemen.

[2]Department of Biological Sciences, Faculty of Science, Sana'a University, Sana'a, Yemen.

[3]Department of Zoology, Faculty of Science, University of Aden, Aden, Yemen.

***Corresponding Author:** Nada M. H. Al Hamdani, Department of Biological Sciences, Faculty of Science, Sana'a University, Sana'a, Yemen. Tel: 00967-772030981 & E-mail: n.alhamdani@su.edu.ye

Received: 15 October 2025. Received (in revised form): 29 November 2025. Accepted: 30 November 2025. Published: 28 December 2025.

Abstract

Background: Gentamicin is an effective aminoglycoside antibiotic widely used in clinical practice; however, its therapeutic application is often limited by adverse effects, particularly liver and kidney toxicity. Experimental evidence suggests that sex hormones may influence susceptibility to gentamicin-induced organ damage. Testosterone, in particular, has been proposed to exert a protective effect against such toxicity. **Objective:** This study evaluated the biochemical and histopathological changes in the liver and kidneys of adult male rabbits treated with gentamicin and testosterone, administered either alone or in combination. **Methods:** Twenty adult male rabbits were randomly assigned to four groups: a control group, a gentamicin-treated group (40 mg/kg body weight), a testosterone-treated group (15 mg/kg body weight), and a group receiving testosterone followed by gentamicin. Serum levels of alanine aminotransferase (ALT), aspartate aminotransferase (AST), urea, and creatinine were measured, and liver and kidney tissues were examined histologically. **Results:** Rabbits treated with gentamicin alone showed marked increases in serum ALT, AST, urea, and creatinine levels, indicating significant hepatic and renal injury. Administration of testosterone alone resulted in lower enzyme and metabolite levels compared with the gentamicin-treated group, suggesting limited organ stress. Co-administration of testosterone with gentamicin significantly reduced ALT and AST levels relative to gentamicin treatment alone, indicating partial hepatoprotection. However, urea and creatinine levels remained elevated, suggesting that the testosterone dose used was insufficient to prevent gentamicin-induced renal damage. Histopathological findings supported the biochemical results, with evident structural alterations in liver and kidney tissues following gentamicin exposure. **Conclusion:** Gentamicin induces pronounced hepatic and renal toxicity in adult male rabbits. Testosterone exerts organ-specific protective effects, providing partial protection to the liver but limited benefit to the kidneys under the conditions of this study.

Keywords: Gentamicin; Testosterone; Liver enzymes; Urea; Creatinine; Rabbits

1. Introduction:

Gentamicin (GM) is a widely prescribed aminoglycoside antibiotic that remains an important option for the treatment of severe infections caused by Gram-positive and Gram-negative aerobic bacteria. Despite its effectiveness, the clinical use of gentamicin is often limited by dose-dependent toxicity, particularly affecting the kidneys and liver [1, 2]. Gentamicin-induced nephrotoxicity is commonly characterized by acute tubular necrosis, elevated serum creatinine, and increased blood urea levels, while hepatotoxicity is reflected by increased serum transaminases and histological alterations in hepatic tissue [2, 3].

The mechanisms underlying gentamicin toxicity are complex and involve the generation of reactive oxygen species (ROS), oxidative stress, inflammation, mitochondrial dysfunction, and activation of apoptotic pathways [4, 5]. The kidneys are especially vulnerable due to the accumulation of gentamicin within proximal tubular epithelial cells through receptor-mediated endocytosis. This accumulation disrupts cellular metabolism and antioxidant defenses, leading to progressive tissue injury. In the liver, gentamicin-induced oxidative damage can compromise hepatocyte membrane integrity and promote inflammatory responses [4, 6]. Recent evidence indicates that susceptibility to gentamicin-induced organ damage may be influenced by sex hormones. Experimental studies suggest that hormonal status plays an important role in modulating renal and hepatic responses to toxic insults [4, 6]. Testosterone, the primary male sex hormone, has been reported to exert protective effects against certain forms of drug-induced nephrotoxicity, although its role appears to be dose-

dependent and tissue-specific. Conversely, gentamicin itself has been shown to disrupt endocrine function by impairing Leydig cell activity and inhibiting steroidogenic enzymes, leading to reduced endogenous testosterone levels [7-9]. These interactions highlight the potential importance of hormonal modulation in determining the severity of gentamicin-induced toxicity.

Testosterone and its synthetic derivatives, collectively referred to as anabolic-androgenic steroids, are used clinically to treat conditions such as hypogonadism, delayed puberty, and osteoporosis. They are also widely misused to enhance muscle mass and physical performance [10, 11]. Physiologically, testosterone plays a central role in male sexual development, spermatogenesis, metabolic regulation, and behavior [12, 13]. While therapeutic use of testosterone addresses conditions such as hypogonadism, osteoporosis, and delayed puberty [14-16], misuse or high doses can induce adverse effects, including hepatotoxicity, cardiac hypertrophy, testicular atrophy, and behavioral disturbances [17-19].

At the cellular level, testosterone has been shown to influence oxidative balance by modulating antioxidant enzyme activity and reducing lipid peroxidation. Through androgen receptor-mediated pathways, testosterone may also affect renal tubular function and hepatocyte metabolism, potentially contributing to tissue protection under certain conditions [4, 5]. Recent clinical and experimental studies have suggested that testosterone therapy may reduce the risk of acute kidney injury and improve systemic outcomes in specific disease contexts, further supporting its potential protective role [20]. Given the dual role of gentamicin as a potent antibiotic and a nephrotoxic/hepatotoxic agent, and considering testosterone's potential protective mechanisms, it is important to further clarify the nature of this interaction [21].

Given the widespread use of gentamicin and the growing evidence of hormone-dependent modulation of drug toxicity, a clearer understanding of the interaction between gentamicin and testosterone is needed. In particular, there is limited experimental information on how testosterone influences gentamicin-induced hepatic and renal injury in animal models. Therefore, the present study aimed to evaluate the biochemical and histopathological effects of testosterone on gentamicin-induced liver and kidney damage in adult male rabbits. By examining changes in liver enzymes, renal function markers, and tissue architecture, this study seeks to clarify whether testosterone confers protective effects against gentamicin toxicity and whether such effects differ between organs.

2. Materials and Methods

2.1 Chemicals

Testosterone hormone was obtained from Ibn Hayyan Pharmacy (Sana'a, Yemen). The commercial preparation used was Testoki® testosterone (Sanzyme Company), supplied as ampoules containing testosterone undecanoate (250 mg/mL), equivalent to 157.9 mg/mL testosterone.

Gentamicin sulfate was purchased from Sam Pharmacy (Sana'a, Yemen) and manufactured by KRKA. Each ampoule contained 80 mg gentamicin in 2 mL solution. Gentamicin was administered intramuscularly without dilution.

2.2 Experimental Animals

Twenty adult male rabbits weighing between 800 and 1500 g were obtained from a local breed and housed individually at the animal care facility of the Faculty of Applied Science, Thamar University. Animals were maintained under standard laboratory conditions at a constant temperature (25 ± 3 °C) with a 12-hour light/dark cycle. Rabbits had free access to food and water throughout the study. All animals were allowed to acclimatize for four weeks prior to the start of the experiment.

2.3 Experiment Design

Rabbits were randomly divided into four groups, with five animals per group, as follows:

- **Group I, GI (Control):** Rabbits received 1 mL of distilled water.
- **Group II, GII (Gentamicin):** Rabbits were administered gentamicin at a dose of 40 mg/kg body weight intramuscularly.
- **Group III, GIII (Testosterone):** Rabbits were administered testosterone at a dose of 15 mg/kg body weight intramuscularly.
- **Group IV, GIV (Testosterone + Gentamicin):** Rabbits received testosterone (15 mg/kg body weight) followed 30 minutes later by gentamicin (40 mg/kg body weight), both administered intramuscularly.

Rabbits were administered testosterone and gentamicin intramuscularly (IM) for a period of 5 days a week for a duration of one treatment [22].

2.4 Blood Collection

At the end of the experimental period, rabbits were fasted for approximately 10 hours. Animals were euthanized by slaughtering, and blood samples were collected by cardiac puncture into non-heparinized tubes. Samples were centrifuged at 3500 rpm for 5 minutes, and serum was separated and stored at 4 °C for enzyme assays [23]. Biochemical analyses were performed at the laboratories of Dhamar General Hospital.

2.5 Biochemical Analysis

Serum samples were used to assess liver function markers, including alanine aminotransferase (ALT) and aspartate aminotransferase (AST), as well as renal function parameters (urea and creatinine). Measurements were performed using standard ELISA-based techniques according to the manufacturer's instructions.

2.6 Histological Examination

At autopsy, liver and kidney specimens were collected from all animals, rinsed with normal saline, and fixed in 10% formalin for 24 hours. Tissues were dehydrated in graded ethanol, cleared in xylene, embedded in paraffin, and sectioned at 5 μm thickness. Sections were stained with hematoxylin and eosin and examined under a light microscope [24]. Histological changes were documented and photographed using a digital imaging system. All procedures followed standard histological techniques [25].

2.7 Statistical Analysis

Data are presented as mean ± standard deviation (SD). Statistical analysis was performed using one-way analysis of variance (ANOVA) with SPSS version 22, followed by post hoc multiple range tests. Differences were considered statistically significant at $p < 0.05$.

3. Results:

3.1 Biochemical Analysis of Liver Function Tests (ALT and AST)

Table 1 shows a significant increase in the mean serum levels of ALT and AST in both the gentamicin (GII) and testosterone (GIII) treated rabbit groups compared with the control group. Treatment with testosterone followed by gentamicin (GIV) produced a significant decrease in serum ALT and AST levels compared to the gentamicin (GII) treated group, but levels remained significantly higher than those of the testosterone (GIII) treated group.

Table 1: Effect of testosterone against the toxicity of gentamicin serum levels of ALT and AST in male rabbits

Group	ALT (U/L)	AST (U/L)
Control (GI)	72.40 ± 3.36	30.60 ± 5.41
Gentamicin-treated group (GII)	102.0 ± 6.48 ^{a**}	44.40 ± 4.56 ^{a***}
Testosterone-treated group (GIII)	85.80 ± 24.71 ^{a*}	37.80 ± 2.16 ^{a*}
Testosterone + Gentamicin treated group (GIV)	95.20 ± 7.59 ^{b*}	40.20 ± 3.96 ^{b**}

Data presented Mean ± SD values in each column were compared by one-way ANOVA followed by Post hoc multiple range test. Values with the same superscript letters are not significantly different, whereas those with different superscript letters are significantly different. *$p < 0.05$; **$p < 0.01$; and *** $p< 0.001$. ^{a} superscript letter indicates the significant differences between treatment groups and the control group; ^{b} superscript letter indicates the significant differences between treatment group no GIV and the GII treatment group.
GI: 1 mL of distilled water, GII: 40 mg/kg bw Gentamicin, GIII: 15 mg/kg bw testosterone, & GIV: 15 mg/kg bw Testosterone + 40 mg/kg bw Gentamicin.

3.2 Renal Function Tests (Urea and Creatinine)

Table 2 indicates a significant elevation in mean serum urea and creatinine levels following treatment with gentamicin (GII) and testosterone (GIII) compared to the control group. However, treatment

with testosterone followed by gentamicin (GIV) showed a significant increase in urea and creatinine levels compared to both GII and GIII.

Table 2: Effect of testosterone against the toxicity of gentamicin on serum levels of Urea and creatinine in male rabbits.

Groups	Urea mg\dl	Creatinine mg\dl
Control (GI)	22.40 ± 1.94	0.48 ± 0.08
Gentamicin-treated group (GII)	35.60 ± 5.59^{a**}	0.68 ± 0.10 ^{a*}
Testosterone-treated group (GIII)	28.00 ± 2.54^{a*}	0.56 ± 0.11 ^{a*}
Testosterone + Gentamicin treated group (GIV)	42.00 ± 7.68^{b***}	0.82 ± 0.13 ^{b**}

Data presented Mean ± SD values in each column were compared by one-way ANOVA followed by Post hoc multiple range test. Values with the same superscript letters are not significantly different, whereas those with different superscript letters are significantly different. *p < 0.05; **p < 0.01; and *** p< 0.001. ^{a}superscript letter indicates the significant differences between treatment groups and the control group, ^{b}superscript letter indicates the significant differences between treatment group no GIV and the GII treatment group.
GI: 1 mL distilled water, GII: 40 mg/kg bw Gentamicin, GIII: 15 mg /kg bw Testosterone, & GIV: 15 mg/kg bw Testosterone + 40 mg/kg bw Gentamicin.

3.3 Liver Histology:

Histological examination of the liver in the control group revealed a normal architecture with a normal central vein, hepatocytes, and sinusoids (Figure 1A). gentamicin-treated rabbits (40 mg/kg bw) exhibited hydropic changes and congestion (Figure 1B). The testosterone-treated group (15 mg /kg bw) showed hydropic changes (Figure 1C). The liver of rabbits treated with testosterone followed by gentamicin exhibited hydropic changes, inflammatory cell infiltration, and congestion (Figure 1D).

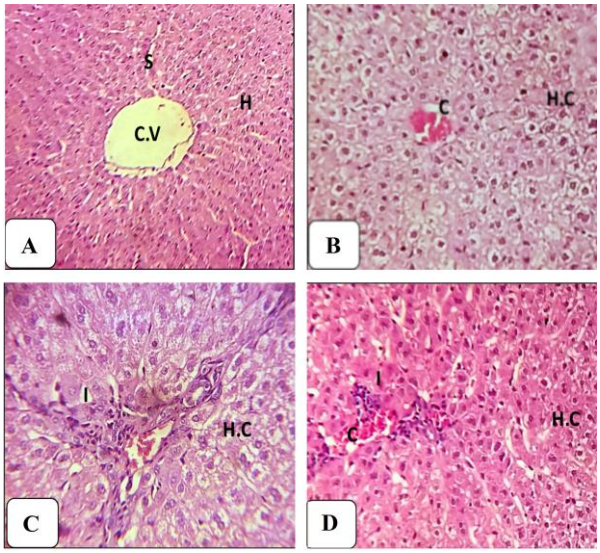

Figure 1: Photograph of rabbits liver sections exhibited **A:** liver section of control group **(GI)** reveal normal central vein (C.V), normal hepatocytes (H) and normal sinusoids (S), **B:** liver section of gentamicin treated rabbits **(GII)** shows hydropic changes (H.C) and congestion (C), **C:** liver section of testosterone treated rabbits **(GIII)** shows hydropic changes (HC) **D:** liver section of testosterone and gentamicin treated rabbits **(GIV)** shows hydropic changes (HC), inflammatory cells infiltration (I) and congestion (C). H & E (X 400).

3.4 Kidney Histology

The control group showed normal glomeruli and normal tubules (Figure 2A). Gentamicin-treated rabbits (GII) demonstrated tubular necrosis, glomerular degeneration, and tubular vacuolation (Figure 2B). The testosterone group (GIII) exhibited tubular necrosis and vacuolation (Figure 2C). The combination treatment group (GIV) showed glomerular degeneration, mild tubular necrosis, and vacuolation, indicating partial structural preservation (Figure 2D).

4. Discussion

Gentamicin administration in GII significantly elevated serum ALT, AST, urea, and creatinine levels compared to the control group, reflecting marked hepatic and renal dysfunction. It is well-known that gentamicin induces renal tubular necrosis, elevates plasma creatinine, and increases blood urea nitrogen, primarily via the generation of reactive oxygen species (ROS) and subsequent oxidative stress, which corresponds with previous findings that associate gentamicin toxicity with oxidative stress, lipid peroxidation, and mitochondrial impairment [2, 3, 26]. Besides, the biochemical disruptions align with previous studies demonstrating the hormone-dependent susceptibility of renal tissue to nephrotoxic insults[6]. Gentamicin nephrotoxicity is mainly attributed to its accumulation within proximal tubular cells via megalin- and cubilin-mediated endocytosis, which disrupts mitochondrial integrity and triggers apoptotic signaling pathways [4, 6]. Similarly, its hepatotoxicity has been linked to oxidative injury, membrane instability, and inflammatory responses within hepatocytes, which might explain the significant rise in serum transaminases observed in the current study. The gentamicin group has been reported to show hepatocellular hydropic degeneration and sinusoidal congestion. Also, the findings of the present study corroborate previous studies that reported structural disorganization due to aminoglycoside-induced oxidative damage [7, 8].

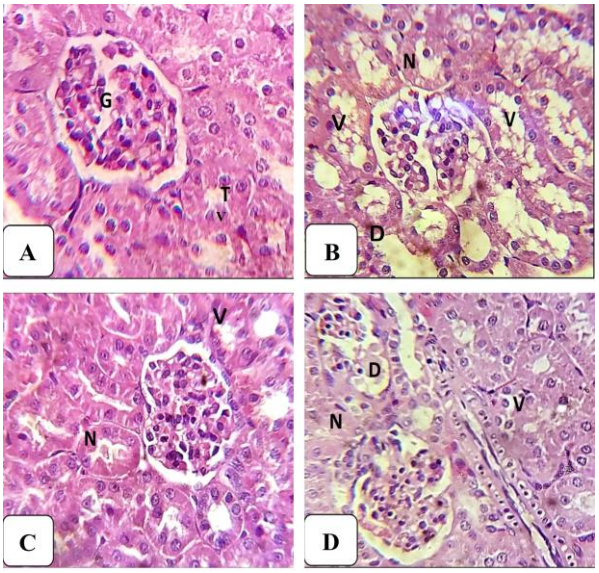

Figure 2: Photograph of rabbits kidney's cross sections exhibit **A**: kidney's cross section of control group **(GI)** shows normal glomerulus (G) and normal tubules (T), **B**: kidney's cross section of gentamicin treated rabbits **(GII)** shows tubular necrosis (N), glomerular degeneration (D) and tubular vacuolation (V) **C**: kidney's section of testosterone treated rabbits **(GIII)** shows tubular necrosis (N) and vacuolization (V), **D**: kidney's cross section of testosterone and gentamicin treated rabbits **(GIV)** shows glomerular degeneration (D), tubular necrosis (N) and tubular vacuolation (V). H & E (X 400).

In testosterone-treated rabbits (GIII), slight elevations in ALT, AST, urea, and creatinine were observed compared with the control group, suggesting mild metabolic stress. Some studies suggested that higher doses of testosterone might induce oxidative and metabolic stress on these organs, causing renal and hepatic damage [17, 19]. However, the changes in the present study were not severe and indicate that testosterone at the administered dose does not cause marked toxicity. Histological examination in testosterone-treated rabbits revealed preserved renal tubular architecture and reduced hepatocyte degeneration compared to the gentamicin treatment group, confirming the absence of major tissue damage.

In this study, when testosterone was administered prior to gentamicin (GIV), biochemical and histopathological findings revealed a mixed response. Hepatic enzyme levels (ALT and AST) were significantly lower than those in the gentamicin-treated group (GII), indicating a partial hepatoprotective effect of testosterone. This effect might be mediated by its antioxidant properties, which enhance the activity of enzymes such as superoxide dismutase (SOD), catalase (CAT), and glutathione peroxidase (GPx), thereby reducing lipid peroxidation and cellular injury in the liver [5]. Histologically, liver sections in GIV showed reduced hepatocellular degeneration, less inflammatory infiltration, and better preservation of lobular architecture compared to GII. Regarding hepatic protection, testosterone has been reported to attenuate ALT and AST elevation, reduce oxidative damage, and preserve hepatocellular architecture in toxic injury models. These effects were attributed partly to its antioxidant properties and its ability to stabilize mitochondrial function and limit ROS generation

[27]. However, the inability of testosterone to effectively protect hepatic and renal tissues against gentamicin-induced toxicity in the present study might be attributed to several interrelated mechanisms. Gentamicin generates intense oxidative stress that markedly suppresses key antioxidant enzymes (GPx, CAT, and SOD), exceeding the compensatory antioxidant potential of testosterone. Moreover, testosterone has been reported to upregulate megalin expression in proximal tubular cells, thereby enhancing gentamicin uptake and aggravating nephrotoxicity [4]. In addition, differences in tissue-specific receptor expression and metabolic capacity may explain the organ-dependent response observed; the liver, with its higher regenerative and detoxifying capacity, exhibited partial protection, whereas the kidney remained highly vulnerable to oxidative and mitochondrial injury. Hence, the overall protective action of testosterone appears insufficient under the current experimental conditions.

In renal tissues, testosterone pre-treatment failed to confer protection and even appeared to aggravate kidney injury. Urea and creatinine levels in GIV were significantly higher than those in both GII and GIII, indicating incomplete or insufficient nephroprotection. This observation might be due to testosterone-induced upregulation of megalin receptors in proximal tubular cells, which could facilitate greater gentamicin uptake and thereby enhance its nephrotoxic potential [4]. Besides, a recent study by Althunibat *et al.* [26] reported that gentamicin accumulates preferentially in the proximal renal tubules, where it disrupts mitochondrial integrity, enhances lipid peroxidation, and suppresses the endogenous antioxidant system, particularly GPx, CAT, and SOD, leading *to severe* marked architectural distortion of the renal tissue. On the other hand, our findings disagreed with those of Sekula *et al.* [6], Soljacic *et al.* [28], and Patil *et al.* [29], who reported that testosterone showed variable protective effects against chemically induced renal and liver injury through enhancement of endogenous antioxidant capacity. Thus, this might be due to the fact that testosterone failed to prevent or alleviate gentamicin's nephrotoxicity, suggesting that the severity of oxidative stress and the marked suppression of key antioxidant enzymes exceeded its protective capacity. Additionally, the antioxidant capacity of the administered testosterone dose might not have been sufficient to counteract the high oxidative burden induced by gentamicin. These findings may be due to a complex interaction between testosterone and gentamicin, in which testosterone exerts beneficial effects on hepatic tissues but fails to provide adequate renal protection at the current dosage. Protective action appears to be dose-dependent and organ-specific, reflecting differences in receptor expression, metabolic capacity, and oxidative vulnerability between the liver and kidney.

5. Conclusion

This study demonstrates that gentamicin induces significant hepatic and renal toxicity in adult male rabbits. Testosterone administration provided partial protection against gentamicin-induced liver injury, as evidenced by reduced serum transaminase levels and improved histological features. However, testosterone did not prevent renal dysfunction or structural kidney damage. These findings suggest that testosterone exerts organ-specific effects and may offer limited hepatoprotection without conferring comparable renal benefits. Further studies are needed to explore optimal dosing, treatment duration, and underlying mechanisms to define better the therapeutic potential and limitations of testosterone in drug-induced toxicity.

Ethical Approval

The study protocol was approved by the Animal Ethics Committee of the Department of Biological Sciences, Faculty of Science, Sana'a University (ethical code: BAHSS101).

Data Availability

The datasets used and analyzed during the current study are available from the corresponding author upon reasonable request.

Funding

This research received no specific grant from any funding agency in the public, commercial, or not-for-profit sectors.

Conflict of Interest

The authors declare that there are no conflicts of interest.

Authors' Contributions:

FSM: Provided supervision, critical revision, and expert advice throughout the study, contributed to data curation and formal analysis, and drafted the first version of the manuscript. **NMAH**: Verified the data, contributed significant manuscript revision, and finalized the manuscript. **EASA** and **FAMQ** reviewed the draft of the manuscript for publication. **MAAQ, AA-S, AA-K, EA-K,** and **OA-A:** carried out experimental work, collected, analyzed the data, and performed data curation, formal analysis, and biochemical findings interpretation.

References

[1] Hansen, M., Christrup, L., Jarløv, J., Kampmann, J., Bonde, J. (2001) Gentamicin dosing in critically ill patients, *Acta Anaesthesiologica Scandinavica* **45**: 734-740.

[2] Dursun, M., Sahin, S., Besiroglu, H., Otunctemur, A., Ozbek, E., Cakir, S., Cekmen, M., Somay, A. (2018) Protective effect of nebivolol on gentamicin-induced nephrotoxicity in rats, *Bratislava Medical Journal-Bratislavske Lekarske Listy* **119**: 718-725.

[3] Gamaan, M.A., Zaky, H.S., Ahmed, H.I. (2023) Gentamicin-induced nephrotoxicity: A mechanistic approach, *Azhar International Journal of Pharmaceutical and Medical Sciences* **3**: 11-19.

[4] Elsakka, E.G., Elsisi, A.M., Mansour, O.A.A.-M., Elsadek, B.E., Abd Elaziz, A.I., Salama, S.A., Allam, S. (2020) Androgen/androgen receptor affects gentamicin-induced nephrotoxicity through regulation of megalin expression, *Life Sciences* **251**: 117628.

[5] Albukhari, T.A., Bagadood, R.M., Bokhari, B.T., Filimban, W.A., Sembawa, H., Nasreldin, N., Gadalla, H.E., El-Boshy, M.E. (2025) Chrysin attenuates gentamicin-induced renal injury in rats through modulation of oxidative damage and inflammation via regulation of Nrf2/AKT and NF-kB/KIM-1 pathways, *Biomedicines* **13**: 271.

[6] Sekuła, M.J., Świerczyńska, B., Smoluchowski, K., Undziakiewicz, A., Piecewicz-Szczęsna, H. (2020) Hepatotoxicity of anabolic androgenic steroids in sport, *Journal of Education, Health and Sport* **10**: 349-356.

[7] Carageorgiou, H.K., Stratakis, C.A., Damoulis, P.D., Varonos, D.D., Messari, I.D., Sideris, A.C., Sfikakis, A.P. (2005) Reversible plasma testosterone levels reduction after gentamicin administration and freund's adjuvant arthritis in rats, *Indian journal of physiology and pharmacology* **49**: 443.

[8] Chen, H., Pechenino, A.S., Liu, J., Beattie, M.C., Brown, T.R., Zirkin, B.R. (2008) Effect of glutathione depletion on Leydig cell steroidogenesis in young and old brown Norway rats, *Endocrinology* **149**: 2612-2619.

[9] Ghosh, S., Dasgupta, S. (1999) Gentamicin induced inhibition of steroidogenic enzymes in rat testis, *Indian Journal of Physiology and Pharmacology* **43**: 247-250.

[10] Niedfeldt, M.W. (2018) Anabolic steroid effect on the liver, *Current Sports Medicine Reports* **17**: 97-102.

[11] Bhasin, S., Woodhouse, L., Casaburi, R., Singh, A.B., Bhasin, D., Berman, N., Chen, X., Yarasheski, K.E., Magliano, L., Dzekov, C. (2001) Testosterone dose-response relationships in healthy young men, *American Journal of Physiology-Endocrinology and Metabolism* **281**: E1172–E1181.

[12] Awad, T., Taha, E., Hassan, M., Amany, F. (2012) Modulatory Effects of Artichock Leave Extract on Nandrolone Decanoate Induced Biochemical Alterations in Rats, *Global Journal of Biotechnology & Biochemistry* **7**: 68-78.

[13] Balthazart, J., Ball, G.F. (2019) Male sexual behavior and hormones in non-mammalian vertebrates, in: *Encyclopedia of Animal Behavior*, (2nd). *Academic Press / Elsevier*, London, UK, pp. 373-387.

[14] Seal, L.J. (2009) Testosterone replacement therapy, *Medicine* **37**: 445-449.

[15] Gooren, L. (2007) Osteoporosis and sex steroids, *Journal of Men's Health and Gender* **4**: 192-198.

[16] Abbas, Y. (2009) Abuse of anabolic androgenic steroids, *Journal of stress physiology & biochemistry* **5**: 22-32.

[17] Casavant, M.J., Blake, K., Griffith, J., Yates, A., Copley, L.M. (2007) Consequences of use of anabolic androgenic steroids, *Pediatric Clinics of North America* **54**: 677-690.

[18] Klaewklad, A., Nakkanong, K., Nathaworn, C.D., Nualsri, C. (2017) Rubber elongation factor (REF) and small rubber particle protein (SRPP) gene expression responses to variation of seasonal change in four selected rubber clones, *Pakistan Journal of Biotechnology* **14**: 115-120.

[19] Sadowska-Krępa, E., Kłapcińska, B., Nowara, A., Jagsz, S., Szołtysek-Bołdys, I., Chalimoniuk, M., Langfort, J., Chrapusta, S.J. (2020) High-dose testosterone supplementation disturbs liver pro-oxidant/antioxidant balance and function in adolescent male Wistar rats undergoing moderate-intensity endurance training, *PeerJ* **8**: e10228.

[20] Bonnet, F., Vaduva, P., Halimi, J.-M., Dosda, A., Ducluzeau, P.-H., Koppe, L., Fauchier, L. (2025) Testosterone therapy is associated with reduced risk of acute kidney injury, kidney failure with renal replacement

therapy, and cardiovascular events in men with diabetes and hypogonadism, *Cardiovascular Diabetology* **24**: 378.

[21] Tsuji, S., Hasegawa-Izaki, A., Ogawa, B., Yamada, H. (2025) Testosterone contributes sex differences of urinary biomarkers for nephrotoxicity in rats, *The Journal of Toxicological Sciences* **50**: 413-424.

[22] Moeloek, N., Asmarinah, A., Siregar, N.C., Ilyas, S. (2008) Testosterone undecanoate and depo medroxyprogesterone acetate induced azoospermia through increased expression of spermatogenic cell caspase 3, *Medical Journal of Indonesia* **17**: 149-56.

[23] Abd Hamza, E., Rashid, K.H. (2017) Some hepatic and renal histological and physiological effects of the artificial testosterone (Sustanon) on female rats, *Pakistan Journal of Biotechnology* **14**: 369-372.

[24] De Rossi, A., Rocha, L.B., Rossi, M.A. (2007) Application of fluorescence microscopy on hematoxylin and eosin-stained sections of healthy and diseased teeth and supporting structures, *Journal of Oral Pathology & Medicine* **36**: 377-381.

[25] Carleton, H.M. (1967) Carleton's Histological Technique, 4th ed., R. A. B. Drury & E. A. Wallington, Rev. & rew. ed., *Oxford University Press*, New York, USA, pp. 442.

[26] Althunibat, O.Y., Abukhalil, M.H., Aladaileh, S.H., Qaralleh, H., Al-Amarat, W., Alfwuaires, M.A., Algefare, A.I., Namazi, N.I., Melebary, S.J., Babalghith, A.O. (2022) Formononetin ameliorates renal dysfunction, oxidative stress, inflammation, and apoptosis and upregulates Nrf2/HO-1 signaling in a rat model of gentamicin-induced nephrotoxicity, *Frontiers in Pharmacology* **13**: 916732.

[27] Xu, L., Yuan, Y., Che, Z., Tan, X., Wu, B., Wang, C., Xu, C., Xiao, J. (2022) The hepatoprotective and hepatotoxic roles of sex and sex-related hormones, *Frontiers in Immunology* **13**: 939631.

[28] Soljancic, A., Ruiz, A.L., Chandrashekar, K., Maranon, R., Liu, R., Reckelhoff, J.F., Juncos, L.A. (2013) Protective role of testosterone in ischemia-reperfusion-induced acute kidney injury, *American Journal of Physiology-Regulatory, Integrative and Comparative Physiology* **304**: R951-R958.

[29] Patil, C.N., Wallace, K., LaMarca, B.D., Moulana, M., Lopez-Ruiz, A., Soljancic, A., Juncos, L.A., Grande, J.P., Reckelhoff, J.F. (2016) Low-dose testosterone protects against renal ischemia-reperfusion injury by increasing renal IL-10-to-TNF-α ratio and attenuating T-cell infiltration, *American Journal of Physiology-Renal Physiology* **311**: F395-F403.

TuJnaS

Original Article

Thamar University Journal of Natural & Applied Sciences 10(2) (2025) 36– 46

DOI: https://doi.org/10.59167/tujnas.v10i2.3017

Investigation of Structural, Optical Characteristics, and Morphological Properties, as well as the Antibacterial Efficacy of MgO-$Bi_{2-x}Ag_xO_3$ Nanocomposites Synthesized via the Solvent-Deficient Method

Annas Al-Sharabi[1,*], Kholod Saleh Sada'a[1], Ahmed Al-Osta[1], Adnan Alnehia[1], Fawaz Al-Badai[2], Ahmed Saleh Alhajj[3], Abdulkarem Alrezaki[4], and Najeeb Al-Hijaini[1]

[1]Physics Department, Faculty of Applied Science, Thamar University, Dhamar 87246, Yemen.

[2]Biology Department, Faculty of Applied Science, Thamar University, Dhamar, 87246, Yemen.

[3]Department of Microbiology, Faculty of Veterinary Medicine, Thamar University, Dhamar 87246, Yemen.

[4]Biology Department, Faculty of Education, Thamar University, Dhamar, 87246, Yemen.

***Corresponding Author:** Annas Al-Sharabi, Physics Department, Faculty of Applied Science, Thamar University, Dhamar 87246, Yemen. E-mail: annas.alsharabi3@gmail.com

Received: 2 November 2025. Received (in revised form): 14 December 2025. Accepted: 17 December 2025. Published: 28 December 2025.

Abstract:

In this work, MgO–$Bi_{2-x}Ag_xO_3$ nanocomposites with different silver contents (x = 0.00, 0.03, 0.05, and 0.07) were synthesized using a simple solvent-deficient method. The structural, optical, morphological, and antibacterial properties of the prepared materials were systematically investigated. X-ray diffraction analysis confirmed that all samples crystallized in the monoclinic α-Bi_2O_3 phase, with no detectable secondary phases related to MgO or AgO, suggesting that these components were either highly dispersed or present in an amorphous form. The average crystallite size was found to increase with Ag content up to x = 0.05, followed by a slight decrease at x = 0.07. Scanning electron microscopy revealed agglomerated particles with relatively uniform distribution, while silver doping led to noticeable improvements in surface morphology. Energy-dispersive X-ray spectroscopy confirmed the presence of Mg, Bi, O, and Ag in compositions close to the intended stoichiometry. Optical studies based on UV–visible spectroscopy showed that the optical bandgap decreased slightly with increasing Ag content, with values of 3.14, 3.13, 3.10, and 3.11 eV for x = 0.00, 0.03, 0.05, and 0.07, respectively. These changes were attributed to the introduction of Ag-related impurity states within the band structure. The antibacterial activity of the nanocomposites was evaluated against both Gram-negative and Gram-positive bacteria using the disc diffusion method. Silver-doped samples exhibited enhanced antibacterial performance compared with the undoped material, with the highest activity observed for the Ag-containing nanocomposites. Notably, inhibition zones exceeding 23 mm were recorded against Gram-negative bacteria, highlighting the strong antibacterial effect associated with Ag incorporation. Overall, the results demonstrate that MgO–$Bi_{2-x}Ag_xO_3$ nanocomposites prepared by the solvent-deficient method possess promising structural, optical, and antibacterial properties, making them potential candidates for applications in medical and environmental fields.

Keywords: MgO–Bi_2O_3; silver doping; Structural properties; Optical bandgap; Antibacterial activity; Solvent-deficient method

1. Introduction

In recent years, nanomaterials have attracted considerable attention because of their unique physical and chemical properties, which differ markedly from those of their bulk counterparts [1, 2]. Owing to their reduced dimensions, high surface-to-volume ratio, and tunable surface characteristics, nanoparticles often exhibit enhanced optical, electrical, and antibacterial behaviors. These features make nanotechnology a powerful tool for improving the performance of inorganic materials, particularly in applications related to antimicrobial activity and environmental protection [2].

Magnesium oxide (MgO) is a wide-bandgap semiconductor that typically crystallizes in a cubic structure and exhibits high thermal and

chemical stability [3]. Mg ionic radii is 0.72 Å and it has +2 oxidation state [4, 5]. In its bulk form, MgO has a large bandgap of approximately 7.8 eV, which limits its direct application in optoelectronic devices. However, when reduced to the nanoscale, the bandgap decreases significantly, often reaching values around 5 eV, thereby improving its optical activity [6]. MgO nanoparticles are also known for their strong surface reactivity and catalytic properties, as well as their effectiveness against a broad range of Gram-positive and Gram-negative bacteria [7, 8]. Importantly, MgO shows relatively low toxicity toward mammalian cells compared with many other metal oxides, which makes it an attractive candidate for biomedical and pharmaceutical applications [9, 10]. As a result, increasing effort has been devoted to the synthesis of MgO-based nanoparticles and nanocomposites for advanced technological uses [11].

The antibacterial activity of MgO nanoparticles is commonly attributed to the generation of reactive oxygen species, particularly superoxide radicals. These species form when oxygen molecules interact with the nanoparticle surface and can disrupt bacterial cell membranes by damaging proteins and phospholipids, ultimately leading to cell death [12]. Despite these advantages, the optical response and antibacterial efficiency of MgO alone remain limited, motivating the development of composite systems that combine MgO with other functional oxides.

Bismuth oxide, also known as bismuth trioxide (Bi_2O_3), is a yellow chemical compound [5]. Bi_2O_3 is another material of significant interest due to its narrow bandgap and versatile physical properties. It exists in several polymorphic forms (α, β, γ, δ, ε, and ω), with the monoclinic α-Bi_2O_3 phase being the most stable at relatively low temperatures [13, 14]. Bi_2O_3 is a p-type semiconductor with a direct bandgap of approximately 2.85 eV, making it responsive to visible light [15, 16]. At the nanoscale, Bi_2O_3 exhibits notable photoluminescence, high dielectric permittivity, good ionic conductivity, and strong catalytic activity, while remaining largely non-toxic [17-20]. These characteristics have enabled its use in a wide range of applications, including gas sensors, optical coatings, photovoltaic devices, optoelectronics, and photocatalysis [21-24]. Moreover, Bi_2O_3 has demonstrated promising antibacterial activity, further expanding its potential utility [25-27].

Several studies have shown that combining Bi_2O_3 with other metal oxides can significantly improve its photocatalytic and antibacterial performance. For example, Bi_2O_3-MgO nanocomposites have been reported to exhibit narrower bandgap values and enhanced photocatalytic activity compared with either component alone [23]. Similar improvements have been observed in CeO_2–Bi_2O_3 and ZnO-Bi_2O_3 nanocomposites, where modifications in microstructure and charge-carrier dynamics led to improved optical and antibacterial behavior [28, 29]. These findings suggest that heterostructure formation plays a key role in tailoring material properties.

Silver nanoparticles have long been recognized for their strong antibacterial activity and relatively low toxicity to humans [30-32]. Owing to their size- and shape-dependent optical and electronic properties, Ag nanoparticles are also attractive for optoelectronic applications [33, 34]. Incorporating silver into metal oxide systems can introduce new electronic states, modify band structures, and enhance charge-carrier separation, which collectively improve optical absorption and antibacterial efficiency.

Based on these considerations, the present study focuses on the synthesis of MgO–$Bi_{2-x}Ag_xO_3$ nanocomposites (x = 0.00, 0.03, 0.05, and 0.07) using a simple and cost-effective solvent-deficient method. The structural, morphological, and optical properties of the synthesized nanocomposites were systematically investigated using X-ray diffraction, scanning electron microscopy, energy-dispersive X-ray spectroscopy, and UV–visible spectroscopy. In addition, the antibacterial activity of the materials was evaluated against both Gram-negative and Gram-positive bacterial strains using the disc diffusion method. The study aims to clarify the role of Ag incorporation in modifying the physical properties and antibacterial performance of MgO–Bi_2O_3-based nanocomposites, with a view toward potential medical and environmental applications.

2. Experimental procedure

2.1 Materials and Methods

The MgO-$Bi_{2-x}Ag_xO_3$ nanocomposites with several doping levels (x = 0, 0.03, 0.05, and 0.07) were fabricated using a straightforward solvent-deficient method. The chemicals used included $Bi(NO_3)_3{\cdot}5H_2O$, ≥ 98 %; Fluka, $Mg(NO_3)_2{\cdot}6H_2O$, $AgNO_3$, > 98.5%; Fluka-Garande, and $NaHCO_3$, > 98.5%; Fluka. All reagents were employed as received without any further purification. The overall reaction governing the synthesis process is abridged as follows:

$$(2\text{-}x)Bi(NO_3)_3{\cdot}5H_2O + Mg(NO_3)_2{\cdot}6H_2O + xAg(NO_3) + 8NaHCO_3 \rightarrow MgO\text{-}Bi_{(2-x)}Ag_xO_3 + (8\text{-}2x)NO_2 + (20\text{-}5x)\,H_2O + 4Na_2O + 8CO_2 + (2\text{-}x)O_2 \quad (1)$$

2.2 Preparation Process

To prepare the nanocomposites, stoichiometrically calculated amounts of $Bi(NO_3)_3{\cdot}5H_2O$, $Mg(NO_3)_2{\cdot}6H_2O$, and $AgNO_3$ were mixed with the appropriate amount of $NaHCO_3$. These components were then ground together for 20 minutes in a mortar at 23±1 °C. During the initial minutes, a degassing reaction occurred due to the release of CO_2, causing the slurry mixture to become more viscous. After drying the mixture overnight at 23 ± 1 °C, a dark powder was obtained. This powder was subsequently washed three times using distilled water and a filter flask. The cleaned powders were then heated in an oven at 773 K for two hours, with the temperature being adjusted at a rate of 10 K/min. Following this calcination step, the final powders were ground again using the mortar and pestle and then subjected to further characterization.

2.3 Antibacterial test

To evaluate the antibacterial efficacy of MgO-$Bi_{2-x}Ag_xO_3$ nanocomposites (x = 0, 0.03, 0.05, and 0.07), a disc diffusion method was employed against Gram-negative bacteria (*Salmonella typhimurium* and *Pseudomonas aeruginosa*) and Gram-positive bacteria (*Staphylococcus aureus*). Prior to testing, the bacterial strains were confirmed using biochemical assays. The nanocomposite samples were prepared by suspending them in sterile distilled water and creating four working dilutions from a stock solution of 50 mg/ml. These dilutions were utilized to impregnate sterile filter paper disks (6 mm diameter) at concentrations of 500, 250, 125, and 62.5 µg/disk (denoted as S_1, S_2, S_3, and S_4, respectively). Agar plates were injected with the bacterial cultures using swabs to form a bacterial lawn, after which the impregnated disks were placed on the surface. The plates were then incubated at 37 °C for 19-21 hours. Following incubation, the zones of inhibition (ZOI) around each disk were measured to the nearest millimeter(mm). A negative control utilizing distilled water (DW) was incorporated into the experimental setup to provide a baseline for comparison. This methodology allowed for the assessment of the antibacterial activities of the MgO–$Bi_{2-x}Ag_xO_3$ nanocomposites against the selected bacterial strains, facilitating a comprehensive evaluation of their potential as antimicrobial agents.

2.4 Characterization Techniques

The crystalline structure of the synthesized nanocomposites was examined using X-ray diffraction (XRD) utilizing an XD-2 X-ray diffractometer operating at 36 kV and 20 mA, sourced from China. X-ray diffraction was recorded with Cu Kα radiation (λ = 1.5406 Å). Diffraction patterns were recorded over a suitable 2θ range to identify phase composition and crystallinity. Average crystallite sizes were estimated using the Scherrer equation. Surface morphology and particle distribution were investigated using scanning electron microscopy (SEM). SEM was conducted using a JEOL-JSM 6360 LV instrument based in Tokyo, Japan, to investigate micro-structural features. Elemental composition and elemental mapping were analyzed by energy-dispersive X-ray spectroscopy (EDX) attached to the SEM: JEOL-JSM 6360 LV instrument. Optical properties were studied using UV–visible absorption spectroscopy in the wavelength range of 200–800 nm. The optical bandgap energies were estimated from Tauc plots by extrapolating the linear portion of $(\alpha h\nu)^2$ versus photon energy ($h\nu$). UV-visible spectra were obtained employing a SPECORD 200 spectrophotometer.

3. Results and discussion

3.1 XRD study

The XRD patterns of as-prepared MgO, α-Bi_2O_3, and MgO over Bi_2O_3 nanocomposite were discussed in our previous study [35]. The crystalline architecture and composition integrity of the synthesized MgO-Bi_2O_3 and Ag-doped MgO-Bi_2O_3 nanocomposites were emphasized through XRD analysis. The diffraction patterns were recorded over a 15° to 65° range, as depicted in Figure 1. The observed peaks aligned well with the JCPDS card number 00-041-1449 [36], corresponding to the monoclinic crystalline structure of α-Bi_2O_3 (space group P21/c), with the (120) peak being the most prominent. No MgO peaks were detected due to its minimal presence

in the nanocomposite and the significant dispersion of MgO particles. However, the presence of MgO was validated through the EDX spectrum. The ionic radius of Bi^{+3} (coordination number = 6) is 1.03 Å, whereas that of Mg^{+2} (coordination number = 6) is only 0.72 Å.

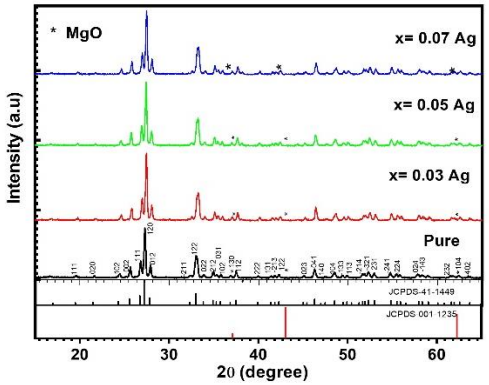

Figure 1: X-ray diffraction patterns of MgO–$Bi_{2-x}Ag_xO_3$ nanocomposites with different Ag contents (x = 0.00, 0.03, 0.05, and 0.07), confirming the monoclinic α-Bi_2O_3 phase.

The results suggest that MgO has an amorphous nature in the samples and/or is highly dispersed on Bi_2O_3 [23]. Therefore, it can be deduced that the existence of MgO suppressed the growth of the Bi_2O_3 crystals. The addition of Mg^{+2} into the Bi_2O_3 lattice led to a change in the cell parameters of the monoclinic phase. Conversely, the existence of Bi_2O_3 appeared to impede the crystallization of MgO [23]. No diffraction peaks were observed besides those of Bi_2O_3, indicating the absence of crystallographic phase impurities in the pure MgO-Bi_2O_3 and Ag-doped MgO-Bi_2O_3 nanocomposites. No peak relating to diffraction from MgO and AgO phases could be identified for x = 0.03, 0.05, and 0.07, indicating that the structure is not disturbed by Ag doping.

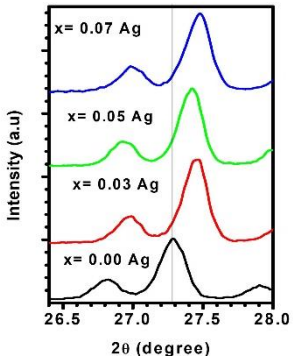

Figure 2: XRD patterns showing a slight peak shift toward the higher angle 2θ of MgO-$Bi_{2-x}Ag_xO_3$ nanocomposites (x = 0.0, 0.03, 0.05, and 0.07).

The intensity of the predominant peak was increased for Ag-doped MgO-Bi_2O_3 nanocomposites as compared to pure MgO-Bi_2O_3 nanocomposites and the diffraction peak shifts towards a higher angle. As observed in Figure 2 at (x = 0.00, 0.03, 0.05, and 0.07), the diffraction pattern of nanocomposites is shifted to a small extent with slight changes in the lattice as compared to pure Bi_2O_3 nanoparticles (The pattern corresponds to monoclinic structure, matching well with JCPDS card number 00-041-1449 for α-Bi_2O_3) indicating the increase in interplanar spacing of MgO-Bi_2O_3 [35]. This might be due to inserting the Ag^{+1} ions in the composite. It indicates Bi^{+3} ions have been successfully substituted by the dopant ions. This is possible because of the closeness in the ionic radii between Bi (1.03 Å) and Ag (1.15 Å), which is more suitable or preferred. Accordingly, oxygen vacancy will be generated to favor the structure reorganization and keep an overall neutral charge after Bi^{+3} in MgO-Bi_2O_3 crystal is replaced by property Ag^{+1} [37-39].

The constants of lattice a, b, and c for the monoclinic phase of α-Bi_2O_3 were computed via the equations:

$$\frac{1}{d^2} = \frac{1}{sin^2\beta}\left(\frac{h^2}{a^2} + \frac{k^2 sin^2\beta}{b^2} + \frac{l^2}{c^2} - \frac{2hl\, cos\beta}{ac}\right) \quad (2)$$

Here, d represents the interplanar distance, while h, k, and l denote the Miller indices. The volume (V) of the unit cell in monoclinic structures was computed from $V = abc \times sin\ \beta$ and given in Table 1. The density (ρ) and d-spacing for monoclinic structures were measured by utilizing the equation: $\rho = (Z \times M)/(N \times a^3)\ g\,.cm^{-3}$ [35] (where M is the molecular weight (g/mol) of the crystal, Z is the number of molecules in a unit cell. V is the volume of the crystalline unit cell, and N is Avogadro's number) and $2dsin\theta = n\lambda$ (where 'd' is the inter-planar spacing of a particular set of crystal plane, 'λ' is the wavelength of the incident X-ray, in our case the wavelength used is that of copper (λ = 1.5407 Å), θ is the diffraction angle, and 'n' is the order of diffraction) [40]. It was observed that the lattice's constant values are approximated to the values of the standard lattice constants. Calculated theoretical density, volume, and interplanar distance (d) between the crystal planes, at major peaks corresponding to the (120) for Bi_2O_3 planes, are in agreement with the standard values. It can be said that the dominant peak angle shifts, the change in d value, and the lattice constants are caused by the Ag^{+1} dopant [39]. It shows a slight change in lattice parameters. The increase in the unit cell volume of MgO-Bi_2O_3 nanocomposite was observed, showing shrinkage in the unit cell as compared to pure α-Bi_2O_3. The unit cell volume and the lattice constant (c) of MgO-$Bi_{(2-x)}Ag_xO_3$ nanocomposites at x = 0.03, 0.05, and 0.07, the phase in the nanocomposite is increased as compared to pure α-Bi_2O_3 (x = 0.00). A slight peak shift toward the higher angle 2θ (Figure 2) and the change in d value and unit cell volume are evidence of the incorporation of Ag ions. The reduction in lattice parameters (a, b) suggests that compressive strain has been introduced into the lattice. Shifts in peak angles and lattice strain can lead to changes in the crystallographic planes (d-spacing). However, the observed changes in lattice constant and unit cell volume with increasing Ag-doping concentration can be attributed to the ionic radius differences between Ag^{+1} and Bi^{+3} ions, as the ionic radius of Ag^{+1} (1.15 Å) is larger than that of Bi^{+3} (1.03 Å). Scherrer's equation was utilized to evaluate the average crystallite size (D) and micro-strain (ε) via XRD data of MgO-$Bi_{2-x}Ag_xO_3$ nanocomposites (x = 0.0, 0.03, 0.05, and 0.07), given as [41]:

$$D = 0.9\lambda/(\varphi\ cos\theta) \quad (3)$$

$$\varepsilon = \varphi/(4\ tan\theta) \quad (4)$$

where φ is the full width at half maximum (FWHM), θ is the angle of the peak maximum, and λ is the CuK_α wavelength (λ = 1.5406 Å) from the XRD calculations given in Table 2. The dislocation density(δ) due to crystal imperfections was estimated by utilizing the equation: $\delta = 1/D^2$, and the evaluated values are recorded in Table 2. The inverse relationship between the dislocation density (δ) and grain size indicates a reduction in the crystallite size due to the large dislocation density value [42].

Table 1: Structural parameters of MgO-$Bi_{2-x}Ag_xO_3$ nanocomposites (x = 0.0, 0.03, 0.05 and 0.07).

Oxides	Oxides	*a* (Å)	*b* (Å)	*c* (Å)	Volume (Å³)	Density (g/cm³)	d-spacing (Å)
JCPDS 011-345	MgO	4.203	-	-	74.25	3.56	2.42
JCPDS 014-1449	Bi_2O_3	5.849	8.169	7.512	330.52	9.36	3.255
***x* = 0.0**	Bi_2O_3 (120)	5.872	8.227	7.363	326.150	9.489	3.266
x = 0.03	Bi_2O_3 (120)	5.845	8.229	7.544	333.751	9.274	3.247
***x* = 0.05**	Bi_2O_3 (120)	5.841	8.202	7.558	333.143	9.290	3.251
***x* = 0.07**	Bi_2O_3 (120)	5.843	8.195	7.541	332.204	9.317	3.245

Table 2: The D, ε, and δ evaluated from Scherrer's equation for MgO-$Bi_{2-x}Ag_xO_3$ nanocomposites (x = 0, 0.03, 0.05 and 0.07).

Oxides Individual	Oxides	D (nm)	$\varepsilon\times10^{-3}$	$\delta\times10^{-4}$ (nm^{-2})
x = 0.0	Bi_2O_3 (120)	36.07	4.07	7.69
x = 0.03	Bi_2O_3 (120)	38.54	3.79	6.73
x = 0.05	Bi_2O_3 (120)	39.74	3.68	6.33
x = 0.07	Bi_2O_3 (120)	39.32	3.70	6.31

The crystallite size (D) of MgO-$Bi_{2-x}Ag_xO_3$ nanocomposites (x = 0, 0.03, 0.05, and 0.07) were increasing with increasing Ag concentration, then decreased at x = 0.07. This indicates that Ag ions doped into the host matrix were strongly capped. Increase the average crystalline size, ascribed to the diffraction peaks of MgO-Bi_2O_3 shift towards higher 2θ values with an increase in the Ag concentration, which is due to Ag^{+1} (1.15 Å) ions that can uniformly substitute into the Bi^{+3} (1.03 Å) ions' sites or interstitial sites in the MgO-Bi_2O_3 lattice [43].

In case of substitution and due to the different ionic radii (Ag = 1.15 Å larger than Bi = 1.03 Å), a lattice distortion occurs, and this distortion increases with the increase in Ag concentration[43]. The δ was increased with a decrease in crystallite size and vice versa. Microstrain was found to be compressive and decreased with the silver doping. The microstrain and dislocation density will have an important effect on the optical parameters of the samples [42].

3.2. SEM and EDX Analysis

The SEM images in Figure 3 were utilized to analyze the morphology of MgO-Bi_2O_3 and MgO-$Bi_{(1.93)}Ag_{0.07}O_3$. The surface of the MgO-Bi_2O_3 sample appeared more agglomerated and irregular in shape, exhibiting significant roughness. In contrast, the Ag-doped sample exhibited a smoother surface with reduced agglomeration, suggesting improved morphology. Some of the nanoparticles appeared spherical; however, they also exhibited variations in shape and irregularity. These changes in surface characteristics were attributed to the influence of silver doping, which enhanced particle interaction and fusion, leading to a more uniform distribution and a decrease in overall surface roughness [44]. The development of uniform, minimal-agglomerated spheres is due to homogeneous nucleation during heating. In contrast, the formation of larger particles and a wider distribution may be due to varied heating zones [45-47]. The chemical compositions of the as-prepared nanocomposite were analyzed by energy-dispersive X-ray spectroscopy (EDX). It was performed to confirm the presence of Ag-ion in MgO/Bi_2O_3 crystal lattice. Figure 4 presents the EDX spectra of the pure MgO/Bi_2O_3 nanocomposite. The results clearly indicate the presence of the elements Bi, Mg, and O as the respective peaks are clearly visible. Moreover, the atomic percentages of Bi, Mg, and O are 88.7%, 0.4% and 10.9% respectively. In addition, EDX spectra of 0.07 for Ag-doped MgO/Bi_2O_3 sample are displayed in Figure 5.5b. Spectra reveal that only four elements, Bi, Mg, Ag, and O, exist in Ag-doped MgO/Bi_2O_3 nanocomposite with their weight percentage of 86.1 %, 0.5 %, 1.8 % and 11.6 % respectively, which indicates the doped Ag ions have entered into the lattice of MgO/$Bi_{(2-x)}Ag_xO_3$ nanocomposite. This also agrees with the foregoing XRD results.

3.3 Optical analysis

3.3.1 Optical Absorption and Transmission Spectra Study

Figure 5 presents the optical absorption spectra of the MgO-$Bi_{2-x}Ag_xO_3$ nanocomposites for various concentrations (x = 0, 0.03, 0.05, and 0.07). The pure MgO-$Bi_{2-x}Ag_xO_3$ nanocomposite (x = 0.00) exhibited a broad absorption band at 363 nm. Conversely, at x = 0.03, 0.05, and 0.07, distinct peaks appeared at 365, 367, and 369 nm, respectively. The primary absorption edge shifted towards longer wavelengths with increasing Ag doping. This overall trend suggests a red shift near the band edge with Ag incorporation. This shift in absorption can be attributed to the potential substitution of Bi ions with Ag ions within the crystal lattice or the mutual exchange of these ions. Additionally, the reduced absorption in the UV and near-visible regions can be attributed to the increased surface roughness caused by higher concentrations of Ag nanoparticles, which enhances scattering and reduces the intensity of incident light [48]. The peak intensity at 363 nm decreased as the Ag doping concentration increased, likely due to the reduced solubility of the highly doped MgO-Bi_2O_3 nanocomposites in solvents compared to the undoped counterparts.

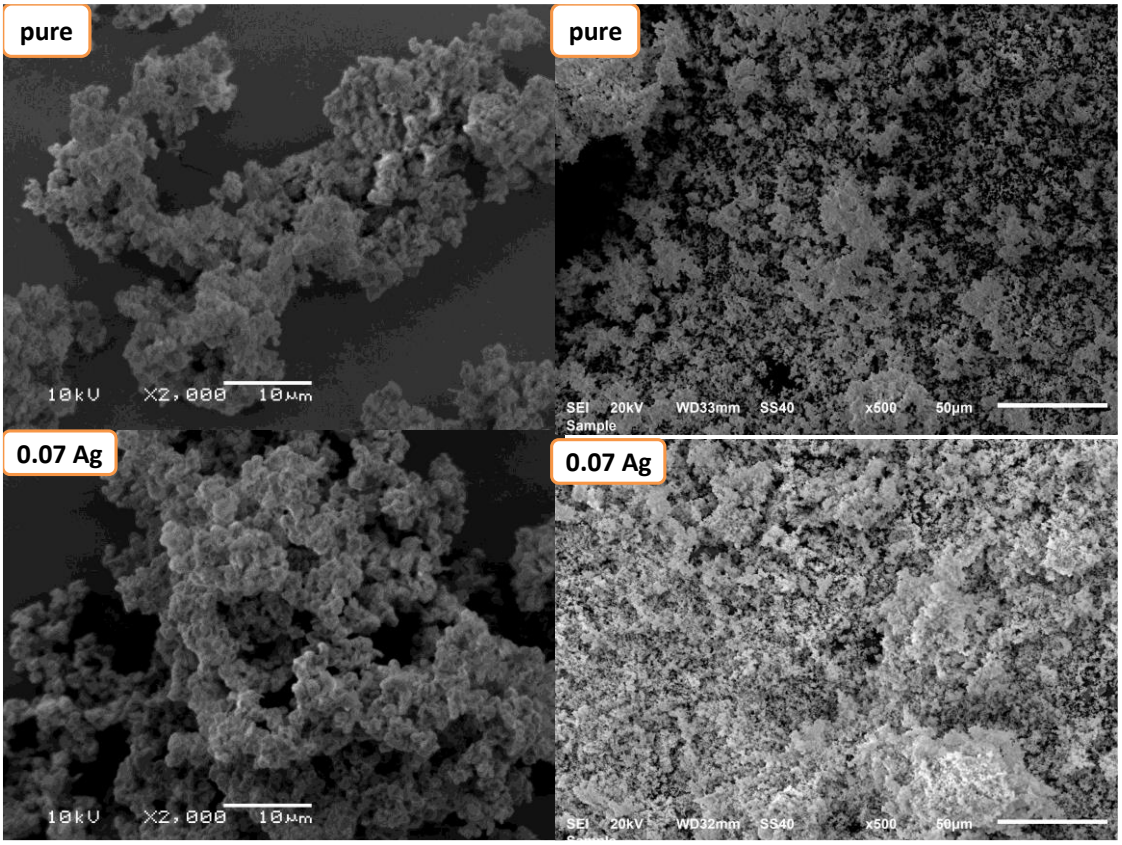

Figure 3: SEM micrographs of MgO–$Bi_{2-x}Ag_xO_3$ nanocomposites showing surface morphology and particle agglomeration as a function of Ag content.

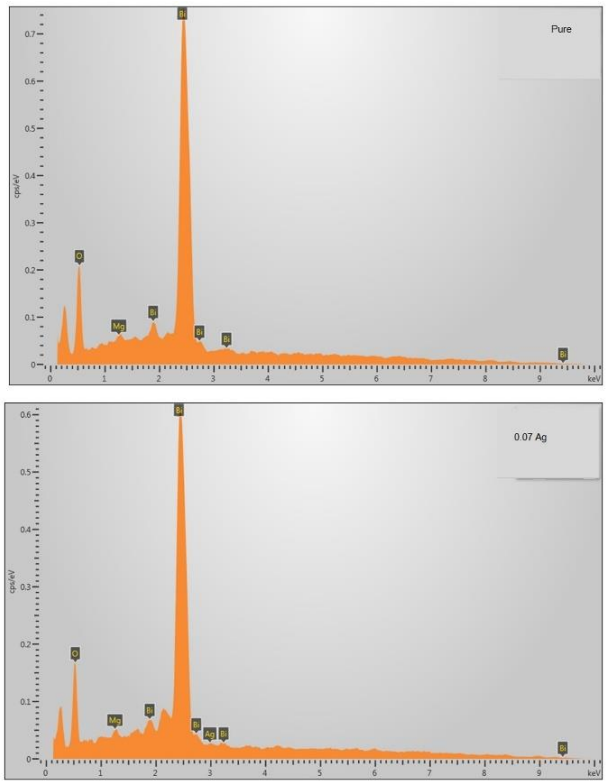

Figure 4: EDX spectra of MgO–$Bi_{2-x}Ag_xO_3$ nanocomposites illustrating the presence of Bi, Mg, O, and Ag elements.

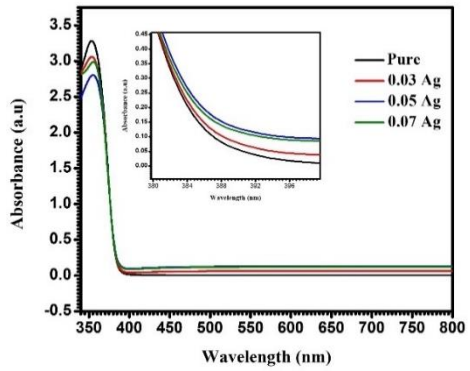

Figure 5: UV–visible absorption spectra of MgO–$Bi_{2-x}Ag_xO_3$ nanocomposites with varying Ag concentrations.

The transmittance (T) measurements for MgO-$Bi_{2-x}Ag_xO_3$ nanocomposites (x = 0, 0.03, 0.05, and 0.07) as a function of wavelength (λ) are depicted in Figure 6. It was observed that T exhibited high values across most measured wavelengths. The nanocomposites demonstrated significant visible-range transmittance, making them suitable candidates for transparent window materials in optoelectronic devices. The optical transmittance values were 99%, 91%, 80%, and 82% for the respective samples, indicating a decrease in the UV and near-visible regions for all samples, with the highest transmittance at x = 0.00. This is attributed to the absence of free electrons (i.e., electrons are bound to atoms via covalent bonds), necessitating a high-energy photon to break the electron linkage and move it to the conduction band [49].

The transmittance in the visible range decreased with increasing Ag^{+1} doping percentage. This reduction in optical transmission can be attributed to increased scattering caused by the surface roughness of the nanocomposites and the presence of oxygen vacancies. It is hypothesized that aggregation and agglomeration decrease grain size with increasing Ag content, further reducing transmittance. The work function of Ag, located between the valence band and conduction band of MgO-Bi_2O_3, enhances the light absorption capability of MgO-Bi_2O_3. The strong interaction between Ag and light arises from the conduction electrons on the Ag surface, which generate surface plasmon resonance (SPR) at specific wavelengths. This SPR phenomenon results in significant scattering and absorption of light [50].

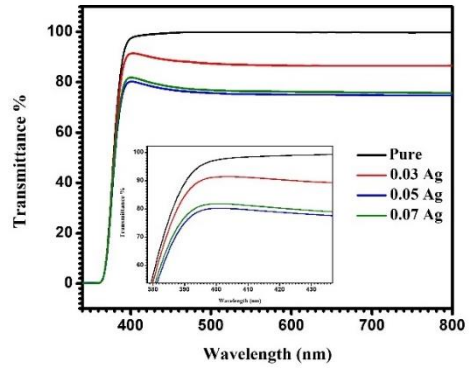

Figure 6: Transmittance as a function of wavelength of MgO-$Bi_{2-x}Ag_xO_3$ nanocomposites (x = 0, 0.03, 0.05, and 0.07).

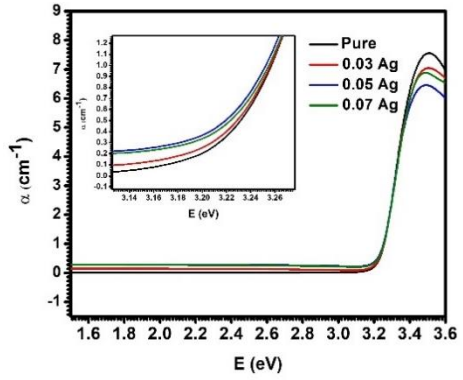

Figure 7: The absorption coefficient versus photon energy of MgO-$Bi_{2-x}Ag_xO_3$ nanocomposites (x = 0.0, 0.03, 0.05, 0.07).

The graph in Figure 7 illustrates the absorption coefficient (α) plotted against the photon energy (E) of the incident light. By establishing a fundamental connection between transmittance (T) and photon absorbance (A), the absorption coefficient (α) was constrained, offering insights into the nature of electron transitions. The calculation of α was based on Lambert's formula [51], as depicted below.

$$I = I_o\, e^{-\alpha t} \qquad (5)$$

where I is the instantaneous photon intensity, Io is the initial photon intensity, and t is the thickness of the cuvette. The α can be computed by utilizing the following equation:

$$\alpha(\lambda) = \left(\frac{1}{t}\right)\left(ln\,\frac{I_o}{I}\right) = \left(\frac{1}{t}\right)\left(ln\,\frac{1}{T}\right) = \frac{2.303\,A}{t} \qquad (6)$$

The variation of α(λ) for MgO-$Bi_{2-x}Ag_xO_3$ nanocomposites (x = 0, 0.03, 0.05 and 0.07) with photon energy is illustrated in Figure 7. The α of both pure and Ag-doped MgO-Bi_2O_3 nanocomposites increased with higher concentrations of Ag nanoparticles. This increase is attributed to the rise in the number of charge carriers, which in turn enhances absorbance and the α of MgO-$Bi_{2-x}Ag_xO_3$ nanocomposites [52-54].

At lower photon energies, absorption is minimal, indicating a reduced possibility of electron transitions because the incident photon energy is insufficient to promote electrons from the valence band (VB) to the conduction band (CB) (hυ < Eg). Conversely, at higher energies, the absorption is more significant, demonstrating a greater probability for electron transitions as the incident photon energy becomes sufficient to move electrons from the valence band to the conduction band. This indicates that the incident photon energy exceeds the forbidden energy gap [49]. A continuous increase in α with increasing E is observed across the entire measured photon energy range (3.1–3.3 eV), with the increase becoming more rapid near the material's optical bandgap energy. The highest absorption coefficient was noted for the sample with 0.05 Ag. Additionally, it was observed that reducing the size of nanoparticles decreases the absorption coefficient in the samples.

3.3.2 Optical Bandgap (E_g) Determination

The optical bandgap (Eg) can be determined using the Tauc plot approach, which correlates the incident light frequency (υ) with the photon energy (hυ) based on the equation [55]:

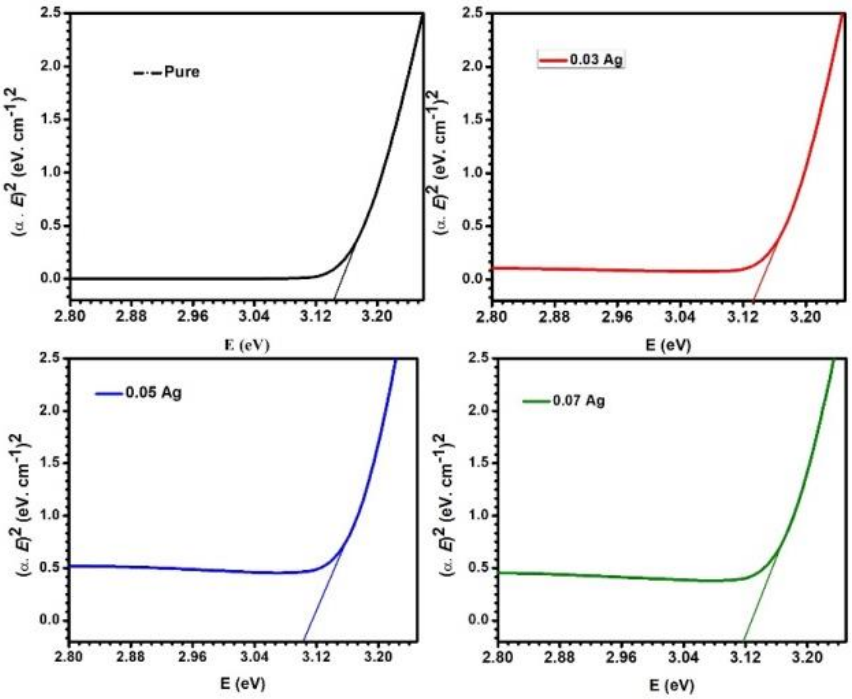

Figure 8: Tauc plots used to estimate the optical bandgap energies of MgO–$Bi_{2-x}Ag_xO_3$ nanocomposites.

$$(\alpha.\, h\upsilon)^n = A\left(h\upsilon - E_g\right) \quad (7)$$

where ν represents the incident light frequency, h is Planck's constant, A is a constant linked to the effective masses of electrons and holes in the material, and n varies depending on the type of electronic transition. For a direct allowed transition, n can be 1/2, for an allowed indirect transition, n is 2, for a forbidden direct transition, n is 3/2, and for a forbidden indirect transition, n is 3[55].

Bandgap energy (Eg) is a crucial parameter to evaluate a material's optical absorption performance. To determine Eg, the plot of $(\alpha h\upsilon)^2$ (for direct transitions) against hν is generated, and the linear portion of these plots is extrapolated to the hυ axis to derive the values of the optical direct bandgap Eg for the samples, as shown in Figure 8.

Direct transition E_g values were obtained for MgO-$Bi_{2-x}Ag_xO_3$ nanocomposites (x = 0, 0.03, 0.05, and 0.07) are listed in Table 3. The change in the bandgap value depends on many parameters, for example, carrier concentration, crystallite size, and the positions of the Ag dopant in the MgO-Bi_2O_3 lattice [56].

Table 3: The band gap values for MgO-$Bi_{2-x}Ag_xO_3$ nanocomposites (x = 0, 0.03, 0.05, and 0.07).

Oxides Individual	Band gap E_g (eV)
***x* = 0**	3.14
x = 0.03 Ag	3.13
***x* = 0.05 Ag**	3.10
***x* = 0.07 Ag**	3.11

The reduction in the bandgap (Eg) with increasing Ag^{+1} content corresponds to a red shift in the λ cut-off. This phenomenon is attributed to the formation of intermediate states between the conduction and valence bands of the MgO-Bi_2O_3 host matrix upon the addition of Ag. These intermediate states are responsible for the reduction in the bandgap of Ag–MgO-Bi_2O_3 nanocomposites. When Ag^{+1} is introduced into MgO-Bi_2O_3, defect states are generated below the conduction band, leading to a decrease in the bandgap. Ag^{+1} ions can be incorporated into the MgO-Bi_2O_3 lattice either by substituting Bi^{+3} ions, resulting in double ionized oxygen vacancies, or by occupying interstitial sites (Ag). The presence of silver impurities in MgO-Bi_2O_3 introduces an extra band within the energy gap, characteristic of a p-type material. This makes Ag act as an acceptor material, altering the bandgap of MgO-Bi_2O_3 nanocomposites and thereby reducing it. In contrast, donor materials exhibit a blue shift and an increase in the bandgap [57]. Consequently, doping MgO-Bi_2O_3 nanocomposites with silver can be advantageous for applications in optoelectronic devices due to the tunable energy bandgap values of the MgO-Bi_2O_3 nanocomposites [58].

3.3.3 Refractive Index(n) and Extinction Coefficient(k)

The α and incident photon wavelength (λ) can be utilized to evaluate the k, given as [59]:

$$k = \frac{\alpha\lambda}{4\pi} \quad (8)$$

Refractive index (n) is an important parameter of optical materials. Refractive index (n) can be given via the equation [59]:

$$n = \frac{1+R^2}{1-R^2} \quad (9)$$

where R is the reflection. Figure 9 (a and b) illustrates the behavior of n and k with the incident photon wavelength for MgO-$Bi_{2-x}Ag_xO_3$ nanocomposites (x = 0, 0.03, 0.05, and 0.07).

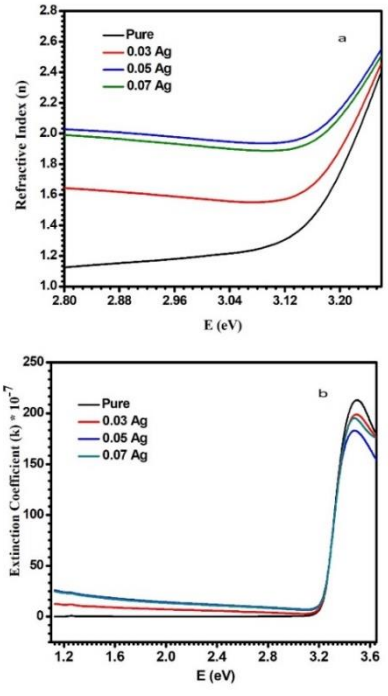

Figure 9: (a) Refractive index and (b) Extinction coefficient versus wavelength of MgO-$Bi_{2-x}Ag_xO_3$ nanocomposites (x = 0, 0.03, 0.05, and 0.07).

The refractive index (n) of MgO-Bi_2O_3 nanocomposites increases with the addition of Ag doping. This increase can be attributed to the rise in the number of free electrons and the consequent improvement in the surface of the nanocomposites, accompanied by a reduction in porosity [60]. Additionally, the increased refractive index with higher Ag doping levels may be due to lattice distortion and structural disorder within the nanocomposites. As illustrated in Figure 9a, the refractive index remains constant with increasing photon energy up to approximately 3.1 eV, after which it increases across all samples with varying Ag concentrations. Notably, the pure MgO-Bi_2O_3 nanocomposite shows a lower refractive index.

Figure 9b illustrates the k as a function of photon energy for all the samples investigated. The calculated extinction coefficient values increase with higher weight percentages of Ag. This coefficient emerges from light absorption when the photon wavelength is greater than or equal to the grain size. The likelihood of grain scattering increases with higher Ag doping, attributed to the enhancement in grain size and density of the nanocomposites. The non-zero extinction coefficient indicates the presence of additional transitions alongside the fundamental transition, suggesting that Ag doping modifies the structure of the host nanocomposites [52].

3.3.4 Optical Conductivity

The number of free charges in a material is termed optical conductivity (σ_{opt}). The σ_{opt} for any material can be expressed as [41]:

$$\sigma_{opt} = \frac{\alpha n c}{4\pi} \quad (10)$$

Here, c represents the velocity of light. Figure 10a illustrates the change of σ_{opt} with photon energy for all the samples. The values of σ_{opt} remained constant as the photon energy increased until approximately 3.1 eV, after which they increased, as shown in Figure 10a. This increase is attributed to variations in the α. The number of free carriers increases with higher Ag^{+1} content. The rise in optical conductivity is due to the creation of new levels within the bandgap, facilitating the movement of carrier charges from the valence band (VB) to the conduction band (CB). Consequently, this leads to a reduction in the bandgap and an increase in conductivity [61, 62].

3.3.5 Dielectric Constant

The real part (ε_r) of the dielectric constant represents a material's capacity to reduce the speed of light and can be computed via the equation:

$$\varepsilon_r = n^2 - k^2 \quad (11)$$

The component of the dielectric constant represented by the imaginary part (ε_i) characterizes the energy absorption resulting from dipole movement within an electric field. To determine (ε_i), the following relation can be used [59]:

$$\varepsilon_i = 2nk \quad (12)$$

The ratio of the ε_i to the ε_r of the dielectric constant yields insights into the loss factor:

$$\tan\delta = \frac{\varepsilon_i}{\varepsilon_r} \quad (13)$$

Figures 10b, 10c, and 10d illustrate the variations in the ε_r and ε_i parts of the dielectric constant, as well as the loss factor, with respect to photon energy. It is evident that the ε_r of the dielectric constant is primarily proportional to the square of the refractive index and therefore increases with the addition of Ag. The imaginary part of the dielectric constant is proportional to the k, as shown in relation (12), and it also increases with higher concentrations of Ag nanoparticles. The results obtained from measurements of the dielectric constant and loss angle show a close correlation with the optical energy gap of the studied materials. It was observed that increasing the doping concentration leads to an increase in the crystallite size calculated from X-ray diffraction (XRD) data. This increase in crystallite size may enhance polarization within the material, thereby increasing the dielectric constant. On the other hand, UV-Vis spectroscopic measurements indicate that the optical energy gap decreases with increasing doping concentration. This reduction in the optical energy gap may facilitate the movement of charge carriers, contributing to an increase in the loss factor. Therefore, the relationship between these properties suggests that modifications in the chemical composition significantly affect the electrical and optical properties of the material [63, 64].

The X-ray diffraction analysis revealed that the nanocomposites exhibited diffraction patterns characteristic of the monoclinic α-Bi_2O_3 phase, with no distinct peaks indicating the presence of MgO or AgO compounds. This suggests that the MgO and AgO phases are either amorphous or highly dispersed within the Bi_2O_3 matrix. The average crystallite size ranged from 36.07 to 39.74 nm, showing an increase with silver concentration, peaking at 0.05, followed by a decrease at 0.07. This trend can be attributed to the substitution of Bi+3 ions by Ag+ ions, which have a larger ionic radius. The increase in crystallite size with increasing silver doping concentration up to 0.05 can be attributed to the enhanced crystallinity of the samples resulting from the incorporation of Ag^+ ions into the Bi_2O_3 lattice. However, at higher silver concentration (x = 0.07), the decrease in crystallite size may be due to the formation of defects or lattice strain caused by the excess Ag^+ ions [65].

The optical properties assessed by UV-visible absorption spectroscopy indicated bandgap energies of 3.14, 3.13, 3.10, and 3.11 eV for silver doping concentrations of 0.00, 0.03, 0.05, and 0.07, respectively. The decrease in bandgap energy with increasing silver concentration can be attributed to the introduction of impurity levels within the bandgap, resulting from the substitution of Bi^{+3} ions by Ag^+ ions. However, at higher silver concentration

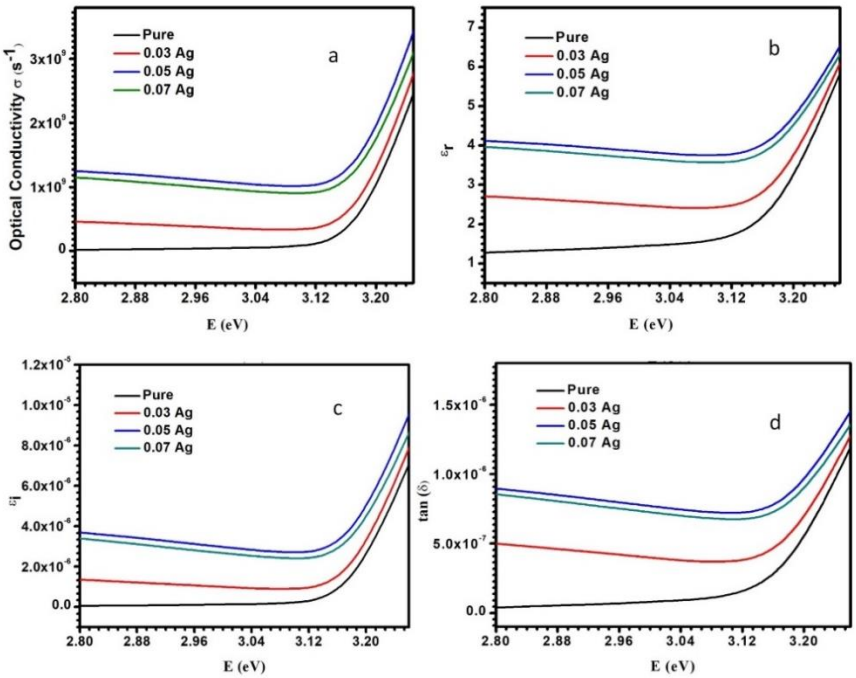

Figure 10: The change of (a) optical conductivity, (b) real dielectric constant, (c) imaginary dielectric constant, and (d) loss factor as a function of E(eV) for the synthesized samples

can be attributed to the introduction of impurity levels within the bandgap, resulting from the substitution of Bi^{+3} ions by Ag^{+} ions. However, at higher silver concentration (x = 0.07), the slight increase in bandgap energy may be due to the Burstein-Moss effect, where the excess Ag^{+} ions lead to a shift in the Fermi level and an increase in the bandgap energy [66].

3.4 Antibacterial activity

The antibacterial activity for MgO-$Bi_{(2-x)}Ag_xO_3$ nanocomposites (x = 0, 0.03, 0.05, and 0.07) were evaluated against gram-negative bacteria (*S. typhimurium and P. aeruginosa*) and gram-positive bacteria (*S. aureus*) (Table 4). Images of antibacterial studies on nanocomposites against bacterial pathogens are shown in Figure 11.

Table 4: Assessment of Antibacterial Efficacy of MgO-$Bi_{2-x}Ag_xO_3$ nanocomposites (x = 0, 0.03, 0.05, and 0.07).

Bacteria	Type of bacteria	ZOI (mm) at concentration in (µg/mL)				
		Con.	Pure	0.03 Ag	0.05 Ag	0.07 Ag
S. typhimurium	Negative	A1	15	20	18	20
		A2	15	19	17	19
		A3	15	18	16	18
		A4	15	17	16	19
P. aeruginosa	Negative	A1	14	21	21	23
		A2	13	18	20	18
		A3	14	18	18	19
		A4	15	19	17	18
S. aureus	Positive	A1	9	10	7	10
		A2	8	11	-	8
		A3	8	11	-	9
		A4	11	11	7	9

The antibacterial activity was determined by measuring the ZOI around the disc using the antibiotic zone scale (mm). The pure sample (at x = 0) nanocomposite has shown greater than 6 mm of inhibition against different types of bacteria. The addition of Ag content (x > 0) leads to an increase in the inhibitory activity of MgO-$Bi_{(2-x)}Ag_xO_3$ nanocomposites against several types of bacteria. This suggests that the growth inhibition ability of MgO-$Bi_{(2-x)}Ag_xO_3$ nanocomposites (x = 0, 0.03, 0.05, and 0.07) against both gram-negative and gram-positive bacteria have been significantly enhanced at the same concentration and growth conditions. The particle size (D) decreased as the doped concentration Ag^{+1}), the small size of the fabricated MgO-$Bi_{(2-x)}Ag_xO_3$ nanocomposites (x = 0.00, 0.03, 0.05, and 0.07) play an important role in their activity upon testing the gram-negative pathogen [67, 68]. MgO-$Bi_{(2-x)}Ag_xO_3$ nanocomposites (0.07) displayed the best antibacterial activity of both gram-negative and gram-positive bacteria, as depicted in Figure 11. The most significant effect of nanocomposites was found for the concentration (500 µg/disc) for all samples against the different types of bacteria. The results illustrated a higher ZOI for all fabricated materials (between 7 and 23 mm).

It is important to highlight that the MgO-$Bi_{(2-x)}Ag_xO_3$ nanocomposites prepared (x = 0, 0.03, 0.05, and 0.07) exhibited greater efficacy against gram-negative bacteria compared to gram-positive bacteria, potentially attributed to variations in bacterial cell structures. A thick lipopolysaccharide cell membrane characterizes gram-positive bacteria [69-71]. The differing antibacterial performance of the developed materials at varying Ag concentrations may be linked to surface defects. The inclusion of heavy metal ions, such as Bi^{+3}, Mg^{+2}, and Ag^{+1}, enhances antibacterial activity. These ions are drawn to the cell membrane through interactions with the thiol group (–SH) found in proteins on the external surface of the cell membrane. This attraction results in the penetration of metallic ions into the cell membrane, leading to protein denaturation and, in turn, damage to the bacterial cell membrane. Additionally, the surface characteristics of the nanocomposite contribute to mechanical disruptions in the membrane [72-77]. Table 5 shows a comparison of antibacterial analysis of MgO-$Bi_{(2-x)}Ag_xO_3$ nanocomposites with other previous studies.

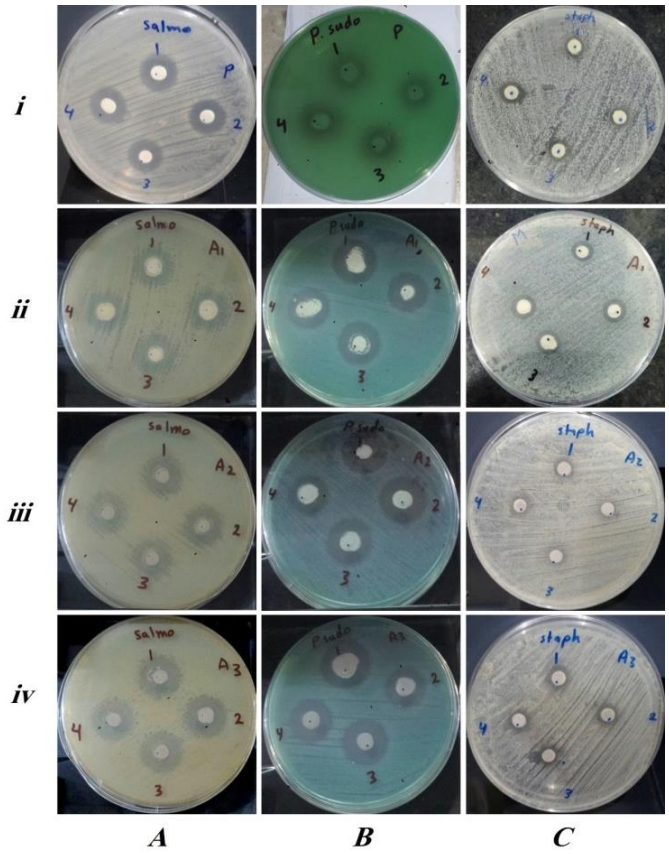

Figure 11: Illustrates the antibacterial activities of MgO-$Bi_{2-x}Ag_xO_3$ nanocomposites with varying silver doping levels against different bacterial strains. The rows represent the different samples: (i) pure, (ii) 0.3 Ag, (iii) 0.5 Ag, and (iv) 0.7 Ag, while the columns correspond to the bacterial strains: (A) *S. typhimurium,* (B) *P. aeruginosa*, and (C) *S. aureus.*

Table 5: A comparison of antibacterial analysis of MgO-$Bi_{2-x}Ag_xO_3$ nanocomposites with other nanocomposites.

Metal oxide nanocomposites	Inhibition Zone (mm)			
	Staphylococcus aureus	*S. typhimurium*	*P. aeruginosa*	Reference
MgO-$Bi_{(2-x)}Ag_xO_3$	10	20	23	Current work
ZnO–V_2O_5-WO_3	17	-	18	[78]
Co_3O_4-CuO-ZrO_2	10	-	-	[79]
CdO–ZnO–MgO	-	-	22	[80]
CuO– CeO_2–ZnO	14	-	12	[81]

4. Conclusion

In this study, MgO-$Bi_{2-x}Ag_xO_3$ nanocomposites were successfully synthesized using a simple solvent-deficient method. Structural analysis confirmed the formation of the monoclinic α-Bi_2O_3phase for all compositions, while the absence of secondary phases indicated good dispersion of MgO and silver within the Bi_2O_3 matrix. The incorporation of Ag influenced crystallite size, surface morphology, and optical behavior, with moderate Ag content producing the most noticeable improvements. Optical studies revealed a slight narrowing of the bandgap with increasing Ag concentration, which was attributed to the introduction of Ag-related electronic states. The antibacterial performance of the nanocomposites was significantly enhanced by silver doping, particularly against Gram-negative bacteria. This improvement is likely due to the combined effects of Ag ion release, reactive oxygen species generation, and increased surface interaction with bacterial cells. Overall, the results demonstrate that controlled Ag incorporation effectively tailors the multifunctional properties of MgO–Bi_2O_3-based nanocomposites. The materials synthesized in this work show promise for applications requiring enhanced antibacterial activity and tunable optical properties, especially in medical and environmental fields.

Data Availability

The datasets used and analyzed during the current study are available from the corresponding author upon reasonable request.

Funding

This research received no specific grant from any funding agency in the public, commercial, or not-for-profit sectors.

Conflict of Interest

The authors declare that there are no conflicts of interest.

References

[1] Zhang, W., Tay, H.L., Lim, S.S., Wang, Y., Zhong, Z., Xu, R. (2010) Supported cobalt oxide on MgO: highly efficient catalysts for degradation of organic dyes in dilute solutions, *Applied Catalysis B: Environmental* **95**: 93-99.

[2] Suryawanshi, S.M., Badwaik, D.S., Shinde, B.S., Gaikwad, K.D., Shkir, M., Chandekar, K.V., Gundale, S. (2023) A comprehensive study on structural, magnetic and dielectric properties of $Ni_{0.3}Cu_{0.3}Zn_{0.4}Fe_{1.8}Cr_{0.2}O_4$ nanoparticles synthesized by sol-gel auto combustion route, *Journal of Molecular Structure* **1272**: 134173.

[3] Spoto, G., Gribov, E., Ricchiardi, G., Damin, A., Scarano, D., Bordiga, S., Lamberti, C., Zecchina, A. (2004) Carbon monoxide MgO from dispersed solids to single crystals: a review and new advances, *Progress in Surface Science* **76**: 71-146.

[4] Edukondalu, A., Stalin, S., Reddy, M.S., Eke, C., Alrowaili, Z., Al-Buriahi, M. (2022) Synthesis, thermal, optical, mechanical and radiation-attenuation characteristics of borate glass system modified by Bi_2O_3/MgO, *Applied Physics A* **128**: 331.

[5] Shannon, R.D. (1976) Revised effective ionic radii and systematic studies of interatomic distances in halides and chalcogenides, *Foundations of Crystallography* **32**: 751-767.

[6] Al-Hammadi, A., Alnehia, A., Al-Sharabi, A., Alnahari ,H., Al-Odayni, A.-B. (2023) Synthesis of trimetallic oxide (Fe_2O_3–MgO–CuO) nanocomposites and evaluation of their structural and optical properties, *Scientific Reports* **13**: 12927.

[7] Richards, R., Li, W., Decker, S., Davidson, C., Koper, O., Zaikovski ,V., Volodin, A., Rieker, T., Klabunde, K.J. (2000) Consolidation of metal oxide nanocrystals. Reactive pellets with controllable pore structure that represent a new family of porous, inorganic materials, *Journal of the American Chemical Society* **122**: 4921.4925-

[8] Ren, A., Liu, C., Hong, Y., Shi, W., Lin, S., Li, P. (2014) Enhanced visible-light-driven photocatalytic activity for antibiotic degradation using magnetic $NiFe_2O_4$/Bi_2O_3 heterostructures, *Chemical Engineering Journal* **258**: 301-308.

[9] Krishnamoorthy, K., Moon, J.Y., Hyun, H.B., Cho, S.K., Kim, S.-J. (2012) Mechanistic investigation on the toxicity of MgO nanoparticles toward cancer cells, *Journal of Materials Chemistry* **22**: 24610-24617.

[10] Elashmawi, I., Menazea, A. (2025) Influence of laser ablation preparation of MgO and Bi_2O_3 nanoparticles on the optical and dielectric behavior of the PVA/PEO polymer blend, *RSC Advances* **15**: 48325-48336.

[11] Wahab, R., Ansari, S., Dar, M.A., Kim, Y.S., Shin, H.S. (2007) Synthesis of magnesium oxide nanoparticles by sol-gel process. Materials Science Forum, **558**, pp. 983-986.

[12] Tang, Z.-X., Fang, X.-J., Zhang, Z.-L., Zhou, T., Zhang, X.-Y., Shi, L.-E. (2012) Nanosize MgO as antibacterial agent: preparation and characteristics, *Brazilian Journal of Chemical Engineering* **29**: 775-781.

[13] Yan, Y., Zhou, Z., Cheng, Y., Qiu, L., Gao, C., Zhou, J. (2014) Template-free fabrication of α-and β-Bi_2O_3 hollow spheres and their visible light photocatalytic activity for water purification, *Journal of Alloys and Compounds*.108-102 :605

[14] Han, W., Xiang, W., Chen, X., Ji, Y., Meng, Z., Qiang, T., Lv, Y. (2024) Enhanced photocatalytic performance of Cr doped MgO/Bi_2O_3 nanocomposite for efficient hydroxylation of benzene to phenol under visible-light irradiation, *Chemical Physics* **577**: 112120.

[15] Bian, Z., Zhu, J., Wang, S., Cao, Y., Qian, X., Li, H. (2008) Self-assembly of active Bi_2O_3/TiO_2 visible photocatalyst with ordered mesoporous structure and highly crystallized anatase, *The Journal of Physical Chemistry C* **112**: 6.6262-258

[16] Gurunathan, K. (2004) Photocatalytic hydrogen production using transition metal ions-doped γ-Bi_2O_3 semiconductor particles, *International Journal of Hydrogen Energy* **29**: 933-940.

[17] Fan, H., Teng, X., Pan, S., Ye, C., Li, G., Zhang, L. (20 (05Optical properties of δ-Bi_2O_3 thin films grown by reactive sputtering, *Applied Physics Letters* **87**: 231916

[18] López-Salinas, F., Martínez-Castañón, G., Martínez-Mendoza, J., Ruiz, F. (2010) Synthesis and characterization of nanostructured powders of Bi_2O_3, BiOCl and Bi, *Materials Letters* **64**: 1555-1558.

[19] Takeyama, T., Takahashi, N., Nakamura, T., Ito, S. (2004) Growth of the high reflectivity Bi_2O_3 glass films by atmospheric pressure halide CVD, *Optical Materials* **26**: 413-415.

[20] Sood, S., Umar ,A., Mehta, S.K., Kansal, S.K. (2015) α-Bi_2O_3 nanorods: An efficient sunlight active photocatalyst for degradation of Rhodamine B and 2, 4, 6-trichlorophenol, *Ceramics International* **41**: 3355-3364.

[21] Bhande, S.S., Mane, R.S., Ghule, A.V., Han, S.-H. (20 (11A bismuth oxide nanoplate-based carbon dioxide gas sensor, *Scripta Materialia* **65**: 1081-1084.

[22] Gujar, T., Shinde, V., Lokhande, C., Han, S.-H. (2006) Electrosynthesis of Bi_2O_3 thin films and their use in electrochemical supercapacitors, *Journal of Power Sources* **161**: 1479-1485.

[23] Li, E.-J., Xia, K., Yin, S.-F., Dai, W.-L., Luo, S.-L., Au, C.-T. (2011) Preparation, characterization and photocatalytic activity of Bi_2O_3–MgO composites, *Materials Chemistry and Physics* **125**: 236-241.

[24] Wachsman, E.D ,.Lee, K.T. (2011) Lowering the temperature of solid oxide fuel cells, *Science* **334**: 935-939.

[25] Hernandez-Delgadillo, R., Velasco-Arias, D., Martinez-Sanmiguel, J.J., Diaz, D., Zumeta-Dube, I., Arevalo-Niño, K., Cabral-Romero, C. (2013) Bismuth oxide aqueous colloidal nanoparticles inhibit Candida

albicans growth and biofilm formation, *International Journal of Nanomedicine* **8**: 1645-1652.

[26] Qin, F., Zhao, H., Li, G., Yang, H., Li, J., Wang, R., Liu, Y., Hu, J., Sun, H., Chen, R. (2014) Size-tunable fabrication of multifunctional Bi_2O_3 porous nanospheres for photocatalysis, bacteria inactivation and template-synthesis, *Nanoscale* **6**: 5402-5409.

[27] Riente, P., Matas Adams, A., Albero, J., Palomares, E., Pericàs, M.A. (2014) Light-driven organocatalysis using inexpensive, nontoxic Bi_2O_3 as the photocatalyst, *Angewandte Chemie International Edition* **53**: 9613-9616.

[28] Li, L., Yan, B. (2009) CeO2–Bi_2O_3 nanocomposite: two step synthesis, microstructure and photocatalytic activity, *Journal of Non-Crystalline Solids* **355**: 776-779.

[29] Jan, T., Azmat, S., Wahid, B., Adil, M., Alawadhi, H., Mansoor, Q., Farooq, Z., Ilyas, S., Ahmad, I., Ismail, M. (2018) Chemically synthesized ZnO-Bi_2O_3 (BZO) nanocomposites with tunable optical, photoluminescence and antibacterial characteristics, *Materials Science in Semiconductor Processing* **84**: 71-75.

[30] Feng, Q.L., Wu, J., Chen, G.-Q., Cui, F.-Z., Kim, T., Kim, J. (2000) A mechanistic study of the antibacterial effect of silver ions on *Escherichia coli* and *Staphylococcus aureus*, *Journal of Biomedical Materials Research* **52**: 662-668.

[31] Pal, S., Tak, Y.K., Song, J.M. (2007) Does the antibacterial activity of silver nanoparticles depend on the shape of the nanoparticle? A study of the gram-negative bacterium *Escherichia coli*, *Applied and Environmental Microbiology* **73**: 1712-1720.

[32] Koga, H., Kitaoka, T., Wariishi, H. (2009) *In situ* synthesis of silver nanoparticles on zinc oxide whiskers incorporated in a paper matrix for antibacterial applications, *Journal of Materials Chemistry* **19**: 2135-2140.

[33] Aziz, A., Khalid, M., Akhtar, M.S., Nadeem, M., Gilani, Z., Hmn, U.H.K.A., Rehman, J., Ullah, Z., Saleem, M. (2018) Structural, Morphological and Optical Investigations of Silver Nanoparticles Synthesized by Sol-Gel Auto-Combustion Method, *Digest Journal of Nanomaterials & Biostructures* **13**: 615 - 623.

[34] Capek, I. (2004) Preparation of metal nanoparticles in water-in-oil (w/o) microemulsions, *Advances in Colloid and Interface Science* **110**: 49-74.

[35] Al-Sharabi, A., Sada'a ,K.S., Al-Osta, A., Abd-Shukor, R. (2022) Structure, optical properties and antimicrobial activities of MgO–$Bi_{2-x}Cr_xO_3$ nanocomposites prepared via solvent-deficient method, *Scientific Reports* **12**: 10647.

[36] Raza, W., Haque, M., Muneer, M., Harada, T., Matsumura, M. (2015) Synthesis, characterization and photocatalytic performance of visible light induced bismuth oxide nanoparticle, *Journal of Alloys and Compounds* **648**: 641-650.

[37] Georgekutty, R., Seery, M.K., Pillai, S.C. (2008) A highly efficient Ag-ZnO photocatalyst: synthesis, properties, and mechanism, *The Journal of Physical Chemistry C* **112**: 13563-13570.

[38] Yıldırım, Ö.A., Unalan, H.E., Durucan, C. (2013) Highly efficient room temperature synthesis of silver-doped zinc oxide (ZnO: Ag) nanoparticles: structural, optical, and photocatalytic properties, *Journal of the American Ceramic Society* **96**: 766-773.

[39] Cai, Y., Wu, D., Zhu, X., Wang, W., Tan, F., Chen, J., Qiao, X., Qiu, X. (2017) Sol-gel preparation of Ag-doped MgO nanoparticles with high efficiency for bacterial inactivation, *Ceramics International* **43**: 1066-1072.

[40] Jeejamol, D., Raj, A.M.E., Jayakumari, K., Ravidhas, C. (2018) Optimization of CdO nanoparticles by Zr^{4+} doping for better photocatalytic activity, *Journal of Materials Science: Materials in Electronics* **29**: 97-116.

[41] Alnehia, A., Al-Sharabi, A., AL-Osta, A. (2023) Effect of Cu^{2+} and Cr^{3+} doping on structural, morphological, optical and electrical properties of zinc sulfide nanoparticles for optoelectronic applications, *Journal of Materials Science: Materials in Electronics* **34**: 2004.

[42] Shkir, M., Khan, A., Chandekar, K.V., Sayed, M., El-Toni, A.M., Ansari, A.A., Adil, S.F., Ghaithan, H., Algarni, H., AlFaify, S. (2021) Dielectric and electrical properties of La@ NiO SNPs for high-performance optoelectronic applications, *Ceramics International* **47**: 15611-15621.

[43] Mohanraj, K., Balasubramanian, D., Chandrasekaran, J., Bose, A.C. (2018) Synthesis and characterizations of Ag-doped CdO nanoparticles for PN junction diode application, *Materials Science in Semiconductor Processing* **79**: 74-91.

[44] Iljinas, A., Marcinauskas, L. (2015) Formation of bismuth oxide nanostructures by reactive plasma assisted thermal evaporation, *Thin Solid Films* **594**: 192-196.

[45] Zhang, J., Han, Q ,.Wang, X., Zhu, J., Duan, G. (2016) Synthesis of δ-Bi_2O_3 microflowers and nanosheets using CH_3COO (BiO) self-sacrifice precursor, *Materials Letters* **162**: 218-221.

[46] Pan, R., Wu, Y., Wang, Q., Hong, Y. (2009) Preparation and catalytic properties of platinum dioxide nanoparticles: A comparison between conventional heating and microwave-assisted method, *Chemical Engineering Journal* **153**: 206-210.

[47] Sonkusare, V.N., Chaudhary, R.G., Bhusari, G.S., Rai, A.R., Juneja, H.D. (2018) Microwave-mediated synthesis, photocatalytic degradation and antibacterial activity of α-Bi_2O_3 microflowers/novel γ-Bi_2O_3 microspindles, *Nano-Structures & Nano-Objects* **13**: 121-131.

[48] Al-Douri, A., Al-Shakily, F., Alias, M., Alnajjar, A. (2010) Optical Properties of Al-and Sb-Doped CdTe Thin Films, *Advances in Condensed Matter Physics* **2010**: 947684.

[49] Dahshan, M. (2002) Introduction to Material Science and engineering, 2nd ed., *McGraw Hill*, New York, USA, pp. 370

[50] Chen, Y., Tse, W.H., Chen, L., Zhang, J. (2015) Ag nanoparticles-decorated ZnO nanorod array on a mechanical flexible substrate with enhanced optical and antimicrobial properties, *Nanoscale Research Letters* **10**: 106.

[51] Al-Sharabi, A., Alnehia, A., Ahmed, A.-O., Yahya, N.A. (2019) Effect of copper doping on structural and optical properties of zinc sulfide (ZnS) nanoparticles, *Albaydha University Journal* **1**: 224-234.

[52]Chau, J.L.H., Lin, Y.-M., Li, A.-K., Su, W.-F., Chang, K.-S., Hsu, S.L.-C., Li, T.-L. (2007) Transparent high refractive index nanocomposite thin films, *Materials Letters* **61**: 2908-2910.

[53] Indolia, A.P., Gaur, M. (2013) Optical properties of solution grown PVDF-ZnO nanocomposite thin films, *Journal of Polymer Research* **20**: 43.

[54] Al-Sharabi, A., Ahmed, A.-O., Alnehia, A., Al-Odayni, A.-B (2023) . Chromium and copper dual-doped zinc sulfide nanoparticles: Synthesis, structural, morphological and optical properties, *Results in Optics* **13**: 100534.

[55] Al-Sharabi, A., Al-Hussam, A.M., Abdullh, S.K. (2019) Synthesis and characterization of metal complexes of Cu (ii) and Cd (ii) with poly vinyl alcohol and studied of electrical and optical properties, *International Journal of Multidisciplinary Research and Development* **6**: 19-26.

[56] Husain, S., Alkhtaby, L.A., Giorgetti, E., Zoppi, A., Miranda, M.M. (2014) Effect of Mn doping on structural and optical properties of sol gel derived ZnO nanoparticles, *Journal of Luminescence* **145**: 132-137.

[57] Thomas, M., Cui, J. (2010) Electrochemical route to p-type doping of ZnO nanowires, *The Journal of Physical Chemistry Letters* **1**: 1090-1094.

[58] Gupta, M.K., Sinha, N., Kumar, B. (2011) p-type K-doped ZnO nanorods for optoelectronic applications, *Journal of Applied Physics* **109**: 083532

[59] Trabelsi, A.B.G., Chandekar, K.V., Alkallas, F.H., Ashraf, I., Hakami ,J., Shkir, M., Kaushik, A., AlFaify, S. (2022) A comprehensive study on Co-doped CdS nanostructured films fit for optoelectronic applications, *Journal of Materials Research and Technology* **21**: 3982-4001.

[60] Chitte, H.K., Bhat, N.V., Karmakar, N.S., Kothari, D.C., Shinde, G.N. (2012) Synthesis and characterization of polymeric composites embeded with silver nanoparticles, *World Journal of Nano Science and Engineering* **2**: 19-24.

[61] Mansour, A., Mansour, S., Abdo, M. (2015) Improvement structural and optical properties of ZnO/PVA nanocomposites, *IOSR Journal of Applied Physics* **7**: 60-69.

[62] Kadham, A.J., Hassan, D., Mohammad, N., Ah-yasari, A.H. (2018) Fabrication of (polymer blend-magnesium oxide) nanoparticle and studying their optical properties for optoelectronic applications, *Bulletin of Electrical Engineering and Informatics* **7**: 28-34.

[63] Chandekar, K.V., Shkir, M., Khan, A., Sayed, M., Alotaibi, N., Alshahrani, T., Algarni, H., AlFaify, S. (2021) Significant and systematic impact of yttrium doping on physical properties of nickel oxide nanoparticles for optoelectronics applications, *Journal of Materials Research and Technology* **15**: 2584-2600.

[64] Shkir, M., Chandekar, K.V., Khan, A., Alshahrani, T., El-Toni, A.M., Sayed, M., Singh, A., Ansari, A.A., Muthumareeswaran, M., Aldalbahi, A. (2021) Tailoring the structure-morphology-vibrational-optical-dielectric and electrical characteristics of Ce@ NiO NPs produced by

facile combustion route for optoelectronics, *Materials Science in Semiconductor Processing* **126**: 105647.

[65] Alsalmah, H.A. (2024) Structural, thermal, optical, morphological, electrical, and photocatalytic characteristics of silver-doped bismuth oxide synthesized by the green route, *Ceramics International* **50**: 14675-14685.

[66] Th, S., Sharma, J., Sanjay, K. (2017) Effect of Silver Doping on Properties of ZnO nanoparticles by chemical Precipitation method, *International Journal of Engineering Technology Science and Research* **4**: 112.

[67] Arakha, M., Saleem, M., Mallick, B., Jha, S (2015) .The effects of interfacial potential on antimicrobial propensity of ZnO nanoparticle, *Scientific Reports* **5**: 9578

[68] El-Sayyad, G.S., Mosallam, F.M., El-Batal, A.I. (2018) One-pot green synthesis of magnesium oxide nanoparticles using Penicillium chrysogenum melanin pigment and gamma rays with antimicrobial activity against multidrug-resistant microbes, *Advanced Powder Technology* **29**: 2616-2625.

[69] El-Batal, A.I., Al-Hazmi, N.E., Mosallam, F.M., El-Sayyad, G.S. (2018) Biogenic synthesis of copper nanoparticles by natural polysaccharides and Pleurotus ostreatus fermented fenugreek using gamma rays with antioxidant and antimicrobial potential towards some wound pathogens, *Microbial Pathogenesis* **118**: 159-169.

[70] He, Y., Ingudam, S., Reed, S., Gehring ,A., Strobaugh Jr, T.P., Irwin, P. (2016) Study on the mechanism of antibacterial action of magnesium oxide nanoparticles against foodborne pathogens, *Journal of Nanobiotechnology* **14**: 54.

[71] Alnehia, A., Al-Sharabi, A., Al-Odayni, A.-B., Al-Hammadi, A ,.Al-Ostoot, F.H., Saeed, W.S., Abduh, N.A., Alrahlah, A. (2023) Lepidium sativum Seed Extract-Mediated Synthesis of Zinc Oxide Nanoparticles: Structural, Morphological, Optical, Hemolysis, and Antibacterial Studies, *Bioinorganic Chemistry and Applications*.4166128 :2023

[72] Verma, S.K., Jha, E., Panda, P.K., Das, J.K., Thirumurugan, A., Suar, M., Parashar, S. (2018) Molecular aspects of core-shell intrinsic defect induced enhanced antibacterial activity of ZnO nanocrystals, *Nanomedicine* **13**: 43-68.

[73] Xia, T., Kovochich, M., Liong, M., Madler, L., Gilbert, B., Shi, H., Yeh, J.I., Zink, J.I., Nel, A.E. (2008) Comparison of the mechanism of toxicity of zinc oxide and cerium oxide nanoparticles based on dissolution and oxidative stress properties, *ACS Nano*.2134-2121 :2

[74] Karthik, K., Dhanuskodi, S., Gobinath, C., Prabukumar, S., Sivaramakrishnan, S. (2018) Multifunctional properties of microwave assisted CdO–NiO–ZnO mixed metal oxide nanocomposite: enhanced photocatalytic and antibacterial activities, *Journal of Materials Science: Materials in Electronics* **29**: 5459-5471.

[75] Alnehia, A., Hadi, M., Alnahari, H., Al-Sharabi, A. (2024) Optical, structural and antibacterial properties of phase heterostructured Fe_2O_3–CuO–$CuFe_2O_4$ nanocomposite, *Scientific Reports* **14**: 14392.

[76] Al-Odayni, A.-B., Alnehia, A., Al-Sharabi, A., Al-Hammadi, A., Saeed, W.S., Abduh, N.A. (2023) Biofabrication of Mg-doped ZnO nanostructures for hemolysis and antibacterial properties, *Bioprocess and Biosystems Engineering* **46**: 1817-18.24

[77] Alnehia, A., Alnahari, H., Al-Sharabi, A. (2024) Characterization and antibacterial activity of MgO/CuO/Cu_2MgO_3 nanocomposite synthesized by sol-gel technique, *Results in Chemistry* **8**: 101620.

[78] Mukhtar, F., Munawar, T., Nadeem, M.S., Rehman, M.N.u., Riaz, M., Iqbal, F. (2021) Dual S-scheme heterojunction ZnO–V_2O_5–WO nanocomposite with enhanced photocatalytic and antimicrobial activity, *Materials Chemistry and Physics* **263**: 124372.

[79] Hadi, M. (2024) Co_3O_4-CuO-ZrO_2 Nanocomposite: Optical, spectral, morphological, structural and antibacterial studies, *Results in Chemistry* **7**: 101311.

[80] Revathi, V., Karthik, K. (2018) Microwave assisted CdO–ZnO–MgO nanocomposite and its photocatalytic and antibacterial studies, *Materials Science: Materials in Electronics* **29** 18519–18530.

[81] Subhan, M.A., Uddin, N., Sarker, P., Azad, A.K., Begum, K. (2015) Photoluminescence,photocatalytic and antibacterial activities of CeO_2-CuO-ZnO nanocomposite fabricated by co-precipitation method, *Spectrochimica Acta Part A* **149** 839–850.

Thamar University Journal of
Natural & Applied Sciences

ISSN-Print: 203-0764
ISSN-Online: 2959-4340

TUJNAS

Volume 10, Issue 2, 2025

CONTENTS

Articles

Published by Thamar University – Dhamar, Yemen